Spatial catchment areas using fuzzy lattice data structures

by

Michelle de Klerk

04377915

Supervisor: Prof. Inger Nicolette Fabris-Rotelli

Submitted in partial fulfillment of the requirements for the degree
Philosophiae Doctor (Mathematical Statistics)
in the Faculty of Natural and Agricultural Sciences
Department of Statistics
University of Pretoria

November 2024

© University of Pretoria

Declaration

I, Michelle de Klerk, declare that this thesis, which I hereby submit for the degree PhD in Mathematical Statistics at the University of Pretoria, is my own work and has not previously been submitted by me for a degree at this or any other tertiary institution. This research is approved by the NAS ethics committee, NAS003/2023.

Signature:

by
Michelle de Klerk
04377915
November 2024

© University of Pretoria

UNIVERSITEIT VAN PRETORIA
UNIVERSITY OF PRETORIA
YUNIBESITHI YA PRETORIA

Spatial catchment areas using fuzzy lattice data structures

by

Michelle de Klerk
E-mail: dklerkm@gmail.com

Abstract

This thesis presents a comprehensive framework for defining and optimising service catchment areas through innovative approaches, addressing accessibility and resource allocation challenges, particularly in low-resource settings. The first methodology introduces fuzzy lattice catchment areas, using a semi-supervised, probabilistic approach to create overlapping service zones. By enabling communities to access multiple points of interest (POIs) within their range and incorporating drive-time thresholds, this approach ensures a more equitable distribution of demand and supply, minimising spatial imbalances. Building on this, the second methodology extends the fuzzy lattice framework by integrating attribute based connections, combining structural and contextual attributes to more accurately capture spatial dynamics. This dual consideration allows for a refined propagation of demand across networks, addressing limitations in traditional connectivity only models. The final methodology applies attribute based spatial segmentation, creating tailored macro-regions that align with local environmental and socio-economic factors. By leveraging probabilistic clustering, it optimises service placements and identifies both spatially accessible and disjoint regions. Collectively, these approaches advance the field of spatial planning by offering flexible, data driven solutions that adapt to regional characteristics, enhancing service accessibility and equitable resource distribution. The applications demonstrate significant potential across healthcare, urban planning, and beyond, providing a robust foundation for addressing evolving accessibility challenges.

Keywords: Catchment areas, Fuzzy lattice data, Semi-supervised, Attribute augmented graph, Label propagation, Spatially disjoint.

© University of Pretoria

"*How do you know which path to take?* the rabbit asked. *Maybe there is no path,* replied the boy. *Maybe the path is simply made by walking.*"

Oxherd Boy (2024)

© University of Pretoria

Acknowledgements

To the two remarkable women who have profoundly shaped my academic journey, Prof. Inger Fabris-Rotelli (UP) and Dr. Lindokuhle Ndlandla (SAMRC), your guidance and influence have been invaluable. Thank you, Prof. Inger Fabris-Rotelli, for being an exceptional supervisor, mentor, and friend. Your dedication and tireless commitment throughout this journey have left me deeply grateful. I am at a loss for words to fully express my appreciation for seeing this through with me. Dr. Lindokuhle Ndlandla, if it were not for your kind words of motivation and support, I would not be here today. Thank you for your empathy and strategic guidance, which gave me the strength to continue.

My husband, Christoffel de Klerk, you have been my rock throughout this journey. Thank you for your unwavering support through the challenges of managing a PhD during COVID times and welcoming a new addition to the family. Thank you for every weekend spent with the children, every dinner prepared, and every word of encouragement. I am truly blessed to have you by my side. Aiden and Ryan de Klerk, thank you for bringing sunshine into my life every day. Thank you for helping me notice the small moments that can easily be overlooked and for reminding me to pause, breathe, and appreciate the little things in life.

To my mother, Christine Botes, thank you for being an extraordinary mother and grandmother. There is nothing that compares to a mother's love. Your words and gestures of encouragement have carried me through this journey. You always believed in me, even when I struggled to believe in myself, and your unwavering support has meant everything to me.

Thank you to my family, friends, and my wonderful colleagues at Lightstone, whose support and encouragement made this journey far less stressful and much more manageable. I would like to extend special recognition to Arminn Potgieter and Paul-Roux de Kock. Arminn, your remarkable technical expertise was invaluable in perfecting the graph figures in LaTeX, and your unwavering support as both a soundboard and a friend throughout this process has meant so much to me. Paul-Roux, you are far more than just the Chief Analytics Officer. Your genuine compassion for the team and the flexibility you provide to help us pursue our dreams are truly inspiring. I am also deeply grateful to

© University of Pretoria

Lightstone (Pty) Ltd for allowing me to use their data resources, which played a crucial role in this research.

Thank you to South African Medical Research Council (SAMRC), University of Pretoria (UP) and National Research Foundation (NRF) for the financial aid throughout this journey. I never felt like just a number in the system, as each institution consistently provided support and guidance. Your understanding and compassion during the challenging times of 2020 will always be deeply appreciated.

The work reported herein was made possible through funding by the South African Medical Research Council through its Division of Research Capacity Development under the Biostatistics Capacity Development partnership with the Belgian Development Agency (Enabel) under its framework of Building Academic Partnerships for Economic Development(BAPED). Additionally, this research received support from the National Research Foundation of South Africa (Grant Number 137785, South Africa DST-NRF-SAMRC SARChI Research Chair in Biostatistics Grant number 114613 and COE-MaSS Grant Number 2022-086-LIF-COVID-19). The content and opinions expressed herein are the sole responsibility of the authors and do not necessarily represent the official views of the NRF, SAMRC or the funders.

© University of Pretoria

Contents

List of Figures iv

List of Tables vii

1 Introduction 1
- 1.1 The full geographical region . . . 2
  - 1.1.1 Spatially accessible areas . . . 3
  - 1.1.2 Spatially inaccessible areas . . . 4
- 1.2 Thesis Outline . . . 5

2 Fuzzy lattice data structure 10
- 2.1 Introduction . . . 11
  - 2.1.1 Background . . . 11
  - 2.1.2 Literature review . . . 12
- 2.2 Methodology . . . 15
  - 2.2.1 Fuzzy lattice data . . . 16
  - 2.2.2 Fuzzy lattice catchment areas . . . 19
  - 2.2.3 Comparing measures of spatial accessibility . . . 21
- 2.3 Application . . . 23
- 2.4 Discussion . . . 29
- 2.5 Conclusion . . . 31

3 Attribute based fuzzy lattice data structure 32
- 3.1 Introduction . . . 33

© University of Pretoria

3.2 Methodology . . . 34
3.2.1 Attribute Augmented Graph . . . 35
3.2.2 Attribute Based Fuzzy Lattice Data . . . 38
3.2.3 Seasonal Catchment Areas . . . 43
3.2.4 Measures of Spatial Accessibility . . . 45
3.3 Application . . . 46
3.4 Discussion . . . 51
3.5 Conclusion . . . 52

4 Attribute based spatial segmentation 54
4.1 Introduction . . . 55
4.2 Literature review . . . 57
4.3 Methodology . . . 58
4.3.1 Transition probability matrix of an attribute augmented graph . . . 59
4.3.2 Cluster memberships and macro-regions of $\mathbf{P}_a$ . . . 63
4.3.3 Optimised cluster memberships and macro-regions . . . 66
4.4 Application . . . 73
4.4.1 Attributes . . . 73
4.4.2 Clusters and macro-regions . . . 77
4.4.3 Attribute segmentation . . . 80
4.4.4 SAR model with attribute segmentation . . . 83
4.5 Discussion . . . 87
4.6 Conclusion . . . 90

5 Conclusion 91
5.1 Chapter discussions . . . 91
5.1.1 Fuzzy lattice data structure . . . 91
5.1.2 Attribute based fuzzy lattice data structure . . . 92
5.1.3 Attribute based spatial segmentation . . . 92
5.2 Attributes, weights and label connectivity . . . 93
5.3 Data limitations . . . 95
5.4 Future work . . . 98

© University of Pretoria

5.5 Summary 100

Bibliography **102**

© University of Pretoria

List of Figures

2.1 Demand for grids $v_n, n = 1, ..., 9$ with POIs P_1 and P_2. 18
2.2 Demand for grids $v_n, n = 1, ..., 9$ with POIs P_1 and P_2 and corresponding drive-time thresholds d^{P_1} and d^{P_2}. 21
2.3 South Africa with hospital accessibility catchment areas application in Gauteng and Eastern Cape provinces. Map data © OpenStreetMap contributors, under the Open Database License (ODbL). 24
2.4 High Accessibility: Illustration of supply-demand ratio (Map A) and accessibility (Map B) at 5 minute drive-time threshold, supply-demand ratio (Map C) and accessibility (Map D) at 10 minute drive-time threshold and supply-demand ratio (Map E) and accessibility (Map F) at 15 minute drive-time threshold of City of JHB. Map data © OpenStreetMap contributors, under the Open Database License (ODbL). 26
2.5 Low Accessibility: Illustration of supply-demand ratio (Map A) and accessibility (Map B) at 5 minute drive-time threshold, supply-demand ratio (Map C) and accessibility (Map D) at 10 minute drive-time threshold and supply-demand ratio (Map E) and accessibility (Map F) at 15 minute drive-time threshold of O.R. Tambo. Map data © OpenStreetMap contributors, under the Open Database License (ODbL). 27

3.1 Graph G_a with structural nodes $v_1, ..., v_9$ and attribute nodes v_{a_1} and v_{a_2} 38
3.2 Graph G_a with structural nodes $v_1, ...v_9$ and attribute nodes v_{a_1} and v_{a_2}. POIs P_1 and P_2 and corresponding drive-time thresholds d^{P_1} and d^{P_2}. . . 44

© University of Pretoria

3.3 Temperature attribute indicating "hot days" and ease of access and accessibility to principal roads. Map data © OpenStreetMap contributors, under the Open Database License (ODbL). 48
3.4 The relative change in demand from FLD to AFLD for 5, 10, and 15-minute drive-time thresholds. Map data © OpenStreetMap contributors, under the Open Database License (ODbL). 49

4.1 Graph G_a with structural nodes $v_1, ..., v_{20}$, associated with attributes λ_1 and λ_2 61
4.2 The network structure of G_a: The structural nodes $(v_1, \ldots, v_{20})$ are depicted as black-outlined circles, with structural edges represented by black lines. Indicator attribute nodes $(v_{a_1}, v_{a_2}, v_{a_3}, v_{a_4})$ are shown as circles in green, purple, blue, and yellow, respectively, with their corresponding attribute edges displayed in the same colours as the nodes. 62
4.3 The left image illustrates the initial cluster assignments $\mathbf{U}(0)$ on P_a with $K = 5$, while the right image shows macro-regions based on $\mathbf{P}_a$ with $Q = 7$. 65
4.4 Spatially coherent optimised macro-regions based on the k-means clustering of $\mathbf{S}(t)$ 70
4.5 Attribute segmentation of clusters 72
4.6 Visualisation of the temperature, ease of access, and demand attributes at node level. The map highlights the spatial distribution of these attributes across individual nodes. Map data © OpenStreetMap contributors, under the Open Database License (ODbL). 75
4.7 The top left panel shows the variogram for maximum temperatures. The top right panel illustrates the observed and predicted maximum temperature values across the City of Cape Town. The bottom left panel displays the variogram for minimum temperatures. The bottom right panel shows the observed and predicted minimum temperature values. Map data © OpenStreetMap contributors, under the Open Database License (ODbL). 76

© University of Pretoria

4.8 Representation of the temperature, ease of access, and demand attribute at cluster and macro-region level. The map illustrates how attributes are aggregated into clusters and macro-regions based on structural edges and spatial connections. Map data © OpenStreetMap contributors, under the Open Database License(ODbL). 78
4.9 Macro-regions constructed using the initial cluster membership ($\mathbf{U}(0)$, left) and the final cluster membership ($\hat{\mathbf{U}}$, right). Map data © OpenStreetMap contributors, under the Open Database License (ODbL). . . . 79
4.10 POI locations and macro-regions over clusters (left) and attribute segmentation (right). Map data © OpenStreetMap contributors, under the Open Database License (ODbL). 82
4.11 Top-left: R-squared and p-value (LRT) trends for varying α in the SAR model. Top-right: Coefficient estimates with reference level PNH. Bottom-left: Coefficient estimates with reference level PHM. Bottom-middle: Coefficient estimates with reference level PNM. Bottom-right: Coefficient estimates with reference level PHH. 86
4.12 Highlighting spatially inaccessible areas and potential spatially accessible (w.r.t this specific POI). Map data © OpenStreetMap contributors, under the Open Database License (ODbL). 87

© University of Pretoria

List of Tables

3.1 Supply, demand and supply-demand ratios for Zevenwacht (P_1), Soneike (P_2) and Brackenfell (P_3) at 5, 10 and 15 minutes drive-time thresholds using a fuzzy lattice data (FLD) and attribute based fuzzy lattice data (AFLD) structure 50

4.1 Distinct clusters with mode value of ease of access, temperature and demand 80

4.2 POI average sales per cluster and attribute segmentation 81

© University of Pretoria

Chapter 1

Introduction

This research was inspired by disparities in healthcare access in South Africa, where some regions have limited service availability compared to metropolitan areas. The work addresses these accessibility challenges by developing a model for catchment areas that captures overlapping and realistic service zones, better reflecting how communities access healthcare facilities and identifying areas with no access to pinpoint potential solutions for improved healthcare accessibility. This method can be applied to any points of interest (POI).

Accessibility to essential facilities and services is a fundamental component of societal well-being and equitable development [50]. Ensuring equal access to resources like healthcare, education, and infrastructure is critical for promoting social equity, particularly for disadvantaged and under served populations. Unfortunately, accessibility is often hindered by a range of geographic and non-geographic barriers, resulting in significant disparities in service provision [23]. This is particularly evident for disadvantaged groups, where factors such as income, minority status, and geographical remoteness can exacerbate accessibility issues [39]. Globally, there is a stark contrast between high-income and low- and middle-income countries when it comes to accessing basic services, with the latter often facing considerable barriers and limited infrastructure [36]. In low-resource settings, capturing accurate catchment areas is essential for estimating population needs and optimising resource distribution. Effective resource planning and demand estimation hinge on understanding both supply and demand dynamics, including the services

© University of Pretoria

UNIVERSITEIT VAN PRETORIA
UNIVERSITY OF PRETORIA
YUNIBESITHI YA PRETORIA

provided by points of interest (POIs), their capacity, the presence of competing service providers as well as natural or man-made barriers that may limit access [32]. On the demand side, accounting for population fluctuations, seasonality and time-sensitive factors such as weather changes is equally important for effective planning [32].

1.1 The full geographical region

A geographical region, in its broadest sense, is a spatially delineated area that encompasses interconnected or proximate pieces of the Earth's surface. These regions are often used in studies or analyses as distinct units of land, defined by their physical, social, or administrative characteristics [16]. The concept of geographical regions has evolved over time, influenced by different disciplines and perspectives.

Geographical regions, do not necessarily have to be contiguous or wholly unfragmented. However, they often appear as compact and cohesive areas due to natural clustering and spatial autocorrelation. This tendency arises from the fact that physical, social, and economic structures are not randomly distributed but rather exhibit patterns of similarity or correlation over space [16].

Spatial autocorrelation on a near-isotropic surface, such as a flat or consistently scaled map, creates compact and contiguous regions. This spatial clustering is further reinforced by human cognition and organisational preferences. Humans tend to perceive and group proximate areas into meaningful units [33]. Moreover, compact and contiguous regions are often practical for administrative, research, and planning purposes, making them integral to understanding and managing spatial dynamics [50].

In this research, when referring to the full geographical region, the geographical region(s) under consideration are sectioned off for their relevance to the specific research question while still being recognised as part of a larger spatial context. The classification of accessibility for the full geographical region is crucial for understanding the levels of accessibility available to different communities and for identifying gaps that require intervention [39]. Regions can be segmented into two main categories: spatially accessible regions (which can be either potential, representing theoretical access, or realised, representing actual access [27]) and spatially inaccessible (disjoint) regions. This

© University of Pretoria

UNIVERSITEIT VAN PRETORIA
UNIVERSITY OF PRETORIA
YUNIBESITHI YA PRETORIA

segmentation provides a foundation for targeted analyses and interventions aimed at enhancing accessibility across the studied region.

1.1.1 Spatially accessible areas

Spatially accessible areas are regions where services or facilities can be reached by a population within a defined geographic boundary, based on factors like distance, travel time or ease of access. These areas are characterised by their proximity to a POI, making them available for potential or actual use by the community [50]. Potential spatially accessible areas are regions where services or facilities theoretically offer access to the population, implying service availability but not guaranteeing actual utilisation. Realised spatially accessible areas represent regions where potential access translates into actual usage, capturing the utilisation of services by the population. This depends on various individual, social, and economic factors [27].

Spatial catchment areas are geographical regions within which services or facilities can be accessed by a population. A catchment area represents the geographical zone from which a POI attracts communities to utilise its services or products [45, 31, 42]. It is typically defined by the maximum distance or travel time users are willing to cover to reach the POI and can be determined naturally (e.g., by geographic boundaries) or as a predefined establishment [30, 23, 37]. Service catchment areas can be classified as either non-overlapping or overlapping [7]. Non-overlapping catchment areas provide a simplified model of spatial access where each geographical region is uniquely associated with a single service facility. While this approach simplifies modelling, it may misallocate demand, particularly when multiple facilities could serve the same region, potentially neglecting user choice and specific needs [7]. Overlapping catchment areas offer a more realistic approach, allowing multiple facilities to serve the same region, acknowledging user choice, and providing a better representation of service accessibility. Overlapping catchments demonstrate how demand can be shared across facilities, potentially reducing disparities in service provision [50]. However, ensuring equitable distribution and avoiding demand concentration at a few nodes can remain challenging. An approach to creating overlapping catchment areas was explored through the use of a *fuzzy lattice data structure* [13] to represent potential spatially accessible regions as outlined in

© University of Pretoria

Chapter 2. This method represents spatially accessible regions while promoting a more balanced distribution of demand and supply. Fuzzy lattice catchment areas are generated using label propagation principles and follow a probabilistic framework that enables proportional demand allocation. In this context, "fuzzy" refers to assigning membership degrees as probabilities between 0 and 1, ensuring a more realistic representation of spatial accessibility. Drive-time thresholds [23] are applied to ensure the probability structure accounts for both the geographical boundaries of POIs and the surrounding population. By contrasting this method with traditional approaches, it underscores the impact of using a weighted distribution of resources and demand compared to uniform weighting. The approach outlined in Chapter 2 primarily focuses on the structural connections within the network and does not incorporate attributes such as environmental or topographic factors that, while not explicitly represented in structural links, still connect nodes through shared properties. To address this limitation, we expanded on the method by developing an *attribute based fuzzy lattice data structure* [14] that integrates both the network's link structure and node attributes [53] to iteratively propagate labels as discussed in Chapter 3. By employing a semi-supervised learning approach, labels are propagated to neighbouring nodes [5], representing the entire geographical region as an attribute based fuzzy lattice structure where each node holds a set of probabilities linked to different labels. This enables unlabelled nodes to retain multiple labels from their neighbours, thus reflecting overlapping catchment areas. The extent of this overlap is captured probabilistically, allowing for the creation of nuanced, seasonal overlapping catchment areas.

1.1.2 Spatially inaccessible areas

Spatially inaccessible areas, also referred to as disjoint areas, lie outside the reach of potential spatially accessible regions and are characterised by exceeding the distance or travel-time thresholds necessary for accessing services [50]. As a result, populations in these areas are effectively excluded from service coverage, posing challenges for equitable access and resource distribution. Communities within these areas are often excluded from further analysis, highlighting the need for targeted interventions [28]. Addressing these gaps may involve expanding infrastructure, increasing service points, or enhan-

© University of Pretoria

UNIVERSITEIT VAN PRETORIA
UNIVERSITY OF PRETORIA
YUNIBESITHI YA PRETORIA

cing connectivity within remote regions. The identification and management of spatially inaccessible areas are critical for achieving broader social equity and ensuring that all populations have access to services. In Chapter 4, an *attribute based spatial segmentation* methodology is developed using the transition probabilities of an attribute augmented graph[12]. By leveraging spatial attributes and creating probabilistic clusters, this methodology can identify areas where POIs are missing and analyse why regions may be spatially inaccessible. When a region lacks a POI within an accessible threshold, it may indicate either a geographic barrier or a lack of demand and accessibility, leading to its categorisation as spatially inaccessible. The probabilistic clusters ensures that, even in cases of limited accessibility, attribute segmentation can identify regions that might benefit from new POIs, transforming otherwise inaccessible areas into potential spatially accessible areas.

1.2 Thesis Outline

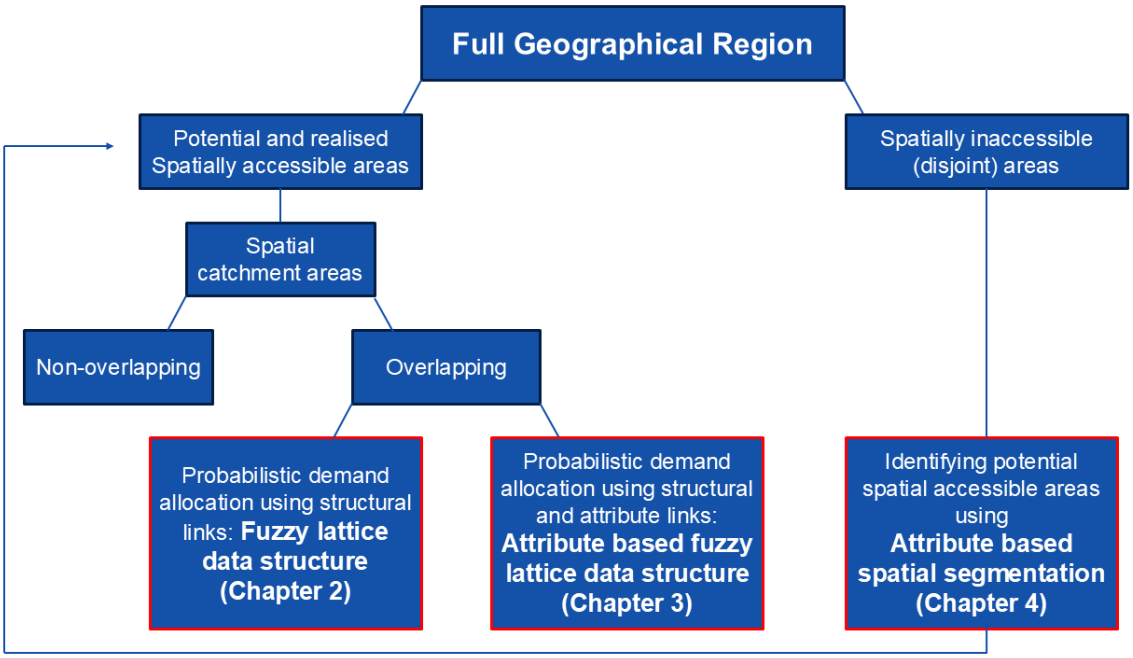

© University of Pretoria

This thesis comprises three key papers, which are presented in Chapters 2 through 4, followed by the conclusion, discussions covering all three papers as well as future work in Chapter 5.

Each chapter represents a significant component of this research, detailing the methodology, findings, and contributions made to the field. The content of each paper is summarised below, along with the venues where these works were presented and the publications in which they appeared, highlighting the academic impact and relevance of this research.

- **Chapter 2** focuses on overlapping catchment areas through the application of a fuzzy lattice data structure, as detailed in the paper titled *Hospital Accessibility Catchment Areas as a Fuzzy Lattice Data Structure*
  - Published work
    - Michelle de Klerk and Inger Fabris-Rotelli. Hospital accessibility catchment areas as a fuzzy lattice data structure. In *ISPRS Annals of the Photogrammetry, Remote Sensing and Spatial Information Sciences*, volume X-4-2024, pages 99–106, 2024[1].
  - Supporting programming code
    - GitHub repository `MichelledKGit/Michelle_PhD_Chap2`
  - Work presented at
    - 2024 International Symposium on Modern Statistics and Biostatistics (SYMSTAT2024), 26–28 June 2024, Future Africa Campus, University of Pretoria, Pretoria, South Africa. SARChi Scholar prize for the best PhD presentation.
    - 2024 ISPRS Technical Commission IV Symposium, 22-25 October 2024, Fremantle, Perth, Australia. Awarded the ISPRS Foundation (TIF) travel grant along with 7 other scholars.
  - Contributed work

[1] https://doi.org/10.5194/isprs-annals-X-4-2024-99-2024

© University of Pretoria

UNIVERSITEIT VAN PRETORIA
UNIVERSITY OF PRETORIA
YUNIBESITHI YA PRETORIA

    * This first contribution focuses on developing a fuzzy lattice data structure to model catchment areas based on spatial proximity and probabilistic membership. By using a semi-supervised approach, overlapping catchment areas are created, providing a realistic representation of service zones and reflecting how communities access services based on geographic distance. This methodology highlights the importance of probabilistic demand allocation and the role of spatial proximity in defining catchment areas

- **Chapter 3** explores overlapping catchment areas by considering both structural and attribute similarities using an attribute based fuzzy lattice data structure, as presented in the paper titled *Seasonal catchment areas using an attribute based fuzzy lattice data structure*

  – Work submitted for publication

    * Michelle de Klerk and Inger Fabris-Rotelli. Seasonal catchment areas using an attribute based fuzzy lattice data structure. 2024. Under review 2024.

  – Supporting programming code

    * GitHub repository `MichelledKGit/Michelle_PhD_Chap3`

  – Work presented at

    * 2024 South African Statistical Association (SASA) Conference, 18-22 November 2024, Stellenbosch, Cape Town, South Africa. Awarded second prize in the SASA Unpublished Postgraduate Paper Competition.

  – Contributed work

    * Building on the initial fuzzy lattice framework, this approach incorporates additional attributes such as environmental and topographical factors to create more complex, attribute based catchment areas. By considering both structural connections and key attributes, this method captures how seasonal changes impact accessibility and resource distribution. The comparison between static and seasonal catchment areas demonstrates the dy-

© University of Pretoria

UNIVERSITEIT VAN PRETORIA
UNIVERSITY OF PRETORIA
YUNIBESITHI YA PRETORIA

namic nature of supply-demand ratios and accessibility, offering insights into how fluctuating environmental conditions affect service provision.

- **Chapter 4** partitions the geographical region under consideration using attribute based spatial segmentation to optimise POI placement, as discussed in the paper titled *Attribute based spatial segmentation for optimising POI placement*
  - Work submitted for publication
    - Michelle de Klerk and Inger Fabris-Rotelli. Attribute based spatial segmentation for optimising POI placement. 2024. Under review 2024.
  - Supporting programming code
    - GitHub repository `MichelledKGit/Michelle_PhD_Chap4`
  - Contributed work
    - This final contribution shifts focus from accessibility to existing POIs to identifying potential spatially accessible areas using attribute based spatial segmentation. This method creates macro-regions with unique structural and attribute properties, such as social factors, topography, and environmental characteristics. By identifying spatially disjoint regions, this approach helps pinpoint potential areas for new POI placement, optimising resource distribution and addressing service gaps

The three papers collectively pioneer novel methodologies for redefining service catchment areas. Paper 1 introduces *fuzzy lattice catchment areas*, a novel semi-supervised probabilistic approach that creates overlapping service zones. Unlike traditional methods, it accommodates shared service use and competition among points of interest (POIs), providing a truly adaptable framework for equitable demand and supply distribution. This is achieved through label propagation in a geographical context, illustrating how areas are interlinked. Paper 2 extends this innovation by integrating *attribute based fuzzy lattice data structures*, incorporating dynamic contextual attributes such as seasonality and temperature to model accessibility shifts over time and space. This approach dynamically captures the interplay between spatial and temporal factors,

© University of Pretoria

UNIVERSITEIT VAN PRETORIA
UNIVERSITY OF PRETORIA
YUNIBESITHI YA PRETORIA

enabling planners to address fluctuating accessibility challenges with precision using a probabilistic structure. Paper 3 further advances the methodology with *attribute based spatial segmentation*, employing probabilistic clustering to delineate macro-regions that reflect nuanced local characteristics such as environmental, socio-economic, and infrastructural factors. This work introduces a novel mechanism for identifying spatially and aspatially similar areas and determining optimal POI placement in spatially disjoint regions, transforming resource allocation strategies. Together, these contributions set a new benchmark for adaptive, data-driven spatial planning.

© University of Pretoria

Chapter 2

Fuzzy lattice data structure

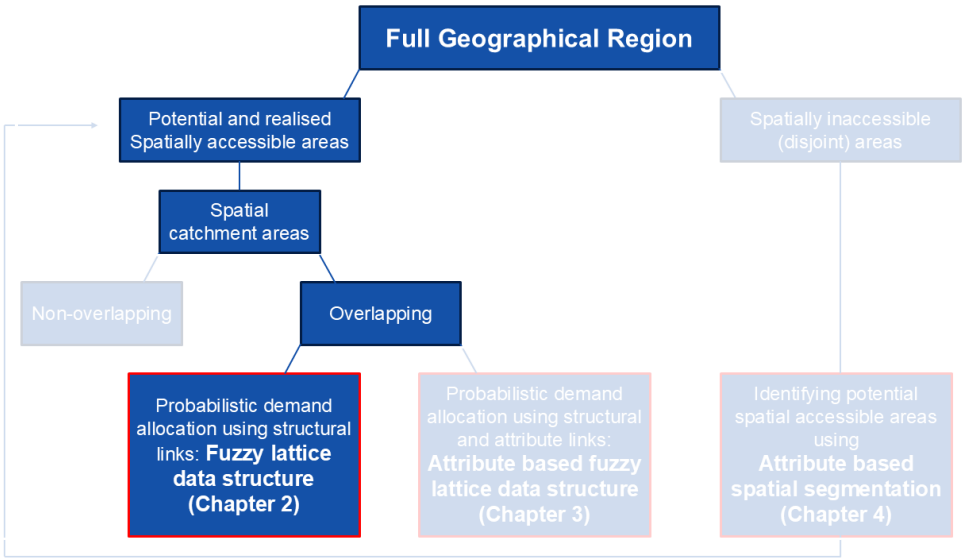

This chapter introduces fuzzy lattice catchment areas, providing a probabilistic approach to generate overlapping service zones and ensure equitable demand distribution across communities.

© University of Pretoria

UNIVERSITEIT VAN PRETORIA
UNIVERSITY OF PRETORIA
YUNIBESITHI YA PRETORIA

Abstract

The accessibility to basic facilities and services plays a pivotal role in every society and city planning. Spatial accessibility can vary between cities and countries and is mainly defined by the ease at which facilities can be accessed by communities. Facilities can provide essential services and/or products such as pharmacies, clinics, schools, universities, etc. Spatial accessibility is dependent on the spatial impedance between a facility and the target population and can be illustrated with catchment areas. We propose a fuzzy lattice catchment area method which uses a semi-supervised learning algorithm to create overlapping catchment areas. This methodology is applied to determine the accessibility to hospitals in South Africa and provides an illustration on the difference for regions with high accessibility compared to low accessibility. The application can easily be adapted in a variety of fields based on industry type, drive-time thresholds, supply capacity and the target population.

2.1 Introduction

2.1.1 Background

Ease of accessibility to essential facilities is an important component of any society. This is important for several reasons, including equality in the provision of resources and services [50]. Unfortunately, due to both geographic and non-geographic barriers, not all communities have equal accessibility to basic facilities [39]. Geographic barriers include distance, infrastructure limitations, and natural obstacles, while non-geographic barriers (also referred to as aspatial barriers) are often demographic and socioeconomic in nature. These include factors such as income disparities, minority status, home ownership, educational attainment, language barriers, and service awareness. For example, low-income households, female-headed households, and those without private transport may face greater difficulties in accessing essential services, even if those services are geographically close [50]. This is especially true for disadvantaged population groups considering factors like income and minority groups. Globally there is also a disparity between countries when considering basic services such as health care, for which low-

© University of Pretoria

UNIVERSITEIT VAN PRETORIA
UNIVERSITY OF PRETORIA
YUNIBESITHI YA PRETORIA

and middle-income countries tend to have poorer accessibility than first world countries [36].

Access can be classified into one of four categories namely: potential spatial, potential aspatial, realised spatial and realised aspatial access as defined by [27]. Aspatial access focusses on social disparities between communities and identifies nongeographic barriers such as wages, gender, race, childcare services, educational attainment, linguistic barriers etc. as discussed in [50, 39]. Potential and realised spatial access is however based on geographic distance as well as the distribution and size of facilities. Services or products offered within geographic accessibility of communities are potential spatial access and only when it is utilised, is it referred to as realised spatial access.

Potential spatial accessibility can be defined by the ease at which a facility, or any point of interest, POI, is arrived at from a demand location [50]. POIs are facilities which provide services and/or products and can be grouped by sub-industry level (laboratories, pharmacies, clinics, schools, universities, etc.) or industry level (health care, education etc.). Spatial accessibility is dependent on the spatial impedance (drive-time or Euclidean distance) between the POI and demand location and on the capacity of the POI in question [45, 31, 42].

This paper proposes a method to identify fuzzy lattice catchment areas, which represent potential spatially accessible regions. Fuzzy in this context refers to assigning degrees of membership as a probability ranging from 0 to 1. The method employs a semi-supervised approach to classify overlapping catchment areas. The fuzzy lattice catchment areas approach is compared to existing methods to highlight how the distribution in resources and demand is affected when using a weighted approach as opposed to assigning equal weights. Finally it is used as an application to create fuzzy lattice catchment areas for hospitals in South-Africa and illustrates how areas with high and low accessibility can be influenced by the weighted distribution of resources.

2.1.2 Literature review

A catchment area is the geographical area from which a POI attracts communities that utilises its services or products. It is usually defined by the maximum traveling distance users are willing to travel to a POI and can either be created naturally to a point that

© University of Pretoria

UNIVERSITEIT VAN PRETORIA
UNIVERSITY OF PRETORIA
YUNIBESITHI YA PRETORIA

people are drawn to, by natural geographic boundaries or as a predefined establishment [30].

There are an array of methods available to determine catchment areas in spatially accessible areas. These methods include the circular buffer approach [1] and Euclidean buffer-based method [28] to more specialised methods such as the floating catchment, two-step floating catchment area (2SFCA) [40, 31], gravity based methods [50], distance decay functions and variable catchment areas as summarised in [45]. As highlighted in [50], spatial accessibility is dependent on the capacity of a POI and/or the spatial impedance between a POI and demand location.

Catchment areas formed around POIs can be classified into one of the following three categories: in potential spatial accessible areas it can either be i) overlapping or ii) non-overlapping [7] and beyond spatial accessible areas, iii) spatially inaccessible [50]. Overlapping catchment areas indicates a choice for the POI being visited and is a more realistic approach than imposing non-overlapping spatial boundaries [7]. Non-overlapping catchment areas provide a simplification to modelling techniques. There is however the disadvantage that demand could be incorrectly assigned. If a community is only assigned to one catchment area, when more than one is available, the result will tend to be spatially uneven [7]. Spatially inaccessible areas, also referred to as off-network areas [28], occur when the distance or time impedance falls beyond the distance or drive-time threshold of the spatially accessible areas [50]. Communities which falls in the spatially inaccessible areas are typically excluded from any further analysis [28].

The spatial impedance or threshold distance between a POI and demand location can be based on different methods such as a distance buffer, distance-decay, drive-times etc. [50]. A welfare approach was taken by [23] to define threshold distances by classifying different services and products by answering the fundamentals of “who gets what, where and how”. Using this approach essential services, such as basic education, healthcare etc., should be available to the majority of the population and should have a smaller threshold distance (and catchment area) than facilities providing inessential services. As discussed in [23], low-order basic facilities define access to essential services such as schools and naturally form small catchment areas around communities. Middle-order POIs serve more communities than low-order POIs and can be located at a further distance such

© University of Pretoria

UNIVERSITEIT VAN PRETORIA
UNIVERSITY OF PRETORIA
YUNIBESITHI YA PRETORIA

as 24-hour health care and Home Affairs/State Department offices. Finally high-order POIs have the largest possible catchment areas as people are willing to commute further to POIs that provide high value services or products such as higher education and leisure centres. According to [23], middle-order POIs should ideally have a maximum distance of 30 km and should be accessible to 91% of the population. The fifteen-minute city concept specifies that all critical urban services and facilities should be within a 15 minute walking, cycling or driving distance for optimal and sustainable city planning and development [38]. The distance and time associated with low-, middle- and high-order POIs can differ vastly between cities and each region should be analysed individually based on its road networks and infrastructure.

It is important to quantify the capacity or supply of a POI and the demand at surrounding communities for optimal resource and facility planning [23]. Supply is quantified based on whether an activity or algorithmic approach is used to model catchment areas [7]. An activity based approach takes into account the daily movement of communities between different regions to access a specific service. An algorithmic approach uses static measures in an area at a specific point in time by considering the size, capacity and ease of access to quantify supply. Demand is calculated in a similar fashion by taking the population size of an area at a point in time. For our application in Section 2.3 an algorithmic approach will be used to compare hospital bed capacity and demand at a specific point in time.

In this paper a similar approach is used as in [7] to define catchment areas using network structures, specifically considering label propagation [41]. Network structures takes into account how nodes (or users) are linked and incorporates information from neighbours to classify unlabelled nodes. There are multiple methods for node classification in network structures available. These include community score, multi-objective optimisation, modularity optimisation, genetic algorithm, label propagation, game theory, clustering etc. as summarised in [4].

The fuzzy lattice catchment areas methodology that is proposed herein will however differ from the approach in [7] where the final result is overlapping catchment areas rather than non-overlapping areas. Non-overlapping catchment areas occur when a node is associated with only one label at the end of the iteration process. In our method a

© University of Pretoria

UNIVERSITEIT VAN PRETORIA
UNIVERSITY OF PRETORIA
YUNIBESITHI YA PRETORIA

probabilistic approach is followed where each node will have a probability to be assigned to each label in the network structure. Drive-time thresholds are applied to ensure that the probability structure also takes into account the geographical boundaries of the POIs and population.

2.2 Methodology

In this section the initial data inputs and the algorithmic approach to creating fuzzy lattice catchment areas will be covered. This is achieved by integrating the foundational work in [5] on node classification in network structures with model-based label propagation techniques for resource allocation as done in [7]. The methodology in [7] focuses on how propagation rates adjust as demand outstrips supply in non-overlapping catchment areas. In contrast, our method suggests overlapping catchment areas where each label has a set of probabilities associated with each node at different drive-time intervals.

A label can be a binary, single or multi-label which can represent any characteristic of the associated node and an edge represents a similarity between two nodes. If a node is an individual in a social network, a label can represent age, marital status etc. and an edge between two individuals can represent a shared characteristic such as a shared family connection, interest etc. In this application, let the network graph be the full geographical region which is subdivided into smaller grid cells (whose centres then represent the nodes) and an edge between two nodes is a shared line segment between two grid cells. Labels according to a chosen connectivity will be the POI associated or classified with each grid cell. Initially only the nodes which spatially overlaps with a POI will be labelled, the remaining nodes will be unlabelled.

Using a semi-supervised learning approach to propagate labels to neighbouring grid cells, the full geographical region can be represented as a fuzzy lattice structure, with each grid cell having a set of probabilities associated with each label, as outlined in Section 2.2.1. Network threshold distances for low-, middle- and high-order POIs will then be overlayed on the fuzzy lattice data structure to create fuzzy lattice catchment areas in Section 2.2.2.

© University of Pretoria

UNIVERSITEIT VAN PRETORIA
UNIVERSITY OF PRETORIA
YUNIBESITHI YA PRETORIA

2.2.1 Fuzzy lattice data

Fuzzy lattice catchment areas uses a random walk approach and label propagation to propagate labels to all nodes by only using the link structure of the graph. Label propagation [41] relies on an iterative process where each node considers its neighbours. Each unlabelled node joins the community to which the maximum number of its neighbours belong to. As discussed in [41] when a tie between two labelled nodes occur, the label is determined by selecting one of the neighbouring labels based on a uniform random approach. In this research we will consider the approach in [52] where a node can keep multiple labels received from neighbouring nodes, allowing for an overlap of catchment areas. The degree of overlap is captured by a probability and hence create a fuzzy lattice data structure.

Using node classification formulation as illustrated in [5], consider graph $G = G(V, E)$ that is subdivided into $N, n = 1, ..., N$ nodes $V = \{v_1, v_2, ..., v_N\}$ and let an edge $(i, j) \in E$ represent a shared line segment between nodes v_i and v_j as defined by the Rook's contiguity [50]. Let $\mathbf{D}$ be a $N \times N$ diagonal degree matrix indicating the number of neighbouring edges to node $v_n, n = 1, ..., N$ and weights matrix $\mathbf{A}$ be an $N \times N$ adjacency matrix defining neighbouring nodes using common edges between grids.

Consider geographical spatial POIs, $P = \{P_1, P_2, ..., P_M\}$, $m = 1, ..., M$ as a known set of M locations. The centre of each grid cell $v_n, n = 1, ..., N$ will represent the nodes in graph G. The grid size should be determined based on the specific geographical region of the study. In addition every node is assumed to contain at most one POI, thus the grid size should be chosen to maintain this at a minimum. Let V_m be the subset of the M labelled nodes which contains a POI and V_u be the subset of remaining $N - M$, initially unlabelled nodes, which doesn't contain a POI. Let V be ordered such that the first M rows are the cells from V_m and the remaining $N - M$ rows are the nodes from V_u such that $V = V_m \cup V_u = \{v_1, ..., v_M, v_{M+1}, ..., v_N\}$ [5].

Let $\mathcal{Y}$ be the full set of M possible labels and $\mathbf{Y}_m$ be an $M \times M$ indicator matrix, carrying the initial M multi-class labels indicating the POI associated with the corresponding node in set V_m. Similarly let $\mathbf{Y}_u$ be an $(N - M) \times M$ matrix indicating the POI associated with corresponding nodes in V_u. The initial label matrix, $\mathbf{Y}$, is an $N \times M$ matrix with the first M rows as $\mathbf{Y}_m$ and the remaining $N - M$ rows as $\mathbf{Y}_u$ or 0 (as the

© University of Pretoria

UNIVERSITEIT VAN PRETORIA
UNIVERSITY OF PRETORIA
YUNIBESITHI YA PRETORIA

nodes in V_u are initially unlabelled).

Assume that all unlabelled nodes can reach a labelled node in a finite number of steps and will therefore have an associated label at the end of the iteration process, i.e. graph G is label connected [3]. A graph is not label connected when there remains unlabelled nodes at the end of the iteration process. This will occur when there exists unlabelled node/s which share no direct edges connecting them with the remaining structure in graph G. When considering a social network structure this can happen when there are people who share no similar interest with the remaining individuals in the network. For a geographical application, a graph can be non label-connected when there are grid cells which doesn't share a direct edge with the remaining grid cells due to natural/man-made boundaries such as rivers, mountains, region/state border boundaries etc.

Consider transition matrix $\mathbf{P}$, with $\mathbf{P}^t$ the corresponding matrix at state t where p_{ij}^t is the probability of reaching node v_j from v_i in t steps. As $t \to \infty$, $p_{ij}^{t\to\infty}$ will indicate the $(i,j)^{th}$ probability in $\mathbf{P}^{t\to\infty}$ at which the process reached node v_j, with associated label $c \in \mathcal{Y}$, from v_i in convergence with $0 \leq p_{ij} \leq 1$ and $\sum_j p_{ij} = 1$. In matrix form

$$\hat{\mathbf{Y}} = \mathbf{P}^{t\to\infty}\mathbf{Y} \tag{2.1}$$

where

$$\hat{\mathbf{Y}} = \begin{bmatrix} \hat{\mathbf{Y}}_m \\ \hat{\mathbf{Y}}_u \end{bmatrix} \text{ and } \mathbf{Y} = \begin{bmatrix} \mathbf{Y}_m \\ \mathbf{0} \end{bmatrix} \tag{2.2}$$

and $\hat{\mathbf{Y}}$ contains the output labels from the converged iteration process for all nodes $v_n \in V$.

Labelled nodes in set V_m are classified as absorbent states such that they exhibit probability 1 of staying in the same node and probability 0 of leaving the node. Therefore the labels of all nodes $v_n \in V_m$ do not change. Since the nodes are ordered in such a way that the first M rows in V are V_m and the last $N - M$ rows are V_u, the transition matrix can be split into 4 sub-matrices, indicating the probability to move between states, namely $\mathbf{P} = \begin{pmatrix} \mathbf{P}_{mm} & \mathbf{P}_{mu} \\ \mathbf{P}_{um} & \mathbf{P}_{uu} \end{pmatrix} = \begin{pmatrix} \mathbf{I} & \mathbf{0} \\ \mathbf{P}_{um} & \mathbf{P}_{uu} \end{pmatrix}$.

The probability of transition from the unlabelled states to the labelled states are

© University of Pretoria

UNIVERSITEIT VAN PRETORIA
UNIVERSITY OF PRETORIA
YUNIBESITHI YA PRETORIA

captured in the $(N-M)\times M$ matrix $\mathbf{P}_{um}$ and from the unlabelled states to the unlabelled states are captured in the $(N-M)\times(N-M)$ matrix $\mathbf{P}_{uu}$. Since all labelled nodes are defined as absorbent states, the probability of staying in a labelled node is 1 and the probability of exiting a labelled node is 0. This simplifies $\mathbf{P}_{mm}$ to an $M\times M$ identity matrix $\mathbf{I}$, and $\mathbf{P}_{mu}$ to an $M\times(N-M)$ zero matrix $\mathbf{0}$.

Since the graph is label connected and there are M absorbent states, the limiting distribution of $\lim_{t\to\infty}\mathbf{P}^t$ is

$$\mathbf{P}^{t\to\infty}=\begin{pmatrix}\mathbf{I} & \mathbf{0}\\ (\mathbf{I}-\mathbf{P}_{uu})^{-1}\mathbf{P}_{um} & \mathbf{0}\end{pmatrix} \tag{2.3}$$

as shown in [5, 3]. Substituting equations (2.3) and (2.2) into (2.1) the labels can be computed by

$$\begin{bmatrix}\hat{\mathbf{Y}}_m\\ \hat{\mathbf{Y}}_u\end{bmatrix}=\begin{pmatrix}\mathbf{I} & \mathbf{0}\\ (\mathbf{I}-\mathbf{P}_{uu})^{-1}\mathbf{P}_{um} & \mathbf{0}\end{pmatrix}\begin{bmatrix}\mathbf{Y}_m\\ \mathbf{0}.\end{bmatrix}. \tag{2.4}$$

From (2.4), the labels for the absorbent state nodes contained in V_m remains unchanged with $\hat{\mathbf{Y}}_m=\mathbf{Y}_m$. The labels of the unlabelled nodes are obtained by computing $\hat{\mathbf{Y}}_u=(\mathbf{I}-\mathbf{P}_{uu})^{-1}\mathbf{P}_{um}\mathbf{Y}_m$. The $(N-M)\times M$ matrix $\hat{\mathbf{Y}}_u$ will contain the probability of each label assigned to grid $v_n\in V_u$ with the sum over each row adding to 1. The process will iterate over all nodes defined in G.

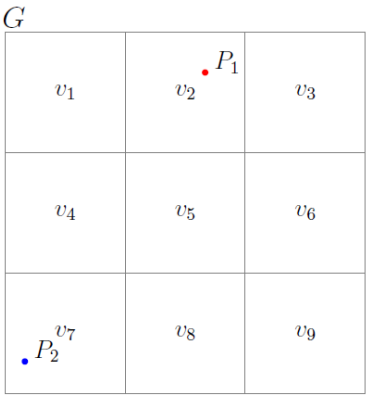

Figure 2.1: Demand for grids $v_n, n=1,...,9$ with POIs P_1 and P_2.

© University of Pretoria

UNIVERSITEIT VAN PRETORIA
UNIVERSITY OF PRETORIA
YUNIBESITHI YA PRETORIA

Consider the simple example illustrated in Figure 2.1. In this example seven regions, $V_u = \{v_1, v_3, v_4, v_5, v_6, v_8, v_9\}$, are unlabelled and two regions, $V_m = \{v_2, v_7\}$, are labelled with associated POIs P_1 and P_2 respectively. Let V be the ordered set, contained in G, consisting of $N = 9$ nodes with the first $M = 2$ rows the labelled nodes and the remaining $N - M = 7$ rows the unlabelled nodes, i.e. $V = \{v_2, v_7, v_1, v_3, v_4, v_5, v_6, v_8, v_9\}$. Let $\mathbf{Y}_m$ be an indicator matrix with the first column representing label P_1 and the second column representing label P_2. Applying the methodology as described above, the probability of labels P_1 and P_2 to be assigned to nodes $v_n \in V, n = 1, ..., 9$ is calculated in (2.5).

$$\hat{\mathbf{Y}} = \begin{bmatrix} \hat{\mathbf{Y}}_m \\ \hat{\mathbf{Y}}_u \end{bmatrix} = \begin{bmatrix} 1 & 0 \\ 0 & 1 \\ 0.72 & 0.28 \\ 0.83 & 0.17 \\ 0.45 & 0.55 \\ 0.62 & 0.38 \\ 0.66 & 0.34 \\ 0.38 & 0.62 \\ 0.52 & 0.48 \end{bmatrix}. \tag{2.5}$$

From the results in (2.5) it can be noted that all nodes in V_m remained in the initial node and label associated with it with probability 1. The nodes contained in set V_u however received a probability associated with labels P_1 and P_2. It can be expected that a unlabelled grid will have a higher probability associated with a labelled grid that is closer in the graph structure than labelled grids that is further away. Node v_3 has the highest probability of being associated with label $P_1(0.83)$ and v_8 with label $P_2(0.62)$ as can be verified by the graph structure of G as illustrated in Figure 2.1.

2.2.2 Fuzzy lattice catchment areas

Using the proposed fuzzy lattice data structure, realistic catchment areas can be obtained on this structure using drive-time thresholds. When assuming G is labelled connected, all nodes will receive a set of probabilities assigned to each label in set $\mathcal{Y}$. This is however

© University of Pretoria

UNIVERSITEIT VAN PRETORIA
UNIVERSITY OF PRETORIA
YUNIBESITHI YA PRETORIA

not practical when considering geographic data and the threshold drive-time distance a person is willing to travel to a given POI.

Consider the set of M POIs, $P = \{P_1, P_2, ..., P_M\}$, $m = 1, ..., M$, with an associated drive-time threshold distance d^{P_m} assigned to each $P_m, m = 1, ..., M$. The threshold drive-time distance d^{P_m} depends on the order of the POIs and will be denoted by $d^{P_m}_{low}, d^{P_m}_{mid}$ or $d^{P_m}_{high}$ for low-, middle- or high-order POIs respectively as discussed in [23]. For each POI, we identify all nodes v_n which are within a threshold drive-time distance d^{P_m} of P_m.

Let G_{P_m} define the region such that $G_{P_m} = \bigcup_n v_n \ni d_{v_n,P_m} \leq d^{P_m}, G_{P_m} \subseteq G$ with d_{v_n,P_m} the drive-time distance between the nearest network point of v_n and P_m. G_{P_m} represents the region of accessibility for POI, P_m, which consists of all nodes v_n that fall within the specified threshold drive-time distance d^{P_m}. The definition of G_{P_m} ensures that only the union of nodes, $\bigcup_n v_n$, satisfying the drive-time constraint $d_{v_n,P_m} \leq d^{P_m}$ are included in the region.

Let $O_{v_n} = \{m : v_n \in G_{P_m}\}$ define the indices of POI, P_m, that is snapped to the same network as v_n. Nodes that are contained in more than one G_{P_m} have an overlap of accessibility to different POIs. There can however exist nodes which are not contained in any set of G_{P_m} resulting in spatially disjoint areas.

Let all nodes which fall beyond the threshold drive-time distance d^{P_m} for each P_m be nullified in $\hat{\mathbf{Y}}_u$ i.e. the probability for a node to be assigned to a label which falls beyond the drive-time threshold is 0. If a region falls beyond the drive-time threshold for all POIs, the region is spatially inaccessible (disjoint) and will be assigned a probability of 0 for all labels $c \in \mathcal{Y}$. The matrix $\hat{\mathbf{Y}}_u$ is row standardised to ensure that all rows adds up to 1.

Consider the example provided in Figure 2.2 with $N = 9$ grids and POIs, P_1 and P_2. Suppose the values for d^{P_1} and d^{P_2} are such that $G_{P_1} = \{v_2, v_3, v_5, v_6\}$, $G_{P_2} = \{v_4, v_5, v_7, v_8\}$, $V_m = \{v_2, v_7\}$ and regions v_1 and v_9 are spatially disjoint. Let all nodes which fall beyond drive-time threshold d^{P_1} for catchment area of P_1 carry a 0 probability to be assigned to label P_1 and similarly P_2. After the matrix $\hat{\mathbf{Y}}_u$ has been row standardised, the results from (2.5) with drive-time thresholds applied is provided in (2.6).

© University of Pretoria

UNIVERSITEIT VAN PRETORIA
UNIVERSITY OF PRETORIA
YUNIBESITHI YA PRETORIA

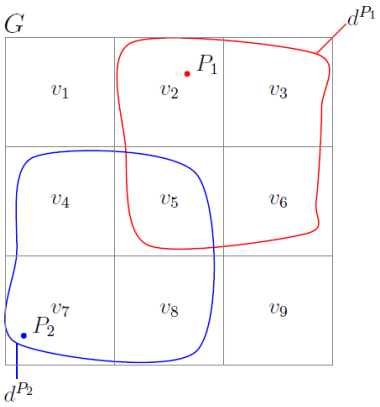

Figure 2.2: Demand for grids $v_n, n = 1, ..., 9$ with POIs P_1 and P_2 and corresponding drive-time thresholds d^{P_1} and d^{P_2}.

$$\hat{\mathbf{Y}} = \begin{bmatrix} \hat{\mathbf{Y}}_m \\ \hat{\mathbf{Y}}_u \end{bmatrix} = \begin{bmatrix} 1 & 0 \\ 0 & 1 \\ 0 & 0 \\ 1 & 0 \\ 0 & 1 \\ 0.62 & 0.38 \\ 1 & 0 \\ 0 & 1 \\ 0 & 0 \end{bmatrix}. \tag{2.6}$$

It can be noted that after standardisation that each node is only associated with the POI falling within the same network. Node v_5 has an overlap of drive-time thresholds d^{P_1} and d^{P_2} and hence retains the probability of being assigned both label P_1 and P_2. Nodes v_1 and v_9 falls beyond the drive-time thresholds for all POIs and is therefore spatially disjoint with probability 0 to be assigned to label $c \in \mathcal{Y}$.

2.2.3 Comparing measures of spatial accessibility

Spatial accessibility can be measured by considering how the distribution of supply and demand is connected in space [50]. Supply can represent the capacity of a supplier such as the number of beds available in a hospital [7], the number of suppliers such as the

© University of Pretoria

UNIVERSITEIT VAN PRETORIA
UNIVERSITY OF PRETORIA
YUNIBESITHI YA PRETORIA

number of primary care physicians in an area [50, 31] or resources that are available such as a doctor's resources as done in [42]. Demand usually represents the population and communities that requires the specified services or products. In this section the difference in spatial accessibility when comparing fuzzy lattice catchment areas to 2SFCA [40, 31] will be illustrated.

Let all POIs, $P_m \in P$ have supply size (capacity) of $S(P_m)$ and all nodes $v_n \in V$ have an associated demand (population size) of $D(v_n)$ as formulated in [7]. Then the supply-demand ratio for supplier m in region G_{P_m} can be expressed by

$$R_{P_m} = \frac{S(P_m)}{D(G_{P_m})} \tag{2.7}$$

and the accessibility for all nodes v_n, $v_n \in V$ is

$$A_{v_n} = \sum_{m \in O_{v_n}} R_{P_m} = \sum_{m \in O_{v_n}} \frac{S(P_m)}{D(G_{P_m})}. \tag{2.8}$$

as illustrated by [50, 31].

Consider the example provided in Figure 2.2 with $N = 9$ grids and POIs, P_1 and P_2. Suppose the demand for all regions are 1 i.e., $D(v_n) = 1, n = 1, ..., 9$ and supply for all suppliers are 4, $S(P_m) = 4, m = 1, 2$. Suppose the values for d^{P_1} and d^{P_2} are such that $G_{P_1} = \{v_2, v_3, v_5, v_6\}$, $G_{P_2} = \{v_4, v_5, v_7, v_8\}$, $V_m = \{v_2, v_7\}$ and regions v_1 and v_9 are spatially disjoint. Using 2SFCA, the supply-demand ratio for P_1 and P_2 are the same as both have the same units of demand and supply i.e. $R_{P_1} = R_{P_2} = 1$. Since region v_5 has access to both P_1 and P_2 the accessibility of v_5 is $A_{v_5} = R_{P_1} + R_{P_2} = 2$. The supply-demand ratio and accessibility is a good indication on how resources are distributed. This approach however doesn't take into account the structure of the data and all demand locations within a catchment area are given equal weights.

Consider the same application, but applied to fuzzy lattice catchment areas to determine accessibility and supply-demand ratio using a probabilistic approach. The supply and demand associated with each grid and supplier will remain the same i.e. $D(v_n) = 1, n = 1, .., 9$ and $S(P_m) = 4, m = 1, 2$ but the demand on catchment area level will change according to the weight assigned by $\hat{\mathbf{Y}}_u$. Let the demand be proportion-

© University of Pretoria

UNIVERSITEIT VAN PRETORIA
UNIVERSITY OF PRETORIA
YUNIBESITHI YA PRETORIA

ally assigned to each supplier's catchment area using the probabilities in (2.6). Then $D(G_{P_1}) = 3.62$ and $D(G_{P_2}) = 3.38$ which results in the supply-demand ratio for P_1 to change to $R_{P_1} = \frac{S(P_1)}{D(G_{P_1})} = 1.105$ and P_2 to $R_{P_2} = \frac{S(P_2)}{D(G_{P_2})} = 1.183$. Since region v_5 still has access to both P_1 and P_2 the accessibility of v_5 is $A_{v_5} = R_{P_1} + R_{P_2} = 2.288$.

Since semi-supervised learning takes into account the structure of the data, a higher weight is placed on label P_1 than for P_2 for region v_5 due to the placement of the supplier. This results in a lower supply-demand ratio for P_1 compared to P_2 since the same level of supply needs to be provided to a slightly higher level of demand.

When comparing fuzzy lattice catchment areas to other overlapping catchment area techniques, such as 2SFCA, the advantage of a probabilistic approach rather than assigning equal weights can be demonstrated when comparing how the population size (or demand in an area) and capacity at a given POI (or supply) is distributed. This provides a better illustration of how demand and supply is allocated based on the structure of the data rather than assigning equal weights to each region. This will also be illustrated in the next section with application to hospital bed capacity and population size in South Africa.

2.3 Application

Access to hospitals for different parts in South Africa will be investigated to test the proposed methodology. The facilities which will be considered are district, central, military, mining, regional and tertiary public hospitals as well as private hospitals. All hospitals which provide basic healthcare services and trauma related emergencies are considered as the POIs, where specialised facilities such as rehabilitation and psychiatric centres are excluded.

To illustrate the difference between areas which are highly accessible and areas with limited accessibility, two district municipalities[1] in Gauteng and Eastern Cape province (as illustrated in Figure 2.3) and their surrounding areas in South-Africa will be considered.

[1] District municipalities consists of multiple local municipalities. They are administrative divisions which is accountable for providing basic services within the area. Source: Education and Training Unit (ETU), www.etu.org.za (accessed February 15, 2024)

© University of Pretoria

Figure 2.3: South Africa with hospital accessibility catchment areas application in Gauteng and Eastern Cape provinces. Map data © OpenStreetMap contributors, under the Open Database License (ODbL).

The first district municipality is City of Johannesburg (JHB) which is situated in the Gauteng province and is categorised as a metropolitan municipality. This is the largest city in South Africa with 4.8 million people of which 44% have completed their high school certificate and 15% holds a higher education qualification. The housing in this district is predominantly formal dwellings (90%) where 95% have access to running water on site as reported in the 2022 South Africa census[2]. The provincial road network of Gauteng consists of majority paved roads (76%) and 24% unpaved roads as reported by the National and provincial Departments of Transport[3].

The second district municipality is O.R. Tambo which is located in the Eastern Cape province and is not categorised as one of the six metropolitan municipalities in South Africa. This district has a population of 1.5 million people of which 22% have completed

[2] Statistics South Africa, *Census 2022 Municipal Factsheet*, census.statssa.gov.za (accessed February 23, 2024)

[3] National Treasury, *Chapter 7 - Roads and Transport*, www.treasury.gov.za (accessed February 23, 2024)

© University of Pretoria

UNIVERSITEIT VAN PRETORIA
UNIVERSITY OF PRETORIA
YUNIBESITHI YA PRETORIA

their high school certificate and 8% hold a higher education qualification. The housing in this district was predominantly informal, with only 43.4% formal housing recorded in 2011, but this value has increased significantly to 77% in 2022. Access to running water on site in this district is however still only 43% as reported in the 2022 South Africa census[4].

Even though the Eastern Cape is geographically larger than Gauteng, this province has limited accessibility where majority of the provincial road network is unpaved at 90% and only 10% is paved as reported by the National and provincial Departments of Transport[3].

Using the proposed fuzzy lattice catchment areas approach let graph G be South Africa which is subdivided into square grids of size $500m \times 500m$. This is the optimal grid size to ensure that only one POI is allocated to each node. The demand allocated to each grid, $D(v_n)$, is population size which is obtained from the overlaying census and deeds office data as captured by Lightstone (Pty) Ltd[4] for 2022. The supply for each POI, $S(P_m)$, is the bed capacity for each hospital. Drive-times thresholds of 5, 10 and 15 minutes for all the POIs will be used as the value for $(d_{low}^{P_m})$ low-, $(d_{mid}^{P_m})$ middle- and $(d_{high}^{P_m})$ high-order facility drive-time thresholds. The highest drive-time threshold considered for this example is at 15 minutes based on the fifteen-minute city concept [38].

Consider Figure 2.4 which illustrates supply-demand ratio and accessibility for POIs situated in the City of JHB, and surrounding areas. The capacity of each POI is illustrated by the size of the dot. The hospital with the largest capacity in South Africa is Chris Hani Baragwanath public hospital[5] with a capacity of 3,200 beds and approximately 6,760 staff members. It is the third largest hospital in the world and is located in the bottom left hand corner for all maps in Figure 2.4.

In Figure 2.4, maps A, C and E illustrate the supply-demand ratio and maps B, D and F the accessibility at drive-time thresholds of 5, 10 and 15 minutes respectively. One

[4] Lightstone (Pty) Ltd procures its data directly from the Deeds office and is comprised of a snapshot of all South Africa property ownership as at 1993, with a full history of all transactions to augment with census data.

[5] Chris Hani Baragwanath Academic Hospital, chrishanibaragwanathhospital.co.za (accessed February 20, 2024).

© University of Pretoria

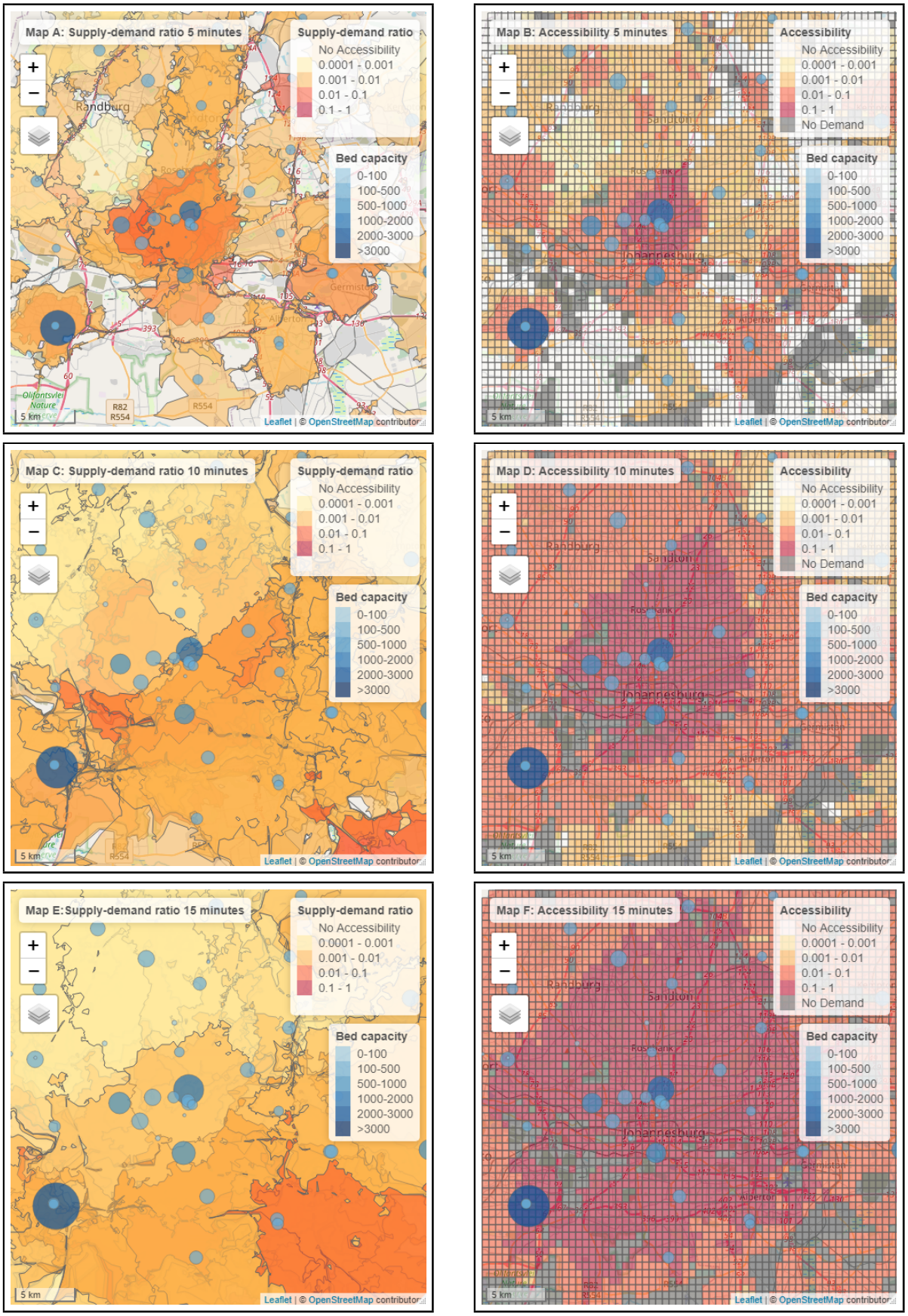

Figure 2.4: High Accessibility: Illustration of supply-demand ratio (Map A) and accessibility (Map B) at 5 minute drive-time threshold, supply-demand ratio (Map C) and accessibility (Map D) at 10 minute drive-time threshold and supply-demand ratio (Map E) and accessibility (Map F) at 15 minute drive-time threshold of City of JHB. Map data © OpenStreetMap contributors, under the Open Database License (ODbL).

© University of Pretoria

UNIVERSITEIT VAN PRETORIA
UNIVERSITY OF PRETORIA
YUNIBESITHI YA PRETORIA

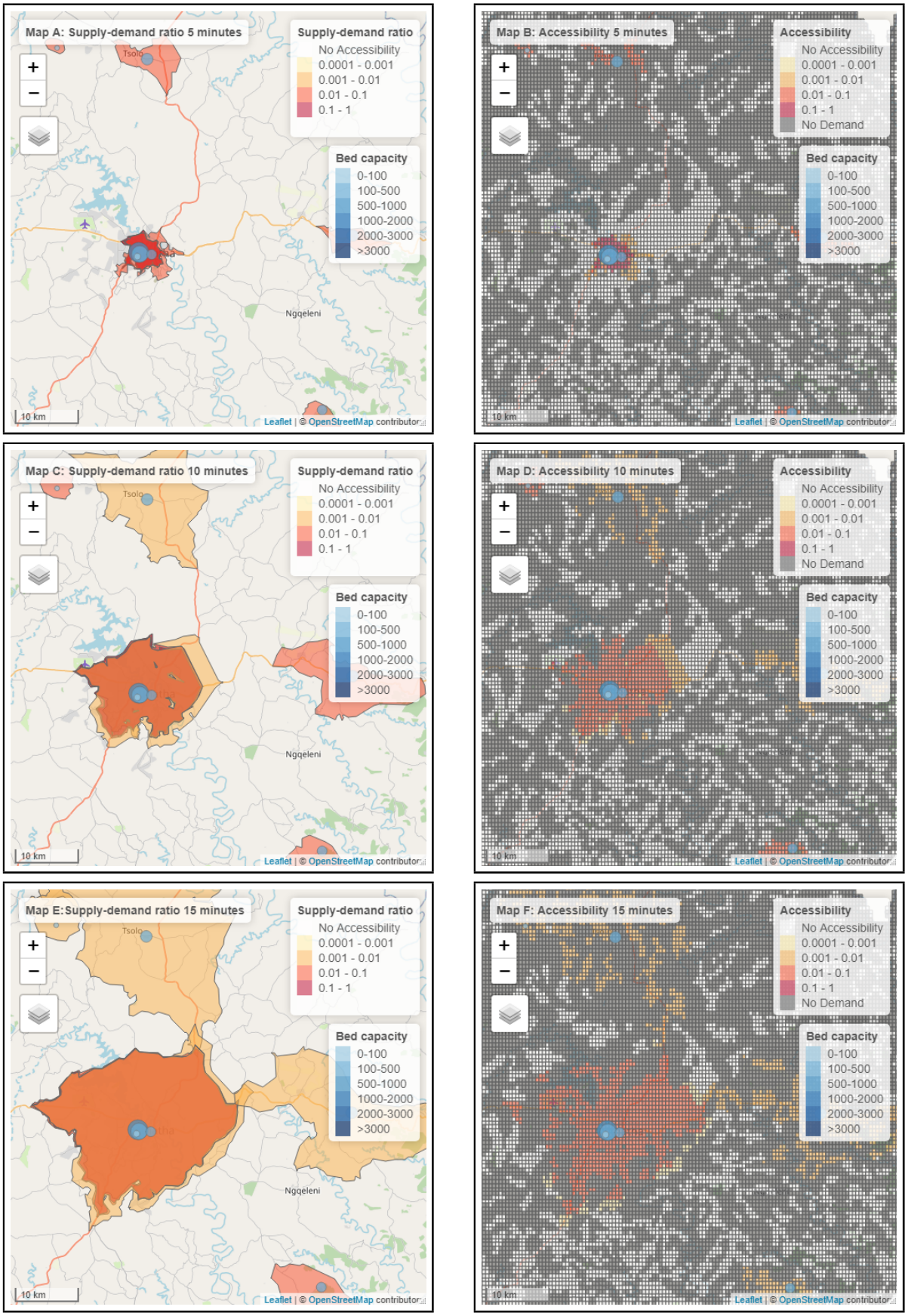

Figure 2.5: Low Accessibility: Illustration of supply-demand ratio (Map A) and accessibility (Map B) at 5 minute drive-time threshold, supply-demand ratio (Map C) and accessibility (Map D) at 10 minute drive-time threshold and supply-demand ratio (Map E) and accessibility (Map F) at 15 minute drive-time threshold of O.R. Tambo. Map data © OpenStreetMap contributors, under the Open Database License (ODbL).

© University of Pretoria

UNIVERSITEIT VAN PRETORIA
UNIVERSITY OF PRETORIA
YUNIBESITHI YA PRETORIA

can note that as the drive-times per POI increases that the supply-demand ratio of each POI decreases as a higher level of demand is expected at the same level of supply. At the lowest drive-time threshold of 5 minutes, the ratio of supply to demand is very high in areas where the POI capacity is high. Maps B, D, and F demonstrate accessibility, and as more POIs are included within the drive-time thresholds, it becomes evident that nodes intersecting multiple POIs have greater accessibility compared to nodes connected to just one POI. When considering accessibility, it can be noted that at the lowest drive-time threshold, high accessibility is only evident where multiple POIs are located in the same vicinity. At the highest drive-time threshold (map F), all nodes have high accessibility, which illustrates that in highly accessible cities, majority of people will have access to all basic services within a 15 minute drive-time threshold.

When considering an area with low accessibility a different view is observed when analysing how resources and demand is distributed. Consider the district municipality O.R. Tambo in Figure 2.5 where maps A, C and E illustrates the supply-demand ratio and maps B, D and F the accessibility at 5, 10 and 15 minutes drive-time thresholds respectively. In the low accessibility region one can note that there is not a significant difference between the supply-demand ratio at 10 and 15 minutes drive-time respectively. This is due to the fact that the number of additional demand that is captured in extending the drive-time is not as much as in a metropolitan area, since the number of people in a square meter is less than in City of JHB. One can note however that the supply-demand ratio for this region is lower than in the highly accessible region for most POIs and this is due to the supply capacity available at each of these POIs.

The capital of O.R. Tambo is the town Mthatha and there are multiple towns and communities that are formed around it. From Figure 2.5, Mthatha (situated close to the midpoint, but slightly off-centre to the left in maps A to F) has one of the highest health service per capita in its district, but since the district O.R. Tambo is largely rural and has a limited budget capacity (as reported by COGTA[6]) one can note that the accessibility to hospitals for other towns in this district is very low. The accessibility for this district, illustrated in maps B, D and F, has the opposite effect as in the highly accessible district.

[6] Department of Cooperative Governance and Traditional Affairs, *Profile and Analysis: OR TAMBO District Municipality EC*, https://www.cogta.gov.za/ddm/wp-content/uploads/2020/11/ORTamnco-September-2020.pdf (accessed February 23, 2024)

© University of Pretoria

UNIVERSITEIT VAN PRETORIA
UNIVERSITY OF PRETORIA
YUNIBESITHI YA PRETORIA

In City of JHB, additional POIs are captured as the drive-time increases, therefore the nodes have access to more hospitals and accessibility increases as drive-time threshold increases. In O.R. Tambo however, the POIs remain the only POIs in the 15 minute catchment area. Therefore, as the drive-time threshold increases, additional demand is added but the supply remains at the same level, which will lead to a decrease in accessibility for nodes that is in a 5 or 10 minute catchment area of the POIs. When considering map F in Figure 2.5 it is noted that some regions have no accessibility even at a 15 minute drive-time threshold. The grayed out blocks indicate open areas with no demand. No demand is identified with census and Lightstone (Pty) Ltd data and occurs where there is vacant land, water bodies, commercial or industrial structures and no residential homes.

On inspection when comparing the high accessible district to the district with lower accessibility it can be noted how the distribution of resources is affected as demand increases and whether the supply can increase to match the level of demand.

2.4 Discussion

We introduce fuzzy lattice catchment areas which are overlapping catchment areas and ensure a spatially even distribution of demand and supply. Fuzzy lattice catchment areas are created using the fundamentals of label propagation and is based on a probabilistic approach. Applying fuzzy lattice catchment areas has the advantage of creating more realistic, overlapping catchment areas, allowing a person to choose from multiple POIs within their accessibility range. This method ensures that demand is proportionally assigned rather than concentrated in a single region, which can lead to spatially uneven catchment areas. Together with this, drive-time thresholds are considered to ensure that the final catchment areas are representative of services or goods being provided by POIs and the target population in that area.

The fuzzy lattice data structure is created by assuming the area is label connected, therefore that each unlabelled node will receive a probability to be associated with labelled node in a finite number of steps. This can be limiting however if there exists a natural barrier in the geographical data where a labelled node cannot be reached and it is

© University of Pretoria

UNIVERSITEIT VAN PRETORIA
UNIVERSITY OF PRETORIA
YUNIBESITHI YA PRETORIA

not labelled connected. Future research includes adjusting the edge weights [5] between nodes which will enable the specification of barriers in the graph structure. Fuzzy lattice catchment areas defines each labelled node as an absorbent state which implies that the node will assume the label with a probability of 1. This assumption can however be relaxed as proposed by [44] where a labelled node is not required to be an absorbent state. The relaxation of this assumption could be applied to cases where the population that is placed in the same node as a POI has a probability to be assigned to all POIs. In this application the grid sizes were small enough that this did not have an effect on creating spatially uneven areas, but if the nodes are chosen at a larger size, relaxing this assumption could be beneficial.

To accurately capture the hospital bed capacity in a third world country such as South Africa can be challenging. How medical resources, staff and accessibility to the resources are reported can also be different between sources especially when comparing public and private hospitals. The list of all public and private[7] health facilities were obtained as reported by the hospital groups or by South African home affairs[8]. A few independent reports, including one from PMG[9], have however raised concerns that the capacity at some of the hospitals are not as reported and some having only half of the capacity available due to budget cuts and lack of health care professionals. Variation on bed capacity other than that officially reported could however not be taken into account and therefore the number of beds per capita that is indicated could be a very conservative estimate. In the approach taken by [7] caution was raised in creating overlapping hospital catchment areas when considering specialised hospitals that doesn't provide the same service but as explained in this application only hospitals that provide basic healthcare services were considered. Hence when applying this method all POIs considered needs to provide the same service or product. Another challenge when calculating catchment areas for low- and middle-income countries is the setup and maintenance of basic infrastructure.

[7] SA Private Hospitals, www.saprivatehospitals.com. (accessed February 02, 2024).

[8] Department of Home Affairs (DHA), *List of Connected Health Facilities per Province*, www.dha.gov.za (accessed February 15, 2024).

[9] PMG (People's Assembly Monitor), *SA Military Health Services briefing on improving capacity and capabilities at Military Hospitals*, https://pmg.org.za/committee-meeting/37138/ (accessed February 23, 2024)

© University of Pretoria

UNIVERSITEIT VAN PRETORIA
UNIVERSITY OF PRETORIA
YUNIBESITHI YA PRETORIA

Depending on the accessibility of a region to main routes and the condition of the roads, the drive-time (given the same distance) can vary greatly between cities. The determination of the threshold for drive-time or distance should be made independently for each unique case, considering the type of service an industry offers and how essential it is to the surrounding communities. Future work will include investigation of a generalised application in the healthcare sector using a simulation study.

Fuzzy lattice catchment areas is a very flexible approach for an array of different industry type services and target population scenarios. It can efficiently depict either an oversupply or undersupply of a services to the nearby population by considering the accessibility criteria based on drive-time or distance.

2.5 Conclusion

A realistic representation of facility catchment areas is crucial for any city resource planning. This will highlight any constraints in a city, such as limited accessibility to basic services. Fuzzy lattice catchment areas give a weighted and spatially even approach to understand the supply-demand ratio for any POI together with the accessibility available to communities.

This approach can be applied in various fields where the target population could only be a subset of the population for a specific industry type, for example only considering children in a local community and their access to parks, schools, or daycare. The algorithm has minimal assumptions and is mainly dependent on the link structure of the geographical region, supply per POI, demand at the desired nodes and drive-time thresholds.

© University of Pretoria

Chapter 3

Attribute based fuzzy lattice data structure

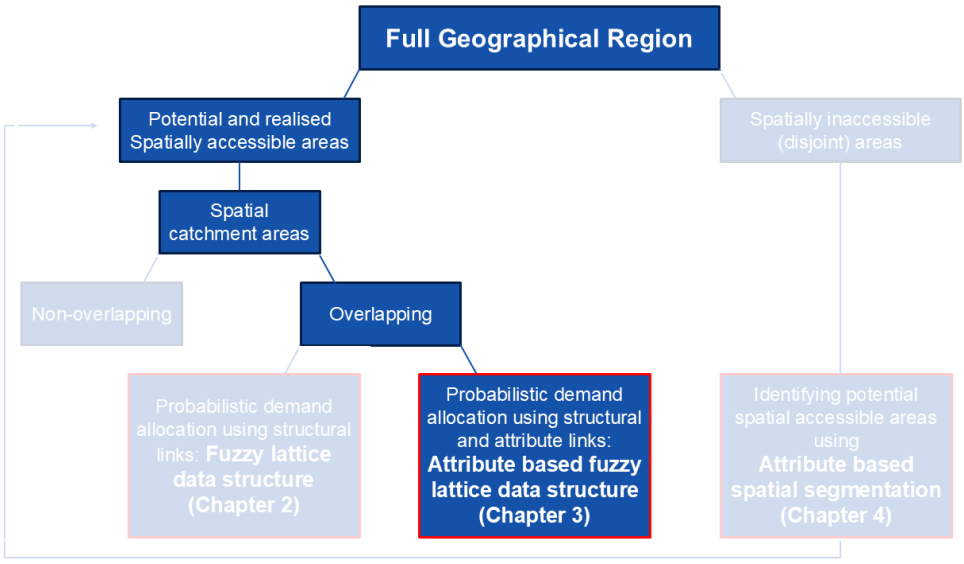

This chapter expands upon Chapter 2 by integrating an attribute-based fuzzy lattice data structure, combining both structural and attribute-based connections within a network.

© University of Pretoria

UNIVERSITEIT VAN PRETORIA
UNIVERSITY OF PRETORIA
YUNIBESITHI YA PRETORIA

Abstract

Seasonality impacts various industries and sectors, influencing agricultural cycles, economic planning, and healthcare resource allocation. We propose a novel approach using an attribute based fuzzy lattice data structure to create overlapping catchment areas using the fundamentals of label propagation and graph clustering. This approach considers both the link structure and attribute similarities between nodes in a network, where the nodes are points of interest in a road network. Nodes may be close or far apart based on connectivity and shared attributes, such as common interests or in a geographical application considering topography features. In this study, we incorporate static and seasonal attributes for geographical nodes, allowing us to explore seasonal catchment areas and provide a more realistic view of accessibility throughout the year. This integrated approach offers a comprehensive framework for assessing spatial accessibility and understanding seasonal variations in regions to enhance planning for essential services.

3.1 Introduction

The need to capture accurate catchment areas is important for estimating population needs in an area as well as resource planning. In low-resource settings or countries with limited infrastructure this is especially important to distribute the available resources optimally and prevent either a over- or under-supply in regions. As mentioned in [32] there is a minimal set of conditions from both the supply and demand side which a catchment area should meet. On the supply side, this involves considering the various services provided by points of interest (POIs), determining whether they are specialised, accounting for competing service providers, assessing the capacity of POIs and identifying any natural or man-made barriers. On the demand side, it is important to identify areas that experience significant fluctuations throughout the year and account for time-sensitive factors such as weather changes and population flows.

Seasonality impacts a variety of industries and sectors. In agriculture, it can influence harvesting times, soil quality, and disease outbreaks [2]. In economics, seasonal trends affect resource planning for tourism and retail sales, requiring careful resource allocation [9]. In healthcare, optimising resources is crucial for addressing seasonal infectious

© University of Pretoria

UNIVERSITEIT VAN PRETORIA
UNIVERSITY OF PRETORIA
YUNIBESITHI YA PRETORIA

diseases, such as colds and flus and gastrointestinal diseases [34].

Overlapping catchment areas are created in [13] which take the supply and demand into consideration by using a fuzzy lattice data structure which relies on the graph's link structure for label propagation. However, nodes often share attributes that are not reflected in the structural links but still connects them to other nodes via a shared property [53]. Our proposed attribute based fuzzy lattice data structure integrates both the link structure and node attributes to iteratively propagate labels. Using a semi-supervised learning approach to propagate labels to neighbouring nodes, the entire geographical region can be represented as an attribute based fuzzy lattice structure, with each node having a set of probabilities associated with various labels. This allows unlabelled nodes to retain multiple labels received from their neighbours, reflecting overlapping catchment areas. The degree of this overlap is captured probabilistically, allowing to create overlapping catchment areas. Using a real-world application in healthcare resource allocation across seasons, we compare seasonal catchment areas to static catchment areas created with a fuzzy lattice data structure. This comparison highlights how accessibility and supply-demand ratios fluctuate seasonally, offering insights into the dynamic nature of catchment areas in regions with changing environmental conditions.

The remainder of this paper is structured in the following order. Section 3.2 covers the methodology, where we define an attribute augmented graph and the transition probability matrix which is then used to create an attribute based fuzzy lattice data structure and seasonal catchment areas. In Section 3.3, we apply this methodology in a practical scenario, demonstrating how the integration of attributes can influence demand patterns and the supply-demand ratio. This is followed by a discussion and conclusion, offering final remarks and insights on the analysis.

3.2 Methodology

This section covers the fundamentals of a network graph, including nodes, edges, weights and introduces a set of attributes associated with the nodes in graph a G. In Section 3.2.1, we define an attribute-augmented graph, G_a, that incorporates these attributes. Section 3.2.2 proposes an attribute-based fuzzy lattice data structure that leverages both

© University of Pretoria

UNIVERSITEIT VAN PRETORIA
UNIVERSITY OF PRETORIA
YUNIBESITHI YA PRETORIA

the link structure and node attributes to iteratively propagate labels. Finally, Section 3.2.3 applies this attribute based fuzzy lattice to a simple toy example, illustrating how the supply-demand ratio and accessibility are impacted.

3.2.1 Attribute Augmented Graph

Using node classification formulation as illustrated in [5], consider a graph $G = G(V, E, W)$, with V the set of nodes, E the set of edges and W the edge weights. Nodes typically represent entities such as individuals in a social network and edges represent the relationships between these entities, such as friendships, or interactions. In this chapter we focus on a spatial graph, that is, the nodes represent geographical areas.

A structural node refers to the position of a node within the graph, independent of any specific attributes. The structure of the graph itself provides information about the network, such as how densely connected certain nodes are, adjacent nodes and how central a node is in comparison to the other nodes. The link structure refers to how the nodes are connected through the edges and can be quantified in a statistical manner by the transition probability from one node to the other. Herein, the link structure uses label propagation such as in [41], to propagate labels across the network to unlabelled nodes, so that structurally close nodes are more likely to share similar labels.

In addition to the link structure in G, consider a set of attributes Λ which is associated with the nodes V in G. Attribute nodes are added to represent specific characteristics or properties of the nodes in a network. These nodes are different from structural nodes, which reflect the network's topology. In an augmented graph, G_a, attribute nodes are added to express similarity based on shared properties. Connections, or attribute edges, are drawn between structural nodes and attribute nodes when the structural nodes share a similar attribute.

Incorporating the attribute nodes into the connectivity between nodes, let $G_a = (V \cup V_a, E \cup E_a, \mathbf{W}_a^*)$ be an attribute augmented graph as defined in [53] with V the structural nodes, V_a the attribute nodes, E the structural edges, E_a the attributes edges and $\mathbf{W}_a^*$ the attribute and structural weights. Let the structural nodes $V = \{v_1, ..., v_N\}$ represent the full geographical region which is subdivided into N smaller grid cells, whose centres then represent the node locations. A structured edge $(v_i, v_j) \in E$ iff

© University of Pretoria

structure node v_i shares a line segment, as defined by the Rook's contiguity [50], with structure node v_j in the geographical area. Let the nodes in V be associated with the attributes $\Lambda = \{\lambda_1, \ldots, \lambda_{\mathcal{A}}\}$. If each attribute $\lambda_i \in \Lambda$ has z_i levels $i \in \{1, ..., \mathcal{A}\}$ then let $A = \{a_1, ..., a_T\}$ be the T-dimesional set of indicator attributes that is associated with each level for attribute $\lambda_i \in \Lambda$ where $T = \sum_{i=1}^{\mathcal{A}} z_i$. Let $V_a = \{v_{a_1}, ..., v_{a_T}\}$ be the set of indicator attribute nodes. The size of node set $V \cup V_a$ is now $N + T$.

The indicator attribute information for structural node v_i is regarded as a T-dimensional binary vector, $\mathbf{x}_i$, and can be represented in an attribute matrix, $\mathbf{X}$, as

$$\mathbf{X} = \begin{pmatrix} \mathbf{x}_1 \\ \mathbf{x}_2 \\ \vdots \\ \mathbf{x}_N \end{pmatrix} = \begin{pmatrix} a_1(v_1) & a_2(v_1) & \ldots & a_T(v_1) \\ a_1(v_2) & a_2(v_2) & \ldots & a_T(v_2) \\ \vdots & \vdots & \ddots & \vdots \\ a_1(v_n) & a_2(v_n) & \ldots & a_T(v_n) \end{pmatrix}$$

where $a_j(v_i) = 1$ indicates an attribute edge in E_a if node v_i is associated with indicator attribute a_j else $a_j(v_i) = 0$ [29]. The structural and attribute weights of G_a is given by $\mathbf{W}_a^* = \begin{pmatrix} \mathbf{W} & 0 \\ 0 & \mathbf{W}_a \end{pmatrix}$ with $\mathbf{W}$ an $N \times N$ matrix indicating the structure edge weights w_{ij} between structure nodes v_i and v_j and $\mathbf{W}_a$ is a $T \times T$ diagonal matrix consisting of the attribute weights, $w_{a_i}, i = 1, ..., T$.

When considering an attribute augmented graph structure, not only can a node transition via a structural edge, but also via an attribute edge. Consider the $(N + T) \times (N + T)$ transition probability matrix $\mathbf{P}_a$ of G_a constructed as

$$\mathbf{P}_a = \begin{pmatrix} \mathbf{P}_s & \mathbf{P}_{sa} \\ \mathbf{P}_{as} & \mathbf{0} \end{pmatrix} \tag{3.1}$$

where $\mathbf{P}_s$ is an $N \times N$ submatrix with the transition probabilities for structural node, v_i, to reach structural node, v_j

$$p_{v_i,v_j} = \begin{cases} \frac{w_{ij}}{w_{i\cdot} + \sum_{i=1}^{T} w_{a_i}}, & \text{if } (v_i, v_j) \in E \\ 0, & \text{otherwise.} \end{cases}$$

© University of Pretoria

UNIVERSITEIT VAN PRETORIA
UNIVERSITY OF PRETORIA
YUNIBESITHI YA PRETORIA

$\mathbf{P}_{sa}$ is an $N \times T$ submatrix containing the transition probability from a structural node, v_i, to an attribute node, v_q

$$p_{v_i,v_q} = \begin{cases} \frac{w_q}{w_i . + \sum_{i=1}^{T} w_{a_i}}, & \text{if } (v_i, v_q) \in E_a \\ 0, & \text{otherwise.} \end{cases}$$

$\mathbf{P}_{as}$ is an $T \times N$ transition probability submatrix for an attribute node, v_p, to reach a structural node, v_j

$$p_{v_p,v_j} = \begin{cases} \frac{1}{N(v_p)}, & \text{if } (v_p, v_j) \in E_a \\ 0, & \text{otherwise} \end{cases}$$

and finally a $T \times T$ submatrix, $\mathbf{0}$, for the transition probability from an attribute node, v_p, to an attribute node, v_q

$$p_{v_p,v_q} = 0, \quad \forall v_p, v_q \in V_a$$

with $w_i.$ the sum of edge-weights for structural node v_i, $N(v_p)$ the number of neighbours to node v_p and $p, q \in \{a_1, ..., a_T\}$ as defined in [29].

Consider a simple example illustrated in Figure 3.1 with structural nodes $V = \{v_1, ..., v_9\}$ such that $N = 9$. Each of the nodes represents a geographical grid with location based attributes captured in Λ. For this example let the nodes be associated with only one attribute, λ_1 which consists of two levels a_1 and a_2 i.e $\mathcal{A} = 1, z_1 = 2$ and $T = 2$. Assume all structure and attribute weights in $\mathbf{W}_a^*$ are 1. In this case then $\mathbf{W}$ will simply be an adjacency matrix that defines structural neighbouring nodes using shared lines between grids. The set of indicator nodes for whether a node is associated with a_1 or a_2 is contained in the set V_a. The transition probability matrix $\mathbf{P}_a$ for G_a is a 11×11 matrix and can be illustrated in equation (3.2).

The transition from a structural node to a structural node is contained in the submatrix $\mathbf{P}_s$ and from equation (3.2) one can note that since node v_1 is only structural neighbours with nodes v_2 and v_4, there is an assigned probability of $1/3$ for moving from v_1 to v_2 or v_4. There is a an additional transition probability of $1/3$ associated with node v_1 contained in the submatrix $\mathbf{P}_{sa}$ which is the probability for structural node v_1

© University of Pretoria

UNIVERSITEIT VAN PRETORIA
UNIVERSITY OF PRETORIA
YUNIBESITHI YA PRETORIA

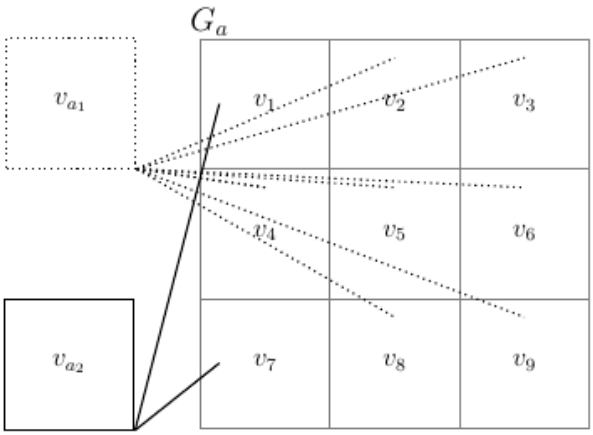

Figure 3.1: Graph G_a with structural nodes $v_1, ..., v_9$ and attribute nodes v_{a_1} and v_{a_2}

to move to attribute node v_{a_2} hence the sum over all rows still adds up to one and $\mathbf{P}_a$ retains its stochastic matrix properties.

$$\mathbf{P}_a = \left(\begin{array}{cccccc|cc} 0 & 1/3 & 0 & 1/3 & \cdots & 0 & 0 & 1/3 \\ 1/4 & 0 & 1/4 & 0 & \cdots & 0 & 1/4 & 0 \\ \vdots & \vdots & \vdots & \vdots & \ddots & \vdots & \vdots & \vdots \\ 0 & 0 & 0 & 0 & \cdots & 0 & 1/3 & 0 \\ -- & -- & -- & -- & -- & -- & -- & -- \\ 0 & 1/7 & 1/7 & 1/7 & \cdots & 1/7 & 0 & 0 \\ 1/2 & 0 & 0 & 0 & \cdots & 0 & 0 & 0 \end{array}\right). \tag{3.2}$$

The transition from the newly created attribute nodes namely v_{a_1} and v_{a_2} can be observed in the submatrix $\mathbf{P}_{as}$ where the attribute node v_{a_1} shares a transition probability of $1/7$ with the structural nodes $v_2, v_3, v_4, v_5, v_6, v_8$ and v_9. The attribute node v_{a_2} shares a transition probability of $1/2$ with structural nodes v_1 and v_7. The probability from an attribute node to an attribute node is 0 and is captured in the 2×2 submatrix $\mathbf{0}$.

3.2.2 Attribute Based Fuzzy Lattice Data

In any network, if a set of labels is known for some nodes, label propagation allows us to predict labels for unmarked nodes by using their connections to the labeled ones.

© University of Pretoria

UNIVERSITEIT VAN PRETORIA
UNIVERSITY OF PRETORIA
YUNIBESITHI YA PRETORIA

This helps assign values, to nodes where data is missing, ensuring that all nodes are considered based on their network links. It is a powerful way to fill missing information and make informed decisions across the entire network.

Using a semi-supervised learning approach to propagate labels to neighbouring nodes, the full geographical region can be represented as an attribute based fuzzy lattice structure, with each node having a set of probabilities associated with each label. As discussed in [13] a fuzzy lattice data structure uses a random walk approach and label propagation to propagate labels to all nodes. A fuzzy lattice data structure only considers the graph's link structure to propagate labels, focusing on how nodes are connected and share common neighbours. However, nodes often have various attributes such as shared interests when examining social networks, or shared geographical features like weather patterns, topography, etc., when analysing geographical data [53]. An attribute based fuzzy lattice data structure is proposed herein using both the link structure and attributes associated with nodes to propagate labels. An unlabelled node can hold multiple labels received from neighbouring nodes, allowing for an overlap of catchment areas. The degree of overlap is captured by a probability and hence create a fuzzy lattice data structure [13].

Let $\mathcal{Y}$ be the full set of M possible labels that is initially applied to the labelled nodes in the network. The foundation of label propagation is to propagate the labels in $\mathcal{Y}$ to the remaining unlabelled nodes based on how nodes are connected to each other. A label can indicate a list of interests (books, movies etc.) and the shared connections propagate these labels to the unlabelled nodes in the graph, predicting who shares similar interests. In a geographical application a node represents a region with an edge indicating neighbouring areas and a label is a POI, which an area is most likely to be associated with.

Consider geographical spatial POIs, $P = \{P_1, P_2, ..., P_M\}$, $m = 1, ..., M$ as a known set of M locations. The centre of each grid cell $v_n, n = 1, ..., N$ will represent the structural nodes in graph G_a. The grid size should be determined based on the specific geographical region of the study. Let $V_m = \{v_1, ..., v_M\}$ be the subset of the M labelled structural nodes which contains a POI and $V_u = \{v_{M+1}, ..., v_N\}$ be the subset of remaining $N - M$, initially unlabelled structural nodes, which doesn't contain a POI.

Let all attribute nodes contained in set V_a initially be unlabelled nodes. Then the

© University of Pretoria

UNIVERSITEIT VAN PRETORIA
UNIVERSITY OF PRETORIA
YUNIBESITHI YA PRETORIA

set of all unlabelled (both structural and attribute) nodes are contained in the ordered set V_u^* with $V_u^* = V_u \cup V_a = \{v_{M+1}, ..., v_N, v_{a_1}, ..., v_{a_T}\}$. Let V be ordered such that the first M rows are the cells from V_m and the remaining $N - M + T$ rows are the nodes from V_u^* such that $V = V_m \cup V_u^* = \{v_1, ..., v_M, v_{M+1}, ..., v_N, v_{a_1}, ..., v_{a_T}\}$.

Let $\mathcal{Y}$ be the full set of M possible labels and $\mathbf{Y}_m$ be an $M \times M$ indicator matrix, carrying the initial M multi-class labels indicating the POI associated with the corresponding node in set V_m. Similarly let $\mathbf{Y}_u^*$ be an $(N - M + T) \times M$ matrix indicating the POI associated with corresponding nodes in V_u^*. The initial label matrix, $\mathbf{Y}$, is an $(N + T) \times M$ matrix with the first M rows as $\mathbf{Y}_m$ and the remaining $N - M + T$ rows as $\mathbf{Y}_u^*$ or 0 (as the nodes in V_u^* are initially unlabelled).

Assume that all unlabelled nodes can reach a labelled node in a finite number of steps and will therefore have an associated label at the end of the iteration process, i.e. graph G is label connected [3]. A graph is considered non-label connected when some nodes remain unlabelled after the iteration process. This can occur when certain nodes are isolated, having no direct edges linking to the rest of graph G. In a social network, this can happen if there are individuals who do not share any common interests with the rest of the network. When considering geographical applications, a graph may be non-label connected when some grid cells are disconnected from the rest, separated by natural or man-made barriers such as rivers, mountains, or boundaries like regional or state borders.

Consider transition matrix $\mathbf{P}_a$ as defined in equation (3.1). Using a random walk approach with $\mathbf{P}_a^t$ the corresponding matrix at time t then $\mathbf{P}_a^{t\to\infty}$ indicates the steady-state distribution matrix at which all nodes are associated with label $c \in \mathcal{Y}$ as $t \to \infty$ as shown in [5]. In matrix form

$$\hat{\mathbf{Y}} = \mathbf{P}_a^{t\to\infty}\mathbf{Y} \tag{3.3}$$

where

$$\hat{\mathbf{Y}} = \begin{bmatrix} \hat{\mathbf{Y}}_m \\ \hat{\mathbf{Y}}_u^* \end{bmatrix} \text{ and } \mathbf{Y} = \begin{bmatrix} \mathbf{Y}_m \\ \mathbf{0} \end{bmatrix} \tag{3.4}$$

and $\hat{\mathbf{Y}}$ contains the output labels from the converged iteration process for all nodes in

© University of Pretoria

UNIVERSITEIT VAN PRETORIA
UNIVERSITY OF PRETORIA
YUNIBESITHI YA PRETORIA

set V.

Labelled nodes in set V_m are classified as absorbent states such that they exhibit probability 1 of staying in the same node and probability 0 of leaving the node. Therefore the labels of all nodes $v_n \in V_m$ do not change. Since the nodes are ordered in such a way that the first M rows in V are V_m and the last $N - M + T$ rows are V_u^*, the transition matrix can be split into 4 sub-matrices, indicating the probability to move between states, namely $\mathbf{P}_a = \begin{pmatrix} \mathbf{P}_{mm} & \mathbf{P}_{mu} \\ \mathbf{P}_{um} & \mathbf{P}_{uu} \end{pmatrix} = \begin{pmatrix} \mathbf{I} & \mathbf{0} \\ \mathbf{P}_{um} & \mathbf{P}_{uu} \end{pmatrix}$.

The probability of transition from the unlabelled states to the labelled states are captured in the $(N - M + T) \times M$ matrix $\mathbf{P}_{um}$ and from the unlabelled states to the unlabelled states are captured in the $(N - M + T) \times (N - M + T)$ matrix $\mathbf{P}_{uu}$. Since all labelled nodes are defined as absorbent states, the probability of staying in a labelled node is 1 and the probability of exiting a labelled node is 0. This simplifies $\mathbf{P}_{mm}$ to an $M \times M$ identity matrix $\mathbf{I}$, and $\mathbf{P}_{mu}$ to an $M \times (N - M + T)$ zero matrix $\mathbf{0}$.

Since the graph is label connected and there are M absorbent states, the limiting distribution of $\lim_{t\to\infty} \mathbf{P}_a^t$ is

$$\mathbf{P}_a^{t\to\infty} = \begin{pmatrix} \mathbf{I} & \mathbf{0} \\ (\mathbf{I} - \mathbf{P}_{uu})^{-1}\mathbf{P}_{um} & \mathbf{0} \end{pmatrix} \tag{3.5}$$

as shown in [5] and [3]. Substituting equations (3.5) and (3.4) into (3.3) the labels can be computed as

$$\begin{bmatrix} \hat{\mathbf{Y}}_m \\ \hat{\mathbf{Y}}_u^* \end{bmatrix} = \begin{pmatrix} \mathbf{I} & \mathbf{0} \\ (\mathbf{I} - \mathbf{P}_{uu})^{-1}\mathbf{P}_{um} & \mathbf{0} \end{pmatrix} \begin{bmatrix} \mathbf{Y}_m \\ \mathbf{0}. \end{bmatrix}. \tag{3.6}$$

From (3.6), the labels for the absorbent state nodes contained in V_m remains unchanged with $\hat{\mathbf{Y}}_m = \mathbf{Y}_m$. The labels of the unlabelled nodes are obtained by computing

$$\hat{\mathbf{Y}}_u^* = (\mathbf{I} - \mathbf{P}_{uu})^{-1}\mathbf{P}_{um}\mathbf{Y}_m. \tag{3.7}$$

The $(N - M + T) \times M$ matrix $\hat{\mathbf{Y}}_u^*$ will contain the probability of each label assigned to the nodes in V_u^* with the sum over each row adding to 1. The process will iterate over all nodes defined in G_a. The solution is only valid when $(\mathbf{I} - \mathbf{P}_{uu})^{-1}$ is non-singular which

© University of Pretoria

UNIVERSITEIT VAN PRETORIA
UNIVERSITY OF PRETORIA
YUNIBESITHI YA PRETORIA

will always be the case when the graph is label connected [5].

Consider the simple example illustrated in Figure 3.1 with added labelled nodes. In this example seven structural nodes, $V_u = \{v_1, v_3, v_4, v_5, v_6, v_8, v_9\}$, and two attribute nodes $V_a = \{v_{a_1}, v_{a_2}\}$ are unlabelled and contained in the set $V_u^* = V_u \cup V_a$. Two structural nodes, $V_m = \{v_2, v_7\}$, are labelled with associated POIs P_1 and P_2 respectively. Let V be the ordered set, contained in G_a, consisting of $N + T = 11$ nodes with the first $M = 2$ rows the labelled nodes and the remaining $N - M + T = 9$ rows the unlabelled nodes, i.e. $V = \{v_2, v_7, v_1, v_3, v_4, v_5, v_6, v_8, v_9, v_{a_1}, v_{a_2}\}$. Let $\mathbf{Y}_m$ be an indicator matrix with the first column representing label P_1 and the second column representing label P_2. Applying the methodology as described above, the probability of labels P_1 and P_2 to be assigned to nodes in set V is calculated in equation (3.8).

$$\hat{\mathbf{Y}} = \begin{bmatrix} \hat{\mathbf{Y}}_m \\ \hat{\mathbf{Y}}_u^* \end{bmatrix} = \begin{bmatrix} 1 & 0 & 0.59 & 0.79 & 0.48 & 0.67 & 0.69 & 0.49 & 0.62 & 0.68 & 0.30 \\ 0 & 1 & 0.41 & 0.21 & 0.52 & 0.33 & 0.31 & 0.51 & 0.38 & 0.32 & 0.70 \end{bmatrix}^T \tag{3.8}$$

From equation (3.8) it can be noted that all nodes in V_m remained in the initial node and label associated with it with probability 1. The nodes contained in set V_u^* however received a probability associated with labels P_1 and P_2. If ignoring the attribute nodes as done in [13], the probability for node v_1 to be associated with label P_1 is 0.72 and with P_2 is 0.28. In this example however, nodes v_1 and node v_7, which is the node associated with label P_2, share a similar attribute a_2 hence even if they are not as structurally close as v_1 and v_2, the node associated with label P_2, they now share a connected link through node v_{a_2}. This can also be observed in the increased probability for node v_1 to be associated with P_2 from 0.28 to 0.41.

The attribute nodes also carry a probability to be associated with labels P_1 and P_2. In a label propagation model, the labels are typically spread across the graph using the connections between structural nodes. When attribute nodes are added they act as additional connections related to the structural nodes. By associating a probability with each attribute node to a label, the model is indicating how likely that attribute is to be connected to a particular label through the structural nodes. This probability reflects the attribute's influence or relationship with the label, as mediated by its connections to the structural nodes. Attribute node v_{a_2} carry a higher probability to be associated with

© University of Pretoria

UNIVERSITEIT VAN PRETORIA
UNIVERSITY OF PRETORIA
YUNIBESITHI YA PRETORIA

label P_2 than with P_1 since the nodes which are associated with attribute a_2 are closer in connectivity to node v_7, which is associated with label P_2 and similar for attribute node v_{a_1} to label P_1.

3.2.3 Seasonal Catchment Areas

Assuming that G is a labelled connected graph, each node receives a set of probabilities corresponding to each label in the set $\mathcal{Y}$. As discussed in [13], the proposed fuzzy lattice data structure enables the identification of realistic catchment areas by applying drive-time thresholds to the structural nodes. This approach involves overlaying polygons representing POIs and ensuring that only nodes which fall within the drive-time polygons are considered when assigning probabilities of association with a POI.

Consider the set of POIs, $P = \{P_1, P_2, ..., P_M\}$, $m = 1, ..., M$, with an associated drive-time threshold distance d^{P_m} assigned to each $P_m, m = 1, ..., M$. The threshold drive-time distance d^{P_m} depends on the order of the POIs and will be denoted by $d^{P_m}_{low}, d^{P_m}_{mid}$ or $d^{P_m}_{high}$ for low-, middle- or high-order POIs respectively as discussed in [23]. The highest drive-time threshold considered is at 15-minutes based on the fifteen-minute city concept [38]. For each POI, we identify all structural nodes $v_n \in V$ which are within a threshold drive-time distance d^{P_m} of P_m.

Let G_{P_m} define the region such that $G_{P_m} = \bigcup_n v_n \ni d_{v_n,P_m} \leq d^{P_m}, G_{P_m} \subseteq G$ with d_{v_n,P_m} the drive-time distance between the nearest network point of structural nodes $v_n \in V$ and P_m. Let $O_{v_n} = \{m : v_n \in G_{P_m}\}$ define the indices of POI, P_m, that is snapped to the same network as $v_n \in V$. Nodes that are contained in more than one G_{P_m} have an overlap of accessibility to different POIs. There can however exist nodes which are not contained in any set of G_{P_m} resulting in spatially disjoint areas.

Since catchment areas can only be applied to structural nodes, $v_n \in V$, only the first $N - M$ rows in $\hat{\mathbf{Y}}^*_u$, i.e. $\hat{\mathbf{Y}}_u = \{\hat{\mathbf{Y}}^*_u[i, :] \mid 1 \leq i \leq N - M\}$ are used in the drive-time threshold calculations. Let all structural nodes which fall beyond the threshold drive-time distance d^{P_m} for each P_m be nullified in $\hat{\mathbf{Y}}_u$ i.e. the probability for a node to be assigned to a label which falls beyond the drive-time threshold is 0. If a region falls beyond the drive-time threshold for all POIs, the region is spatially inaccessible (disjoint) and will be assigned a probability of 0 for all labels $c \in \mathcal{Y}$. The matrix $\hat{\mathbf{Y}}_u$ is

© University of Pretoria

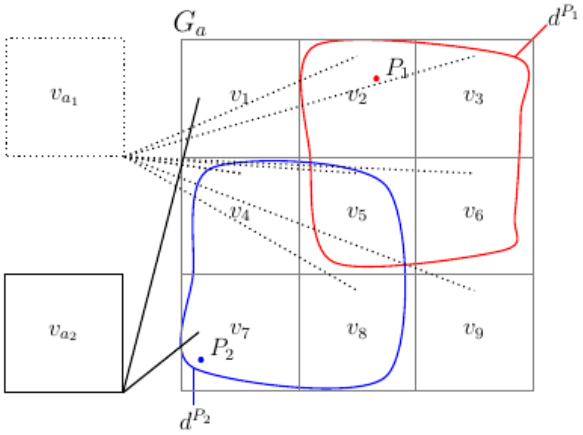

Figure 3.2: Graph G_a with structural nodes $v_1, ...v_9$ and attribute nodes v_{a_1} and v_{a_2}. POIs P_1 and P_2 and corresponding drive-time thresholds d^{P_1} and d^{P_2}.

row standardised to ensure that all rows adds up to 1.

Consider the example provided in Figure 3.2 with drive-time thresholds for POIs, P_1 and P_2. Suppose the values for d^{P_1} and d^{P_2} are such that $G_{P_1} = \{v_2, v_3, v_5, v_6\}$, $G_{P_2} = \{v_4, v_5, v_7, v_8\}$, $V_m = \{v_2, v_7\}$ and regions v_1 and v_9 are spatially disjoint. Let all structural nodes which fall beyond drive-time threshold d^{P_1} for catchment area of P_1 carry a 0 probability to be assigned to label P_1 and similarly P_2. After the matrix $\hat{\mathbf{Y}}_u$ has been row standardised, the results from equation (3.8) with drive-time thresholds applied are,

$$\hat{\mathbf{Y}}_u = \begin{bmatrix} 0 & 1 & 0 & 0.67 & 1 & 0 & 0 \\ 0 & 0 & 1 & 0.33 & 0 & 1 & 0 \end{bmatrix}^T . \tag{3.9}$$

It can be noted that after standardisation that each node is only associated with the POI falling within the same network. Node v_5 has an overlap of drive-time thresholds d^{P_1} and d^{P_2} and hence retains the probability of being assigned both label P_1 and P_2. Nodes v_1 and v_9 falls beyond the drive-time thresholds for all POIs and are therefore spatially disjoint with probability 0 to be assigned to label $c \in \mathcal{Y}$.

© University of Pretoria

UNIVERSITEIT VAN PRETORIA
UNIVERSITY OF PRETORIA
YUNIBESITHI YA PRETORIA

3.2.4 Measures of Spatial Accessibility

In this section, we apply supply-demand ratios and accessibility measures to demonstrate the distribution of resources when using attribute based fuzzy lattice data. Supply may refer to a provider's capacity, such as the number of available hospital beds [7], the quantity of providers like primary care physicians in a given region [50, 31], or the resources offered by a provider, such as a doctor's available services or stock availability at a store, as in [42]. Demand typically represents the population and communities in need of the specified services or products.

Let all POIs, $P_m \in P$ have supply size (capacity) of $S(P_m)$ and all nodes $v_n \in V$ have an associated demand (population size) of $D(v_n)$ as formulated in [7]. Then the supply-demand ratio for supplier m in region G_{P_m} can be expressed by

$$R_{P_m} = \frac{S(P_m)}{D(G_{P_m})}, \tag{3.10}$$

and the accessibility for all structural nodes $v_n \in V$ is

$$A_{v_n} = \sum_{m \in O_{v_n}} R_{P_m} = \sum_{m \in O_{v_n}} \frac{S(P_m)}{D(G_{P_m})}, \tag{3.11}$$

as illustrated by [50, 31].

Consider the example provided in Figure 3.2 with $N = 9$ grids and POIs, P_1 and P_2. Suppose the demand for all regions are 1 i.e., $D(v_n) = 1, n = 1, ..., 9$ and supply for all suppliers are 4, $S(P_m) = 4, m = 1, 2$. Suppose the values for d^{P_1} and d^{P_2} are such that $G_{P_1} = \{v_2, v_3, v_5, v_6\}$, $G_{P_2} = \{v_4, v_5, v_7, v_8\}$, $V_m = \{v_2, v_7\}$ and regions v_1 and v_9 are spatially disjoint. Using attribute based fuzzy lattice catchment areas to determine accessibility and supply-demand ratio using a probabilistic approach, the demand on catchment area level will change according to the weight assigned by $\hat{\mathbf{Y}}_u$. Let the demand be proportionally assigned to each supplier's catchment area using the probabilities in equation (3.9). Then $D(G_{P_1}) = 3.67$ and $D(G_{P_2}) = 3.33$ which results in the supply-demand ratio for P_1 to change to $R_{P_1} = \frac{S(P_1)}{D(G_{P_1})} = 1.09$ and P_2 to $R_{P_2} = \frac{S(P_2)}{D(G_{P_2})} = 1.2$. Since region v_5 still has access to both P_1 and P_2 the accessibility of v_5 is $A_{v_5} = R_{P_1} + R_{P_2} = 2.288$.

© University of Pretoria

UNIVERSITEIT VAN PRETORIA
UNIVERSITY OF PRETORIA
YUNIBESITHI YA PRETORIA

Comparing this to the same example in [13], the demand in region G_{P_1} has increased which in turn has decreased the supply-demand ratio for P_1. The only overlapping node v_5 has a higher probability to be associated with label P_1 because of the shared attribute node v_{a_1} with structural nodes $v_2, v_3, v_4, v_5, v_6, v_8$ and v_9. The accessibility for node v_5 remains unchanged whether fuzzy lattice catchment areas or attribute based fuzzy lattice catchment areas are used because even though the demand is proportionally different, the sum over supply-demand ratios remains the same. The decreased supply-demand ratio for P_1 indicates that supplier P_1 is under greater pressure to provide the same level of supply while facing increased demand. The attribute based fuzzy lattice data offers the added advantage of incorporating factors that influence both demand and supply, rather than relying solely on the proximity of a community to a POI. This allows for a more comprehensive analysis, accounting for attributes beyond just geographical distance. This will be illustrated with an example in the next section by not only considering the link structure but also underlying attributes such as ease of accessibility and seasonal characteristics.

3.3 Application

To test the proposed methodology on real-world applications, the population size and sales of one of South-Africa's leading pharmaceutical chains (with close to 880 stores located in South Africa) was considered. The supply allocated to each of the stores is determined by sales and demand by population size at an EA[1] level.

Let region G be the district municipality City of Cape Town[2] located in the Western Cape province in South Africa. Region G is subdivided into 592 square grids of size 2km $\times$ 2km, which is the optimal grid size to ensure adequate variation in landscape features and changes across the nodes.

[1] An enumerations area (EA) is the smallest geographical unit (piece of land) into which the country is divided for enumeration purposes. Enumeration areas contain between 100 to 250 households. Source: Stats SA.

[2] District municipalities consists of multiple local municipalities. They are administrative divisions which is accountable for providing basic services within the area. Source: Education and Training Unit (ETU), www.etu.org.za (accessed February 15, 2024)

© University of Pretoria

UNIVERSITEIT VAN PRETORIA
UNIVERSITY OF PRETORIA
YUNIBESITHI YA PRETORIA

In addition to the link structure, a set of geographical attributes assigned to all nodes in G will be considered. Seasonal attributes such as extreme temperature and rainfall patterns are considered since gastrointestinal illnesses increase at higher temperatures or rainfall shortages as highlighted by the Department of Health South Africa[3]. Research from [34] also indicates that high temperatures can promote the growth of bacteria, viruses, and parasites in food and water which increases the risk of waterborne diseases like diarrhoea.

Daily minimum and maximum temperature as well as rainfall for 86 weather stations in Western Cape was provided by SAWS[4]. The average rainfall, minimum and maximum temperatures from 2016 to 2019 for the four different seasons were calculated. In the grids which have no overlap with a SAWS weather station, ordinary Kriging was used to estimate the average rainfall, minimum and maximum temperatures for the different seasons.

The seasonal relationship between total seasonal sales and weather variables was tested using a simple linear regression, with average seasonal sales (from 2016 to 2019) as the dependent variable and average maximum temperature, average minimum temperature, and average rainfall (all averaged from 2016 to 2019) as the independent variables. These variables were captured in 2km $\times$ 2km grids for which sales and weather data was available, which was 46 distinct areas in the City of Cape Town. The results indicate that the average minimum temperature has the most significant positive effect on average sales ($p = 0.0295$) and average maximum temperature somewhat of an effect ($p = 0.0791$) which aligns with findings from [34]. However, rainfall does not appear to significantly influence sales ($p = 0.9453$). It should be noted that Cape Town experienced a water crises from 2017-2019 and 574 of the 592 nodes indicated rainfall at the 10th percentile or lower. Hence very low rainfall measures were captured over majority of Cape Town. The multiple R-squared value of 0.1628 suggests that only about 16.3% of the variability in sales can be explained by the model, indicating other factors may play a role. For the continuation of this research we will only be using temperature and

[3] Department of Health South Africa, *NATIONAL HEAT HEALTH ACTION GUIDELINES: Guide to extreme heat planning in South Africa for the human health sector*, https://www.health.gov.za/ (accessed August 20, 2024)

[4] South African Weather Services, https://www.weathersa.co.za/

© University of Pretoria

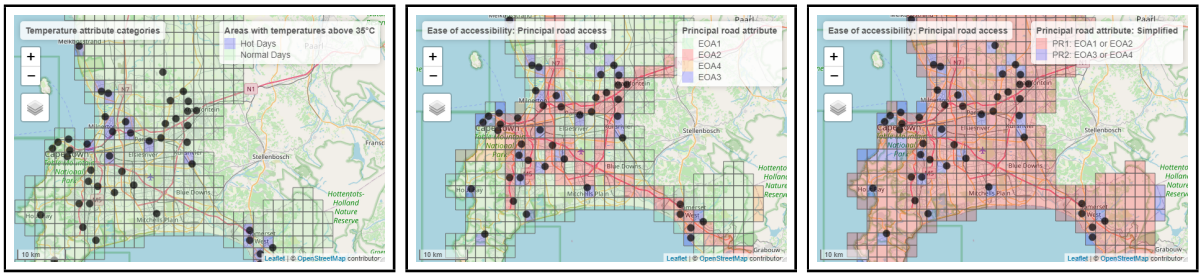

Figure 3.3: Temperature attribute indicating "hot days" and ease of access and accessibility to principal roads. Map data © OpenStreetMap contributors, under the Open Database License (ODbL).

ease of access as attributes.

Let the attribute temperature have two levels namely "hot days" and "normal days". All structural nodes in G will be associated with either one of these two levels. The first, "hot days," will include all structural nodes, overlapping with at least one POI and experiences maximum temperatures above 35°C in summer. The structural nodes associated with "hot days" correspond with the same areas identified by Heat Watch Cape Town[5]. All other remaining structural nodes are assigned to "normal days," reflecting the tendency to select areas that are less impacted by extreme weather as illustrated in Figure 3.3. This also accounts for potential shortages of essential medicines for gastrointestinal illnesses in heat-affected regions. In addition to temperature, ease of access to a POI will be considered as an attribute. Each structural node will have an indication on whether it has easy access to a principal road or not. A principal road can be either a major road, such as a highway, or a main road, typically serving as a key route for local traffic within a town or city[6]. This designation signifies whether the node is connected to key transportation routes that facilitate faster and more direct travel between nodes. The principal road attribute will have four levels that each structural node can be associated with. The first level, "EOA1", indicates that the structural node has demand but no easy access to a principal road. The second level, "EOA2", indicates

[5] StoryMap by CAPA Strategies, *Heat Watch Cape Town: Community Heat Mapping in Cape Town, South Africa*, https://storymaps.arcgis.com/stories/35fd2bf7e70c448ab0a58245d2f2cd0b (accessed August 20, 2024)

[6] Department of Health South Africa, *TRH 26: South African Road Classification and Access Management Manual*, https://wayleave.tshwane.gov.za/ (accessed August 15, 2024)

© University of Pretoria

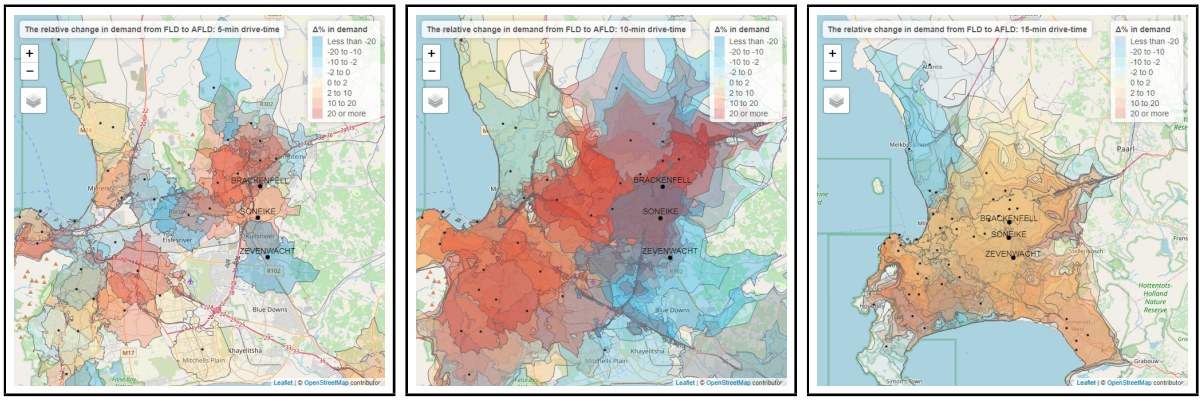

Figure 3.4: The relative change in demand from FLD to AFLD for 5, 10, and 15-minute drive-time thresholds. Map data © OpenStreetMap contributors, under the Open Database License (ODbL).

that a structural node has easy access to a principal road. The third level, "EOA3", is associated with structural nodes that are overlapping with a POI, but not within easy access of a principal road, and level four, "EOA4", includes all other structural nodes not within easy access to principal roads. Given the assumption that people will prefer POIs that are easily accessible, the nodes associated with "EOA1" and "EOA2" should share a connection through the same attribute. For this reason, the principal road attribute will be simplified into two levels: "PR1", which includes all nodes from levels "EOA1" and "EOA2," and "PR2", which includes all nodes from levels "EOA3" and "EOA4", as illustrated in Figure 3.3.

The demand allocated to each grid, $D(v_n)$, is the population size which is obtained from the overlaying census and deeds office data as captured by Lightstone Pty Ltd[7] from 2016 to 2019. The supply capacity at each node is the total sales over summer (December, January and February) of an affordable over-the-counter diarrhoea medication, averaged over 2016 to 2019.

The accessibility and supply-demand ratio will be computed using both an attribute based fuzzy lattice data structure and a fuzzy lattice data structure to compare how the probabilities assigned to each POI differs when ease of access and temperature are

[7] Lightstone (Pty) Ltd procures its data directly from the Deeds office and is comprised of a snapshot of all South Africa property ownership as at 1993, with a full history of all transactions to augment with census data. Ethics clearance number: NAS003/2023.

© University of Pretoria

UNIVERSITEIT VAN PRETORIA
UNIVERSITY OF PRETORIA
YUNIBESITHI YA PRETORIA

Table 3.1: Supply, demand and supply-demand ratios for Zevenwacht (P_1), Soneike (P_2) and Brackenfell (P_3) at 5, 10 and 15 minutes drive-time thresholds using a fuzzy lattice data (FLD) and attribute based fuzzy lattice data (AFLD) structure .

		FLD		AFLD	
$S(P)$	Drive-time	Demand	SD-Ratio	Demand	SD-Ratio
$S(P_1) = 1,252$	5min	93,638	0.013	93,638	0.013
	10min	252,558	0.005	211,542	0.006
	15min	225,203	0.006	118,533	0.011
$S(P_2) = 1,654$	5min	57,993	0.029	57,238	0.029
	10min	69,743	0.024	81,338	0.020
	15min	86,922	0.019	108,908	0.015
$S(P_3) = 674$	5min	30,950	0.022	31,253	0.022
	10min	45,415	0.015	64,683	0.010
	15min	45,468	0.015	79,372	0.009

taken into account. The supply considered here includes only one pharmaceutical chain in South Africa, which is not an exhaustive list of all suppliers providing diarrhea medication. As a result, the supply-demand ratio values are very small due to the under representation of supply. Therefore, when comparing the 5, 10, and 15-minute drive-time thresholds visually, the differences in demand are mapped to illustrate how demand changes when using the fuzzy lattice data structure (FLD) compared to the attribute based fuzzy lattice data structure (AFLD). Figure 3.4 shows the proportionate difference between demand using AFLD and demand using FLD, relative to the demand using FLD, indicating how much demand has increased or decreased as a percentage when using AFLD instead of FLD.

Areas with easy access to principal roads and normal temperature fluctuations tend to see an increase in demand, while areas farther from main routes and experiencing temperatures above 35°C typically experience a decrease in demand. Note that in this example, both attributes were given equal weights, though these weights can be adjusted to reflect differing levels of importance.

When comparing Brackenfell, Soneike, and Zevenwacht (indicated with labels in Figure 3.4), as done in Table 3.1, it's important to note their proximity and how their

© University of Pretoria

UNIVERSITEIT VAN PRETORIA
UNIVERSITY OF PRETORIA
YUNIBESITHI YA PRETORIA

5-minute drive-time catchment areas overlap slightly, becoming fully overlapping at the 15-minute drive-time threshold catchment areas. Brackenfell benefits from easy access to a principal road, an attribute that Soneike and Zevenwacht lack. Additionally, Zevenwacht is associated with the "hot days" category in the temperature attributes. As a result, Brackenfell holds a stronger connection with the surrounding population due to its shared attributes while Zevenwacht has attributes that aren't shared by the surrounding population and demand will be allocated only on the link structure.

When examining Zevenwacht's demand across different drive-time thresholds, we see that as we move from fuzzy lattice data to attribute based fuzzy lattice data, demand decreases significantly with increased drive-time, which causes the supply-demand ratio to rise. Soneike, although not linked to a principal road, still experiences a demand increase because it shares the temperature attribute, absorbing some of the demand that would have shifted to Zevenwacht.

The greatest increase in demand, however, occurs in Brackenfell. Demand nearly doubles when using the AFLD, driven by the two shared attributes: normal temperature and ease of access. As Brackenfell's population grows, the supply-demand ratio decreases, indicating that the store will need to adjust its supply to meet the increased demand.

The comparison between the attribute based fuzzy lattice data structure (AFLD) and the fuzzy lattice data structure (FLD) highlights the impact of incorporating attribute nodes on demand allocation. This helps to capture more realistic demand allocation to areas based on additional factors other than the link structure. Adjusting the weights of these attributes can further refine the calculation of accessibility and supply-demand ratios, allowing for more accurate predictions to varying conditions and priorities.

3.4 Discussion

The benefits of an attribute based fuzzy lattice data structure is evident in its ability to propagate labels more effectively within a network. By combining both structural connections and attribute similarities, nodes can share a connection through a similar attribute node. Traditional methods typically rely on link structures, but many real-world networks contain shared attributes between nodes that are not captured by structural

© University of Pretoria

UNIVERSITEIT VAN PRETORIA
UNIVERSITY OF PRETORIA
YUNIBESITHI YA PRETORIA

connectivity alone. This approach leverages both aspects, enabling labels to propagate based on structural connections and shared characteristics such as common interests, similar topography etc.

In this application, edge weights were equally assigned across different attributes and structural edges, it can however be adjusted. If there are natural or man-made barriers, structural weights can be reduced or even set to zero. Similarly, if certain attributes hold varying levels of importance, weights can be adjusted accordingly to ensure that these attributes are prioritised.

Only temperature and ease of access were considered as factors influencing the sales of diarrhoea medication. The low R-squared value when testing sales against temperature suggests that other factors, which were not investigated, likely play a significant role in these sales. Factors such as socioeconomic conditions, economic considerations, marketing strategies etc. could also be pivotal. Additionally, the model only accounted for the supply of one easily accessible over-the-counter diarrhoea medication from one pharmaceutical chain store in South Africa. As multiple other pharmacies and medications are available, the supply figures indicated per region are likely an underestimate.

3.5 Conclusion

Traditional community detection methods focus primarily on a network's topology, but integrating attribute information can enhance these methods by improving the understanding of node similarities and capturing relationships that go beyond structural connectivity. Incorporating attributes into the fuzzy lattice data structure allows for a more accurate estimate of demand distribution. In networks where nodes share common attributes, such as similar accessibility or environmental conditions, the attribute based fuzzy lattice data structure can propagate labels across the network more accurately. This approach overcomes limitations of purely structural connectivity by accounting for both the link structure and attributes, resulting in a more detailed and accurate depiction of the network's interactions. The attribute based fuzzy lattice data structure offers significant advantages for modelling and analysing networks. By considering both attribute and structural links, attribute based fuzzy lattice data provides a balance between

© University of Pretoria

UNIVERSITEIT VAN PRETORIA
UNIVERSITY OF PRETORIA
YUNIBESITHI YA PRETORIA

proximity and shared attributes.

© University of Pretoria

Chapter 4

Attribute based spatial segmentation

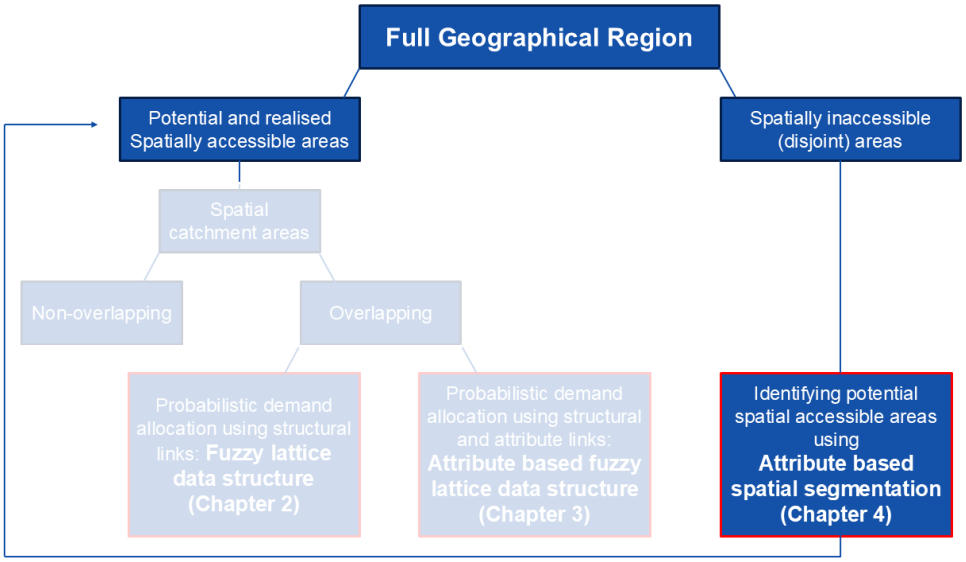

This chapter focuses on attribute based spatial segmentation to create tailored macro-regions aligned with local characteristics and needs. By incorporating geographic and contextual attributes, this approach optimises resource allocation and service planning.

© University of Pretoria

UNIVERSITEIT VAN PRETORIA
UNIVERSITY OF PRETORIA
YUNIBESITHI YA PRETORIA

Abstract

Effective spatial planning and resource optimisation require precise demarcation of potential spatial accessible areas and optimal placement of points of interest (POIs). Our approach introduces a novel attribute based spatial segmentation methodology that utilises an iterative clustering approach to create unique macro-regions, each associated with key structural and attribute specific properties. By integrating a probabilistic attribute based structure with k-means clustering, we adaptively segment spatial regions to balance area based attributes and topological characteristics. The full geographical network is segmented into attribute based macro-regions for all spatially accessible and spatially disjoint regions. Attribute based spatial segmentation offers insights into why certain areas may be spatially disjoint and if it is identified as potential spatially accessible areas to determine which POIs can be placed to maximise accessibility. This approach transforms city planning and resource allocation by aligning POI placement with regional needs and characteristics.

4.1 Introduction

When considering spatial planning and resource optimisation, determining accurate service catchment areas and POI placement is crucial for city planning. As discussed in [32], ideal catchment areas should balance both supply and demand, account for geography and physical barriers to access, and differentiate by service type and capacity. Additionally, they should be adaptable to seasonal changes, ensuring service delivery aligns with local needs and infrastructure limitations, particularly in low-resource settings.

In [13], a fuzzy lattice data structure was introduced to identify catchment areas based on spatial proximity and probabilistic membership. This methodology was expanded to consider not only spatial proximity but also key attributes, such as topography and environmental factors, to create seasonal catchment areas [14]. Both approaches primarily focused on spatially accessible regions by assessing the accessibility of surrounding areas from existing POIs. In contrast, this work reverses the perspective by utilising the transition probabilities from an attribute augmented graph structure [14] to identify where new POIs should ideally be placed by creating attribute based spatial

© University of Pretoria

UNIVERSITEIT VAN PRETORIA
UNIVERSITY OF PRETORIA
YUNIBESITHI YA PRETORIA

segments which will assist in addressing gaps in service coverage and planning for future needs.

Attribute based spatial segmentation creates macro-regions, each characterised by a unique structural layout and attribute properties, including social factors, topographical features or environmental characteristics. For regions that are spatially disjoint, where communities lack access to a specific POI among a set of POIs providing a particular product or service [50], these attribute segments offer a framework for identifying potential spatial areas. Effective clustering methodologies are key to defining these macro-regions, which are associated with distinct attribute segments. Traditional clustering techniques often rely on either shared edges or attribute-based properties but rarely integrate both in a unified geographical framework.

In this work, clustering plays a vital role in grouping regions based on shared characteristics or proximity, enabling planners to delineate coherent regions for efficient service distribution. We leverage an iterative clustering process applied to a transition probability matrix derived from an attribute-augmented graph to create attribute based spatial segments. These segments reflect both structural connectivity and attribute similarity, ensuring the formation of spatially coherent macro-regions. When incorporated into a spatial autoregressive (SAR) model, attribute based spatial segmentation can model supply, identify regions with the greatest need or potential benefit from new POIs and transform potential spatial regions into realised spatial areas. This comprehensive methodology bridges the gap between spatial accessibility needs and facility planning, aligning potential POI locations with regional attributes and improving resource distribution.

The remainder of this paper is structured as follows. First, we review the historical developments in graph clustering and its application to spatial planning. This is followed by a detailed discussion of the transition probability matrix derived from an attribute-augmented graph, which forms the foundation for initial clustering. We then describe the iterative clustering process used to optimise and produce spatially coherent macro-regions. Following this, the attribute based spatial segmentation methodology is applied to a real-world case study, predicting average POI sales and identifying ideal POI placements. Finally, we examine regions that remain spatially disjoint and discuss the implications of this approach for improving resource allocation and accessibility.

© University of Pretoria

UNIVERSITEIT VAN PRETORIA
UNIVERSITY OF PRETORIA
YUNIBESITHI YA PRETORIA

4.2 Literature review

Clustering on networks has been extensively explored as a means to reveal underlying structures, identify communities, and optimise connectivity within complex systems. Approaches such as modularity maximisation [15], spectral clustering [35], and graph partitioning algorithms [37] have been instrumental in detecting cohesive subgroups within various networks.

Spectral clustering [35] has gained significant attention for its ability to partition graphs by leveraging eigenvectors of the graph Laplacian. It identifies clusters based on the similarity between data points in a transformed spectral space. However, spectral clustering often relies on the assumption of linear separability in the spectral space, which can limit its effectiveness in complex or highly non-linear network structures. Additionally, its reliance on global eigenvector calculations introduces computational inefficiencies for large-scale networks [49], making it less suitable for applications with extensive geographic or contextual variability.

SimRank [25] introduced a similarity measure for graph nodes based on their structural context, where two objects are considered similar if they are related to similar objects. This approach relies on iterative computation of similarity scores using a graph theoretic model. Graph mincuts [6], a graph based semi-supervised learning technique, uses min-cut optimisation to classify data by exploiting both labelled and unlabelled data, partitioning the graph into regions that minimise cut costs while respecting label constraints. Another approach, the k-means clustering enhancement through a feature weight self-adjustment (FWSA) mechanism [47], adaptively assigns weights to features to improve clustering quality by minimising intra-cluster separations and maximising inter-cluster separations. These methods optimise how nodes are grouped by only considering either structural, attribute or feature-based similarities to achieve improved clustering or segmentation outcomes.

A method that balances both structural and attribute-based similarities is the SA-Cluster (structural and attribute) algorithm [53]. This approach uses a unified distance measure and incorporates a neighbourhood random walk model to generate cohesive clusters with homogeneous attributes and dense connectivity. However, the random walk parameters must be carefully specified, as they directly influence the extent and

© University of Pretoria

UNIVERSITEIT VAN PRETORIA
UNIVERSITY OF PRETORIA
YUNIBESITHI YA PRETORIA

localisation of connectivity exploration within the network. In geographic contexts, determining appropriate parameter values can be particularly challenging due to the inherent complexity and variability of spatial regions, necessitating careful tuning to ensure meaningful clustering results.

While the methods discussed above primarily focus on network graph structures, they lack direct applicability to geographic contexts. To address this gap, we propose a novel attribute based spatial segmentation methodology that integrates structural and attribute-based similarities to cluster geographic nodes into spatially coherent regions. This is done by applying an iterative clustering process directly to the transition probability structure derived from an attribute augmented graph, as detailed in [14]. By doing so, it eliminates the reliance on computationally intensive spectral transformations, offering a more efficient and adaptable solution. This approach balances structural connectivity and attribute-based similarities, enabling the formation of spatially coherent areas that reflect diverse regional characteristics. Furthermore, the methodology is highly scalable, requiring only a single parameter, the number of clusters, allowing for practical implementation without the complexity of extensive parameter tuning.

Our approach is particularly impactful in grouping the full geographical region into attribute based spatial segments, encompassing both spatially accessible and spatially disjoint regions. By identifying areas lacking POIs within an accessible drive-time threshold, our method highlights geographic barriers or limited accessibility, categorising such regions as spatially disjoint. This segmentation not only identifies regions that could benefit from new POIs but also explains why certain areas remain inaccessible. The proposed methodology transforms otherwise inaccessible regions into potential service catchment areas, providing a powerful tool for improving resource allocation, accessibility planning and service delivery across urban and rural contexts.

4.3 Methodology

In this section, the methodology of attribute based spatial segments will be discussed, beginning with the creation of the transition probability matrix, $\mathbf{P}_a$, derived from an attribute-augmented graph structure, as illustrated with a small toy example in Section

© University of Pretoria

UNIVERSITEIT VAN PRETORIA
UNIVERSITY OF PRETORIA
YUNIBESITHI YA PRETORIA

4.3.1. Following this, the initial clustering on $\mathbf{P}_a$ will be explored to obtain preliminary cluster memberships and macro-regions, as described in Section 4.3.2. Based on the results from Section 4.3.2, it is evident that the macro-regions in the toy example can be further refined. This leads to the exploration of spatially optimal cluster memberships and attribute based segmentation in Section 4.3.3.

4.3.1 Transition probability matrix of an attribute augmented graph

Let $G = G(V, E)$ be a network graph, where V represents the set of nodes and E the edges connecting them [5]. In this context, nodes typically correspond to entities such as individuals within a social network, while edges depict relationships like friendships or interactions. In this study, we focus specifically on spatial graphs, where nodes correspond to geographical locations.

The graph's structural connectivity, referred to as its link structure, describes how nodes are interconnected via edges, which can be quantified using transition probabilities. Beyond this structural framework, graphs can be enriched by incorporating attributes, denoted as Λ, that capture additional properties of the nodes V. In an augmented graph G_a, these attributes are represented by attribute nodes, distinct from the structural nodes that embody the graph's spatial layout and link structure. Attribute nodes create connections between structural nodes based on shared characteristics, forming an integrated representation [53].

To incorporate attribute nodes into the node connectivity, we define an attribute-augmented graph as $G_a = (V \cup V_a, E \cup E_a, \mathbf{W}_a^*)$, following the definition in [53]. Here, V represents the structural nodes, V_a denotes the attribute nodes, E refers to the structural edges, E_a indicates the attribute edges and $\mathbf{W}_a^*$ the structural and attribute weights with $\mathbf{W}_a^* = \begin{pmatrix} \mathbf{W}_s & 0 \\ 0 & \mathbf{W}_a \end{pmatrix}$ where $\mathbf{W}_s$ is an $N \times N$ matrix of structural edge weights and $\mathbf{W}_a$ is an $T \times T$ diagonal matrix for the attribute edge weights.

Consider the structural nodes $V = \{v_1, \ldots, v_N\}$, which represent the full geographical region that is subdivided into N grid cells, with the centres of these cells serving as the node representative locations. A structured edge $(v_i, v_j) \in E$ exists if and only if node

© University of Pretoria

UNIVERSITEIT VAN PRETORIA
UNIVERSITY OF PRETORIA
YUNIBESITHI YA PRETORIA

$v_i \in V$ shares a boundary point with node $v_j \in V$ for $i \neq j$ in the geographical area, as defined by queen's contiguity [50]. Each node in V is associated with a set of attributes $\Lambda = \{\lambda_1, \ldots, \lambda_{\mathcal{A}}\}$. If each attribute $\lambda_i \in \Lambda$ has z_i levels, where $i \in \{1, \ldots, \mathcal{A}\}$, then let $A = \{a_1, \ldots, a_T\}$ represent the T-dimensional set of indicator attributes associated with each level of $\lambda_i \in \Lambda$, where $T = \sum_{i=1}^{\mathcal{A}} z_i$. The indicator attribute information for each structural node v_i is represented as a T-dimensional binary vector $\mathbf{b}_i$ such that attribute matrix $\mathbf{B}$ is structured as

$$\mathbf{B} = \begin{pmatrix} \mathbf{b}_1 \\ \mathbf{b}_2 \\ \vdots \\ \mathbf{b}_N \end{pmatrix} = \begin{pmatrix} a_1(v_1) & a_2(v_1) & \ldots & a_T(v_1) \\ a_1(v_2) & a_2(v_2) & \ldots & a_T(v_2) \\ \vdots & \vdots & \ddots & \vdots \\ a_1(v_N) & a_2(v_N) & \ldots & a_T(v_N) \end{pmatrix} \tag{4.1}$$

where $a_j(v_i) = 1$ signifies the presence of an attribute edge in E_a if node v_i is associated with indicator attribute a_j otherwise, $a_j(v_i) = 0$ [29]. Let $V_a = \{v_{a_1}, \ldots, v_{a_T}\}$ be the set of indicator attribute nodes resulting in the combined node set $V \cup V_a$ to be of size $N + T$.

In an attribute-augmented graph structure, transitions between nodes can occur either through structural edges (connecting structural nodes) or attribute edges (linking nodes to their associated attributes). The transition probability matrix $\mathbf{P}_a$ for G_a is an $(N + T) \times (N + T)$ matrix

$$\mathbf{P}_a = \begin{pmatrix} \mathbf{P}_s & \mathbf{P}_{sa} \\ \mathbf{P}_{as} & \mathbf{0} \end{pmatrix} \tag{4.2}$$

where $\mathbf{P}_s$ is an $N \times N$ submatrix representing transition probabilities between structural nodes, $\mathbf{P}_{sa}$ an $N \times T$ submatrix representing the transition probabilities from structural to attribute nodes, $\mathbf{P}_{as}$ is a $T \times N$ submatrix for transitions from attribute to structural nodes and the transition probability matrix between two attributes nodes is captured in the $T \times T$, $\mathbf{0}$ submatrix since there is no shared edges between two attribute nodes [14].

Consider Figure 4.1, which illustrates a simple example with structural nodes $V = \{v_1, ..., v_{20}\}$. Each structural node corresponds to a geographical grid, with attributes captured in Λ. In this case, the structural nodes are associated with two attributes,

© University of Pretoria

UNIVERSITEIT VAN PRETORIA
UNIVERSITY OF PRETORIA
YUNIBESITHI YA PRETORIA

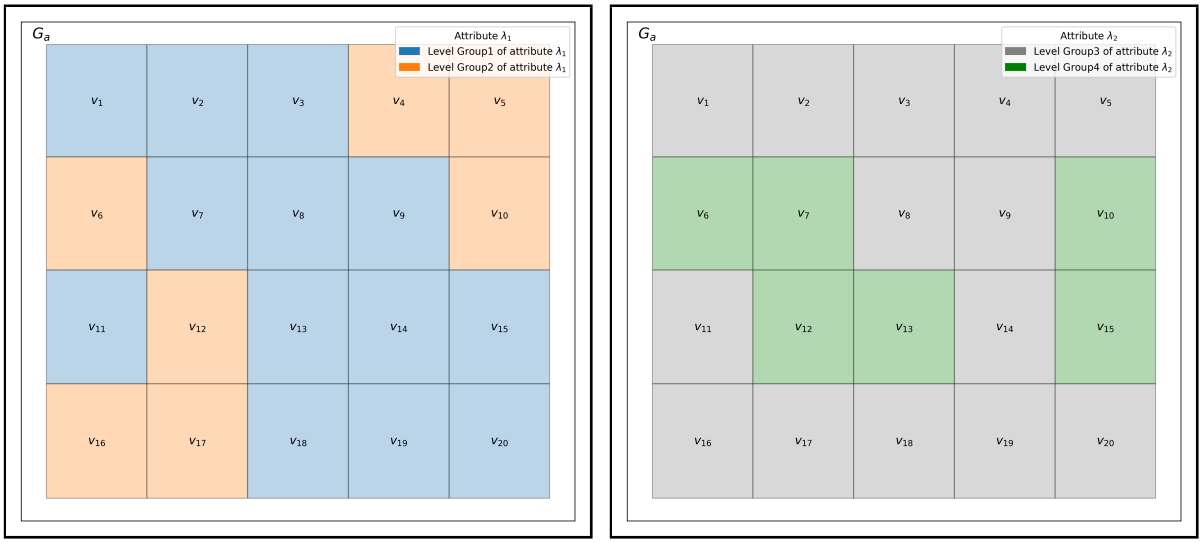

Figure 4.1: Graph G_a with structural nodes $v_1, ..., v_{20}$, associated with attributes λ_1 and λ_2

λ_1 and λ_2, comprising two levels each. Attribute λ_1 consists of levels "Group1" and "Group2" and attribute λ_2 of levels "Group3" and "Group4" such that $\mathcal{A} = 2$, $z_1 = 2$, $z_2 = 2$, $N = 20$ and $T = 4$. Let $a_1(v_i) = 1$ signify that structural node v_i is associated to "Group1" and $a_1(v_i) = 0$ otherwise, similarly for "Group2" to a_2, "Group3" to a_3 and "Group4" to a_4. For attribute λ_1, nodes $v_4, v_5, v_6, v_{10}, v_{12}, v_{16}$, and v_{17} are associated with level "Group2", while the remaining nodes are linked to level "Group1". When considering attribute λ_2, nodes $v_6, v_7, v_{10}, v_{12}, v_{13}$, and v_{15} are associated with level "Group4", while the remaining nodes are linked to level "Group3". From equation (4.1) the attribute matrix $\mathbf{B}$ for the simple example illustrated in Figure 4.1 is provided by

$$\mathbf{B} = \begin{pmatrix} \mathbf{b}_1 \\ \mathbf{b}_2 \\ \mathbf{b}_3 \\ \mathbf{b}_4 \\ \vdots \\ \mathbf{b}_{20} \end{pmatrix} = \begin{pmatrix} 1 & 0 & 1 & 0 \\ 1 & 0 & 1 & 0 \\ 1 & 0 & 1 & 0 \\ 0 & 1 & 1 & 0 \\ \vdots & \vdots & \ddots & \vdots \\ 1 & 0 & 1 & 0 \end{pmatrix}.$$

The set V_a contains indicator nodes $\{v_{a_1}, v_{a_2}, v_{a_3}, v_{a_4}\}$ reflecting associations with "Group1", "Group2", "Group3" and "Group4" respectively. Assume all structural and

© University of Pretoria

UNIVERSITEIT VAN PRETORIA
UNIVERSITY OF PRETORIA
YUNIBESITHI YA PRETORIA

attribute weights in $\mathbf{W}_a^*$ are set to 1. Consequently, $\mathbf{W}_s$ is simplified to the adjacency matrix that defines structural neighbouring nodes based on shared boundary points between grids. The network structure of G_a is illustrated in Figure 4.2.

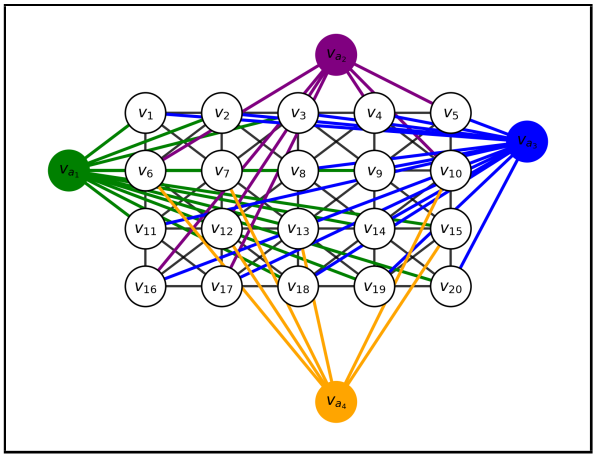

Figure 4.2: The network structure of G_a: The structural nodes $(v_1, \ldots, v_{20})$ are depicted as black-outlined circles, with structural edges represented by black lines. Indicator attribute nodes $(v_{a_1}, v_{a_2}, v_{a_3}, v_{a_4})$ are shown as circles in green, purple, blue, and yellow, respectively, with their corresponding attribute edges displayed in the same colours as the nodes.

The transition probability matrix $\mathbf{P}_a$ for G_a is a 24×24 matrix, as illustrated in equation (4.3)

$$\mathbf{P}_a = \begin{pmatrix} \mathbf{p}_{a,1} \\ \mathbf{p}_{a,2} \\ \vdots \\ \mathbf{p}_{a,N+T} \end{pmatrix} = \left(\begin{array}{cccc|cccc} 0 & \frac{1}{5} & \cdots & 0 & \frac{1}{5} & 0 & \frac{1}{5} & 0 \\ \frac{1}{7} & 0 & \cdots & 0 & \frac{1}{7} & 0 & \frac{1}{7} & 0 \\ \vdots & \ddots & \vdots & \vdots & \vdots & \vdots & \vdots & \vdots \\ 0 & 0 & \cdots & 0 & \frac{1}{5} & 0 & \frac{1}{5} & 0 \\ -- & -- & -- & -- & -- & -- & -- & -- \\ \frac{1}{13} & \frac{1}{13} & \cdots & \frac{1}{13} & 0 & 0 & 0 & 0 \\ 0 & 0 & \cdots & 0 & 0 & 0 & 0 & 0 \\ \frac{1}{14} & \frac{1}{14} & \cdots & \frac{1}{14} & 0 & 0 & 0 & 0 \\ 0 & 0 & \cdots & 0 & 0 & 0 & 0 & 0 \end{array}\right) \tag{4.3}$$

where the embedded representation of every node i is captured in the $N+T$-dimensional feature vector $\mathbf{p}_{a,i}, i = 1, ..., N+T$.

© University of Pretoria

UNIVERSITEIT VAN PRETORIA
UNIVERSITY OF PRETORIA
YUNIBESITHI YA PRETORIA

4.3.2 Cluster memberships and macro-regions of $\mathbf{P}_a$

Clustering is a fundamental technique in data analysis aimed at grouping objects into homogeneous categories based on their similarity. Clustering uncovers the inherent structures of high-dimensional data, such as the transition probabilities captured in $\mathbf{P}_a$, without relying on predefined hypotheses or models [51].

Cluster analysis will be applied on the feature vectors $\mathbf{p}_{a,i}, i = 1, ..., N+T$ in $\mathbf{P}_a$ to identify natural patterns in the nodes based on shared attribute and structural connections. The feature vectors, $\mathbf{p}_{a,i}, i = 1, ..., N+T$, will be split into $K < N+T$ clusters $\mathcal{C} = (C_1, ..., C_K)$, where every cluster needs to contain at least one feature vector and each feature vector will belong to only one cluster.

Initially, clusters are formed using the k-means [43] algorithm by partitioning $\mathbf{p}_{a,i}, i = 1, ..., N+T$ into K clusters. The optimal number of clusters, K, is determined using the elbow method [24], where the point at which the rate of decrease in inertia slows significantly is identified, indicating diminishing returns from additional clusters. Initial cluster centres, $\boldsymbol{\mu}_j, j = 1, ..., K$ are randomly selected from $\mathbf{P}_a = (\mathbf{p}_{a,1}, ..., \mathbf{p}_{a,N+T})^T$. The remaining feature vectors are assigned to the respective clusters based on which has the closest cluster centre by minimising the distance between each feature vector $\mathbf{p}_{a,i}$ and its assigned cluster centroid $\boldsymbol{\mu}_j$ i.e. $\sum_{i=1}^{N+T}\sum_{j=1}^{K} u_{ij}(\mathbf{p}_{a,i} - \boldsymbol{\mu}_j)(\mathbf{p}_{a,i} - \boldsymbol{\mu}_j)^T$. $\mathbf{U} = (\mathbf{u}_1, ..., \mathbf{u}_{N+T})^T = [u_{ij}]$ is the $(N+T) \times K$ matrix indicating the assignment of the i-th feature vector, $\mathbf{p}_{a,i}$, to the j-th class i.e. $u_{ij} = 1$ if feature vector i is assigned to cluster j for $i = 1, ..., N+T; j = 1, ...K$ and $u_{ij} = 0$ otherwise. After the remaining feature vectors are assigned to one of the K clusters $\mathcal{C} = (C_1, ..., C_K)$, new cluster centres are calculated by $\boldsymbol{\mu}_j = \frac{1}{n_j}\sum_{i=1}^{N+T} u_{ij}\mathbf{p}_{a,i}$ where n_j is the number of feature vectors assigned to cluster $j, j = 1, ..., K$. This process continues until there is no more change in the assignment of feature vectors to clusters. This process provides the initial cluster assignments, $\mathbf{U}(0)$ with $u_{ij} \in \{0, 1\}$ a crisp partition [51] as outlined in algorithm (1).

Applying this initial clustering process on the simple example illustrated in Figure 4.1 the optimal number of clusters obtained using the elbow method was $K = 5$ clusters. The final cluster assignments $C_1 = \{\mathbf{p}_{a,4}, \mathbf{p}_{a,5}\}$, $C_2 = \{\mathbf{p}_{a,9}, \mathbf{p}_{a,14}, \mathbf{p}_{a,15}, \mathbf{p}_{a,18}, \mathbf{p}_{a,19}, \mathbf{p}_{a,20}\}$, $C_3 = \{\mathbf{p}_{a,16}, \mathbf{p}_{a,17}\}$, $C_4 = \{\mathbf{p}_{a,6}, \mathbf{p}_{a,7}, \mathbf{p}_{a,8}, \mathbf{p}_{a,10}, \mathbf{p}_{a,12}, \mathbf{p}_{a,13}, \mathbf{p}_{a,21}, \mathbf{p}_{a,22}, \mathbf{p}_{a,23}, \mathbf{p}_{a,24}\}$ and $C_5 = \{\mathbf{p}_{a,1}, \mathbf{p}_{a,2}, \mathbf{p}_{a,3}, \mathbf{p}_{a,11}\}$ is indicated in $\mathbf{U}(0)$ in equation (4.4) and a graphical rep-

© University of Pretoria

UNIVERSITEIT VAN PRETORIA
UNIVERSITY OF PRETORIA
YUNIBESITHI YA PRETORIA

Algorithm 1 Initial k-means clustering on P_a

Require: $\mathbf{P}_a = (\mathbf{p}_{a,1}, ..., \mathbf{p}_{a,N+T})^T$ - dataset, K - number of clusters
Ensure: $C = \{C_1, C_2, \ldots, C_K\}$ - set of clusters, initial cluster assignment $\mathbf{U}(0)$

```
Select K initial centroids μ_j, j = 1, ..., K randomly from P_a
repeat
    Create K empty clusters C_1, C_2, ..., C_k
    for i = 1 to N + T do
        Assign p_{a,i} to the cluster C_j with the closest centroid μ_j
        for j = 1 to K do
            Update centroid μ_j as the mean of all points in cluster C_j
        end for
    end for
until no more changes in the assignment of points to clusters, U
```

resentation is provided in the first image of Figure 4.3.

$$\mathbf{U}(0) = \begin{pmatrix} 0 & 0 & 0 & 0 & 1 \\ 0 & 0 & 0 & 0 & 1 \\ 0 & 0 & 0 & 0 & 1 \\ 1 & 0 & 0 & 0 & 0 \\ 1 & 0 & 0 & 0 & 0 \\ 0 & 0 & 0 & 1 & 0 \\ \vdots & \vdots & \vdots & \vdots & \vdots \\ 0 & 0 & 0 & 1 & 0 \\ 0 & 0 & 0 & 1 & 0 \end{pmatrix}. \tag{4.4}$$

From the cluster assignments illustrated in Figure 4.3, it can be observed that there are structural nodes $v_i \in V$ which are adjacent to each other and belong to the same cluster. Since this clustering is applied to spatial data, the goal is to create spatially coherent regions rather than clusters of aspatial data. To achieve this, a new spatial entity, termed a macro-region, is constructed.

Macro-regions are formed by merging structural nodes $v_i \in V$ that share a structural edge $(v_i, v_j) \in E$ and whose feature vectors $\mathbf{p}_{a,i}$ and $\mathbf{p}_{a,j}$ belong to the same cluster C_k. Specifically, two nodes v_i and v_j are grouped into the same macro-region if they are connected by a structural edge and their feature vectors satisfy the condition $u_{ik} =$

© University of Pretoria

UNIVERSITEIT VAN PRETORIA
UNIVERSITY OF PRETORIA
YUNIBESITHI YA PRETORIA

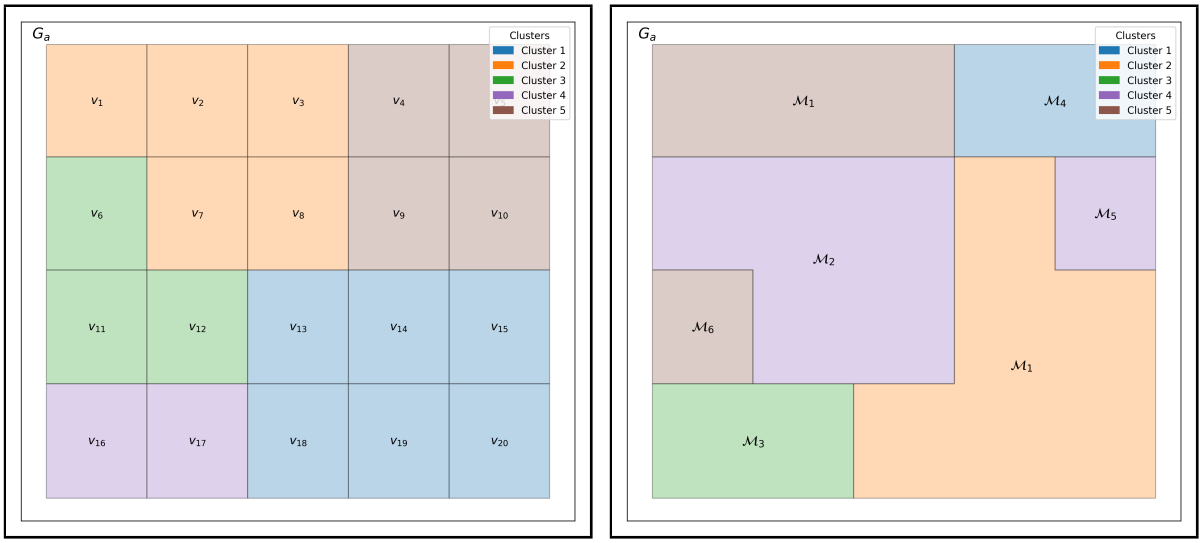

Figure 4.3: The left image illustrates the initial cluster assignments $\mathbf{U}(0)$ on P_a with $K = 5$, while the right image shows macro-regions based on $\mathbf{P}_a$ with $Q = 7$.

$u_{jk} = 1$, where $u_{ik} = 1$ indicates that the feature vector $\mathbf{p}_{a,i}$ is assigned to cluster C_k. The attribute nodes from V_a are not included when creating the macro-regions, as they have no geographical properties.

Macro-regions, denoted as $\mathbf{M} = \{\mathcal{M}_1, \ldots, \mathcal{M}_Q\}$, are thus formed by the union of all structural nodes that meet this criteria. Formally, a macro-region $\mathcal{M}_q$, where $q = 1, \ldots, Q$, is defined as the set of all connected structural nodes that belong to the same cluster, expressed as

$$\mathcal{M}_q = \bigcup_{\substack{(v_i,v_j)\in E \\ k\in\{1,\ldots,K\}, u_{ik}=u_{jk}=1}} \{v_i, v_j\}. \tag{4.5}$$

Each macro-region is uniquely associated with one of the clusters $C_k \in \mathcal{C}$, but a single cluster can produce multiple macro-regions if its constituent nodes form disconnected subgraphs within the network G_a. Consequently, the total number of macro-regions Q satisfies $K \leq Q$, where K is the number of clusters. This framework ensures that macro-regions are defined both by spatial connectivity and clustering assignments, providing a cohesive representation of spatially coherent regions.

Using equation (4.5) to construct macro-regions for the simple example shown in Figure 4.1, $Q = 7$ macro-regions where identified as shown in the second image of Figure

© University of Pretoria

UNIVERSITEIT VAN PRETORIA
UNIVERSITY OF PRETORIA
YUNIBESITHI YA PRETORIA

4.3.

Upon close inspection of the macro-regions created in Figure 4.3, it becomes evident that there are many smaller-sized macro-regions, such as $\mathcal{M}_5$ and $\mathcal{M}_6$. This is a result of the k-means clustering of $\mathbf{P}_a$, which primarily focuses on minimising the distance between each feature vector $\mathbf{p}_{a,i}$ and its assigned cluster centroid $\boldsymbol{\mu}_j$. However, this approach does not fully account for spatial dependencies and neighbouring nodes.

Although the feature vectors for the attribute nodes $\mathbf{p}_{a,21}, \mathbf{p}_{a,22}, \mathbf{p}_{a,23}, \mathbf{p}_{a,24}$ are not directly part of the macro-regions, they play a crucial role in clustering the nodes by incorporating both structural and attribute links. Notably, $\mathbf{p}_{a,21}, \mathbf{p}_{a,22}, \mathbf{p}_{a,23}, \mathbf{p}_{a,24}$ were all assigned to cluster 4. By examining the attributes in Figure 4.1 and comparing them to the macro-regions in Figure 4.3, it can be observed that regions $\mathcal{M}_2$ and $\mathcal{M}_5$ are not associated with all levels of attributes λ_1 and λ_2. This discrepancy suggests that while $\mathbf{p}_{a,21}, \mathbf{p}_{a,22}, \mathbf{p}_{a,23}, \mathbf{p}_{a,24}$ and macro-regions $\mathcal{M}_2$ and $\mathcal{M}_5$ are all assigned to cluster C_4, the initial clustering does not fully account for all attribute and structural links to achieve spatially optimal solutions. In the following section, an iterative process will be explored to spatially smooth the initial clusters obtained in $\mathbf{U}(0)$ and generate more spatially coherent macro-regions.

4.3.3 Optimised cluster memberships and macro-regions

The macro-regions generated through the clustering of $\mathbf{P}_a$ provide an insightful yet preliminary segmentation of the graph. While the k-means approach effectively partitions the data based on feature similarity, its focus on minimising intra-cluster distances, neglects the spatial relationships between neighbouring nodes. As a result, the initial macro-regions may lack spatial coherence, as seen with smaller macro-regions, which emerge due to localised feature similarities rather than broader spatial patterns. To address this limitation and improve spatial contiguity, further refinement of the cluster memberships is required. This refinement leverages the inherent network structure and spatial dependencies embedded in $\mathbf{P}_a$. The next section explores a method to iteratively enhance the spatial cohesion of these macro-regions while maintaining their distinctiveness.

To identify more spatially coherent macro-regions, we need to re-cluster the member-

© University of Pretoria

UNIVERSITEIT VAN PRETORIA
UNIVERSITY OF PRETORIA
YUNIBESITHI YA PRETORIA

ships obtained in $\mathbf{U}(0)$ by incorporating the network structure represented in $\mathbf{P}_a$. Let $\mathbf{S}(t) = \mathbf{P}_a \cdot \mathbf{U}(t-1)$ be an $(N+T) \times K$ matrix of the probability distribution of the cluster memberships based on the connectivity structure in $\mathbf{P}_a$. Each K-dimensional feature row vector in $\mathbf{S}(t)$, $\mathbf{S}(t) = (\mathbf{s}_1, \ldots, \mathbf{s}_{N+T})^T$, provides weighted averages of the nodes' affiliations to their respective clusters. $\mathbf{S}(t) = [s_{ij}(t)]$ is the $(N+T) \times K$ matrix indicating the assignment of the i-th node to the j-th cluster membership at iteration t with $s_{ij}(t) \in [0, 1]$ which indicates a fuzzy or probabilistic membership as opposed to $u_{ij}(t) \in \{0, 1\}$ which indicates a crisp membership of 0 or 1. If the nodes in $\mathbf{P}_a$ are more tightly grouped around one cluster centroid, higher probabilities will be observed for that cluster in the corresponding rows of $\mathbf{S}(t)$.

For $t = 1$, the cluster membership from the initial cluster assignment $\mathbf{U}(0)$ is $\mathbf{S}(1) = \mathbf{P}_a \cdot \mathbf{U}(0)$. When applied to the example illustrated in Figure 4.1, the cluster memberships of $\mathbf{U}(0)$ are

$$\mathbf{S}(1) = \begin{pmatrix} 0 & 0 & 0 & 0.8 & 0.2 \\ 0 & 0 & 0 & 0.714 & 0.286 \\ 0.143 & 0.143 & 0 & 0.57 & 0.143 \\ 0.143 & 0.143 & 0 & 0.57 & 0.143 \\ 0.2 & 0.2 & 0 & 0.6 & 0 \\ 0 & 0 & 0 & 0.571 & 0.429 \\ \vdots & \vdots & \vdots & \vdots & \vdots \\ 0.143 & 0.357 & 0.143 & 0.071 & 0.286 \\ 0 & 0.167 & 0 & 0.833 & 0 \end{pmatrix}. \tag{4.6}$$

From the results of $\mathbf{S}(1)$, it can be observed that nodes strongly associated with a particular cluster (rows dominated by a single value close to 1) are more tightly grouped around one cluster centroid. For example, nodes v_1 to v_6 exhibit a high affinity to cluster 4, as reflected in the fourth column of $\mathbf{S}(1)$. This is because most nodes are initially assigned to cluster 4, which dominates the probability structure in $\mathbf{S}(1)$.

If we re-cluster $\mathbf{S}(1)$ using the k-means algorithm described in Algorithm (1), but with $\mathbf{S}(t) = (\mathbf{s}_1, \ldots, \mathbf{s}_{N+T})^T$ as the input data and initial centroids $\boldsymbol{\mu}_j, j = 1, \ldots, K$ chosen randomly from $\mathbf{S}(t)$, the cluster memberships change to

© University of Pretoria

UNIVERSITEIT VAN PRETORIA
UNIVERSITY OF PRETORIA
YUNIBESITHI YA PRETORIA

$$\mathbf{U}(1) = \begin{pmatrix} 0 & 0 & 0 & 1 & 0 \\ 0 & 0 & 0 & 1 & 0 \\ 0 & 0 & 1 & 0 & 0 \\ 0 & 0 & 1 & 0 & 0 \\ 0 & 0 & 1 & 0 & 0 \\ 0 & 0 & 0 & 1 & 0 \\ \vdots & \vdots & \vdots & \vdots & \vdots \\ 1 & 0 & 0 & 0 & 0 \\ 0 & 0 & 1 & 0 & 0 \end{pmatrix} \tag{4.7}$$

and the resulting cluster membership probability distribution matrix $\mathbf{S}(2) = \mathbf{P}_a \cdot \mathbf{U}(1)$ becomes

$$\mathbf{S}(2) = \begin{pmatrix} 0.4 & 0 & 0 & 0.6 & 0 \\ 0.286 & 0 & 0.286 & 0.429 & 0 \\ 0.286 & 0 & 0.429 & 0.286 & 0 \\ 0.143 & 0.143 & 0.571 & 0 & 0.143 \\ 0.2 & 0.2 & 0.4 & 0 & 0.2 \\ 0 & 0 & 0.143 & 0.429 & 0.429 \\ \vdots & \vdots & \vdots & \vdots & \vdots \\ 0 & 0.214 & 0.5 & 0.143 & 0.143 \\ 0 & 0.5 & 0 & 0.333 & 0.167 \end{pmatrix}. \tag{4.8}$$

As the iteration progresses, the memberships in $\mathbf{S}(t)$ begin to balance between clusters, reflecting both structural and attribute-based dependencies as can be seen in $\mathbf{S}(2)$ where the cluster memberships for $\mathbf{s}_1, \mathbf{s}_2, \mathbf{s}_3, \mathbf{s}_6$ are now different from $\mathbf{s}_4, \mathbf{s}_5$ as when compared to $\mathbf{S}(1)$.

Continuing the process, the cluster memberships between $\mathbf{U}(t)$ and $\mathbf{U}(t+1)$ will gradually stabilise. This stabilisation reflects the influence of the connectivity structure in $\mathbf{P}_a$. The final clusters account for transition probabilities between nodes and smooth cluster memberships based on the underlying graph structure.

The iterative process continues until convergence is achieved in terms of mutual

© University of Pretoria

UNIVERSITEIT VAN PRETORIA
UNIVERSITY OF PRETORIA
YUNIBESITHI YA PRETORIA

information [46] between $\mathbf{U}(t)$ and $\mathbf{U}(t+1)$ given by

$$I(\mathbf{U}(t), \mathbf{U}(t+1)) = \sum_{j=1}^{K} \pi_{s_j}(t) \sum_{i=1}^{N+T} u_{ij}(t+1) \log \frac{u_{ij}(t+1)}{\pi_{u_i}(t+1)}. \tag{4.9}$$

where $\pi_{s_j}(t) = \frac{1}{N+T} \sum_{i=1}^{N+T} s_{ij}(t), j = 1, 2, ..., K$ is the prior probabilities of the cluster memberships at iteration t and $\pi_{u_i}(t+1) = \frac{1}{N+T} \sum_{j=1}^{N+T} \delta\left(\mathbf{u}_i(t+1), \mathbf{u}_j(t+1)\right)$ is the average cluster membership for each node i at iteration t+1 with $\delta\left(\mathbf{u}_i(t+1), \mathbf{u}_j(t+1)\right) =$ 1 if $\mathbf{u}_i(t+1) = \mathbf{u}_j(t+1)$ and 0 otherwise.

When the iterative process outlined in equation (4.9) converges, the optimal crisp cluster memberships will be captured in $\hat{\mathbf{U}}$ with corresponding fuzzy membership in $\hat{\mathbf{S}}$.

By computing mutual information during each iteration, we ensure that the current clustering structure captures as much information as possible about the distribution of the input data, gradually approaching an optimal clustering solution.

Since the probabilities are split as fractions for structural and attribute nodes in $\mathbf{P}_a$, the likelihood of observing the same pattern of probabilities per node is high. This can result in two or more optimal solutions, which may cause the iterative process in equation (4.9) to oscillate. If this happens, priority will be given to the solution where more nodes share a structure edge as the primary objective of the clustering is to form mutual spatial regions. To formalise this, let $\sum_{i=1}^{N+T} \sum_{j=1}^{N+T} \delta\left(\mathbf{u}_i, \mathbf{u}_j\right) \mathbf{A}_{ij}$ be a spatial coherence score, where $\mathbf{A}$ is the adjacency matrix of all nodes in the set $V \cup V_a$ and $\delta\left(\mathbf{u}_i, \mathbf{u}_j\right)$ indicates whether the cluster assignment for node i and node j are the same with $\delta\left(\mathbf{u}_i, \mathbf{u}_j\right) = 1$ if $\mathbf{u}_i = \mathbf{u}_j$ and 0 otherwise. This score is calculated for all solutions obtained through equation (4.9), if more than one optimal solution was identified, and the cluster membership with higher structural spatial coherence will be assigned as $\hat{\mathbf{U}}$.

Once the optimal solution $\hat{\mathbf{U}}$ along with $\hat{\mathbf{S}}$ is obtained, the macro-regions can be determined as formulated in equation (4.5). Revisiting the example illustrated in Figure 4.1, the newly defined macro-regions based on $\hat{\mathbf{U}}$ are shown in Figure 4.4.

Continuing with this example, the stabilised value $\hat{\mathbf{S}}$ in equation (4.10) provides

© University of Pretoria

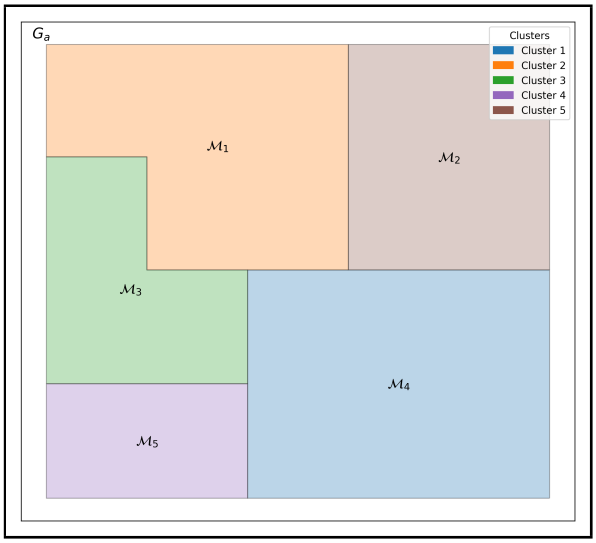

Figure 4.4: Spatially coherent optimised macro-regions based on the k-means clustering of $\mathbf{S}(t)$

cluster assignments coherent with the connectivity structure in $\mathbf{P}_a$,

$$\hat{\mathbf{S}} = \begin{pmatrix} 0.2 & 0.4 & 0.4 & 0 & 0 \\ 0.143 & 0.571 & 0.286 & 0 & 0 \\ 0.143 & 0.429 & 0.143 & 0 & 0.286 \\ 0 & 0.286 & 0.143 & 0.143 & 0.429 \\ 0 & 0 & 0.2 & 0.2 & 0.6 \\ \vdots & \vdots & \vdots & \vdots & \vdots \\ 0.286 & 0.286 & 0.071 & 0.143 & 0.214 \\ 0.333 & 0.167 & 0.333 & 0 & 0.167 \end{pmatrix}. \tag{4.10}$$

When comparing the macro-regions in Figure 4.3 and Figure 4.4, it can be noted that the number of macro-regions has decreased from $Q = 7$ to $Q = 5$ while maintaining the same number of clusters $K = 5$. The regions are also larger in size. Although the number of macro-regions has been reduced, there is still a combination of key attributes that are repeated across different clusters.

To further understand and describe the spatial configuration, attribute segmentation can be introduced as a higher-level categorisation of the macro-regions based on shared

© University of Pretoria

UNIVERSITEIT VAN PRETORIA
UNIVERSITY OF PRETORIA
YUNIBESITHI YA PRETORIA

prominent attribute combinations. Unlike macro-regions, which are defined spatially, attribute segmentations focus on grouping macro-regions with similar modal attribute profiles into categorical values. For example, if $\mathcal{M}_1$ and $\mathcal{M}_4$ share the same dominant attribute combination "Group1" and "Group3", they will belong to the same attribute segmentation. Similarly, $\mathcal{M}_2$ and $\mathcal{M}_5$ may share a different attribute combination "Group2" and "Group3", forming a separate segmentation. This results in fewer attribute segmentations than macro-regions, as multiple macro-regions can map to a single attribute segmentation.

Formally, let Q denote the number of macro-regions, R the number of attribute segmentations, and K the number of clusters. Then, $R \leq Q$, where each macro-region is associated with exactly one attribute segmentation, but multiple macro-regions can map to the same attribute segmentation.

Since the optimal clusters are based on structural links between nodes and shared attributes, the final clusters can share similar attributes but can be located in different geographical regions. Hence, attribute segmentation provides a meaningful, higher-level description for each macro-region.

Clusters with identical modal attributes across all attribute levels are grouped into the same attribute segmentation to facilitate visualisation and to serve as covariates in a model. Attribute segmentation applied to the example in Figure 4.4 provides the results shown in Figure 4.5.

The macro-regions that share the most prominent attributes (or levels of an attribute) are grouped together in the same attribute-based spatial segmentation. For example, macro-regions $\mathcal{M}_1$ and $\mathcal{M}_4$ both share the attribute combination "Group1" and "Group3", $\mathcal{M}_2$ and $\mathcal{M}_5$ both share "Group2" and "Group3" and $\mathcal{M}_3$ is characterised by "Group2" and "Group4".

In this work, we developed an enhanced clustering framework that integrates structural and attribute-based information to identify spatially coherent macro-regions. Starting from the initial clustering of $\mathbf{P}_a$ using k-means, it was observed that traditional clustering methods primarily focus on minimising intra-cluster distances in the feature space, often neglecting spatial dependencies between neighbouring nodes. This limitation resulted in smaller, disjointed macro-regions and inconsistent spatial coherence. To

© University of Pretoria

UNIVERSITEIT VAN PRETORIA
UNIVERSITY OF PRETORIA
YUNIBESITHI YA PRETORIA

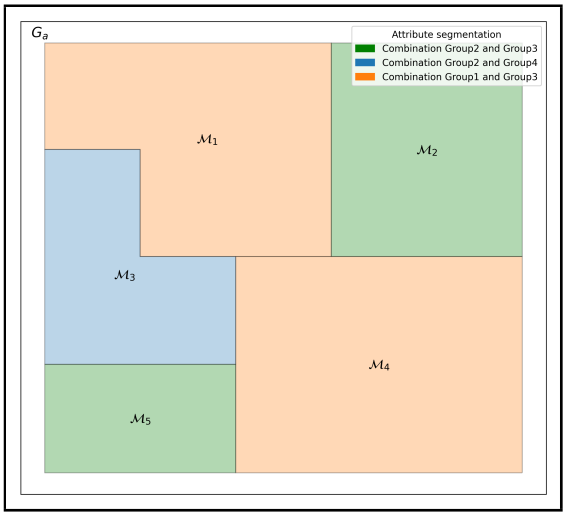

Figure 4.5: Attribute segmentation of clusters

address this, we introduced an iterative refinement process that incorporates the structural relationships embedded in $\mathbf{P}_a$, ensuring that the final clusters are both spatially contiguous and meaningful in terms of their feature vectors.

The refinement process was guided by a mutual information framework, which evaluates the similarity between cluster membership matrices across consecutive iterations, ensuring convergence to stable and interpretable solutions. By integrating structural links and attribute-based information, the framework allows for a unified clustering approach that is capable of capturing complex spatial and attribute-level dependencies. This novel methodology bridges the gap between traditional clustering approaches and practical applications, offering a scalable solution for spatial planning and geographic analysis. The integration of structural coherence and attribute alignment lays the foundation for future applications in optimising resource allocation, defining service areas, and segmenting spatial systems with multimodal data.

© University of Pretoria

UNIVERSITEIT VAN PRETORIA
UNIVERSITY OF PRETORIA
YUNIBESITHI YA PRETORIA

4.4 Application

To evaluate the proposed methodology in a practical application we consider region G_a to be the district municipality City of Cape Town[1] located in the Western Cape province in South Africa. Region G_a is subdivided into 2042 square grids of size $1\text{km} \times 1\text{km}$ whose centres will be the structural nodes.

The POIs in this study are pharmaceutical stores, part of a subset from one of South Africa's largest pharmaceutical chains. The supply data for these POIs consists of the average summer sales (December, January, and February) of an affordable over-the-counter diarrhoea medication, recorded from 2015 to 2019. In South Africa, a low- to middle-income country, access to affordable medication is vital for public health. The over-the-counter medication used in this application is widely available and commonly used to manage diarrhoea, a condition with significant health implications, particularly in regions facing challenges related to water quality and sanitation [34].

This section will explore the attributes associated with the nodes in G_a, followed by the identification of clusters, macro-regions and attribute segments. The application will conclude by evaluating the performance of a SAR model to predict the average sales per POI when incorporating attribute segmentations into a covariate-dependent spatial weights matrix.

4.4.1 Attributes

Key attributes influencing sales, which are allocated to all structural nodes in G_a include ease of access, demand and temperature. Ease of access represents how conveniently a POI can be reached, reflecting the importance of physical proximity in settings where travel costs and time may limit access. Demand is influenced by the socio-economic characteristics of the area, including population density and disposable income, which affect the purchasing behaviour of local communities. Temperature is included because diarrhoeal diseases are more prevalent in warmer months, making it a significant seasonal

[1] District municipalities consists of multiple local municipalities. They are administrative divisions which is accountable for providing basic services within the area. Source: Education and Training Unit (ETU), www.etu.org.za (accessed February 15, 2024)

© University of Pretoria

UNIVERSITEIT VAN PRETORIA
UNIVERSITY OF PRETORIA
YUNIBESITHI YA PRETORIA

factor in medication demand [34].

The first attribute, ease of access, categorises nodes based on the primary type of road access, which has three levels: principal, suburb, and other[2]. Nodes with principal road access are either connected by major roads, such as highways, or main roads that serve as key routes within towns or cities. These roads offer the highest level of accessibility and play a crucial role in connecting POIs to densely populated or high-traffic areas. Nodes classified as suburb roads are connected by secondary roads or local streets, typically found in residential or suburban areas. The other category includes unpaved paths, trails, or less accessible roads, indicating lower accessibility for POIs in these locations.

The second attribute, demand, is represented by the average population size from 2015 to 2019 associated with each node, derived from overlaying census and deeds office data provided by Lightstone (Pty) Ltd[3]. To segment demand, we used quartiles based on the distribution of population data in City of Cape Town, defining four categories: no demand for population totals below Q1, low demand for totals between Q1 and Q2, mid demand for totals between Q2 and Q3, and high demand for totals equal to Q3 or more. This approach ensures that regions with similar population-driven demand characteristics are grouped, simplifying the integration of this attribute and removing the complexity of continuous population data. By focusing on quartiles, the attribute reflects both high-density urban areas and sparsely populated regions, capturing the heterogeneity of demand across the City of Cape Town.

The final attribute, temperature, includes two levels: hot days and normal days. High temperatures are particularly relevant as they can have a direct impact on public health and infrastructure. Hot days, defined as days with maximum temperatures exceeding a threshold indicative of heat stress conditions, promote the growth of bacteria, viruses, and parasites in food and water, thereby increasing the risk of waterborne diseases such as diarrhoea [34]. Normal days, on the other hand, represent typical temperature conditions that are less likely to exert such extreme impacts. The levels for all attributes on all

[2] Department of Health South Africa, *TRH 26: South African Road Classification and Access Management Manual*, https://wayleave.tshwane.gov.za/ (accessed August 15, 2024)

[3] Lightstone (Pty) Ltd procures its data directly from the Deeds office and is comprised of a snapshot of all South Africa property ownership as at 1993, with a full history of all transactions to augment with census data. Ethics clearance number: NAS003/2023.

© University of Pretoria

structural nodes in G_a is illustrated in Figure 4.6.

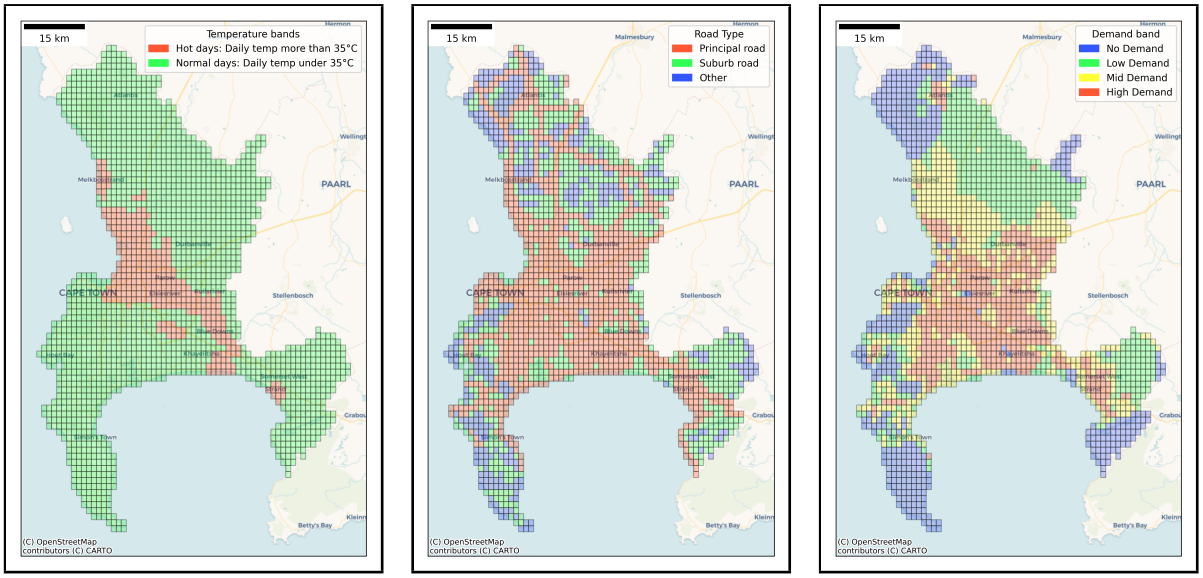

Figure 4.6: Visualisation of the temperature, ease of access, and demand attributes at node level. The map highlights the spatial distribution of these attributes across individual nodes. Map data © OpenStreetMap contributors, under the Open Database License (ODbL).

Temperature data was sourced from the South African Weather Services (SAWS), which provided daily minimum and maximum temperatures recorded at various weather stations in the Western Cape. Since only 10 SAWS stations were located in the City of Cape Town, OpenWeather[4] was used as an additional data source to ensure adequate variability across the city. The combined temperature inputs from the two sources were used to represent the spatial variability across the region, but the coverage was insufficient to represent the entire geographical network G_a. Weather stations were mapped to $4\,\text{km} \times 4\,\text{km}$ grids because weather patterns do not vary significantly over smaller spatial scales, making this resolution appropriate for temperature interpolation. Out of the total 177, $4\,\text{km} \times 4\,\text{km}$ grids covering the City of Cape Town, observed minimum and maximum temperatures were available for only 101 grids. This meant that predictions were required for the remaining 76 grids to fill gaps in the temperature dataset.

To address this, Ordinary Kriging [10] was applied on a grid size of $4\,\text{km} \times 4\,\text{km}$, and the results were subsequently mapped down to the corresponding $1\,\text{km} \times 1\,\text{km}$ grids to

[4] Open Weather, https://openweathermap.org/ (accessed October 17, 2024)

© University of Pretoria

estimate minimum and maximum temperatures. The midpoints of the 4 km × 4 km grids that overlapped with a SAWS or OpenWeather station were used as the x, y coordinates of the observed value $z(x_i)$, while the remaining grids required interpolation using Ordinary Kriging, defined by $\hat{z}(x_0) = \sum_{i=1}^{N} \lambda_i z(x_i)$ where $z(x_i)$ are the observed values at neighbouring locations, and λ_i are the Kriging weights. These weights are determined by solving a system of linear equations that incorporate the distances between observed points, the distances between observed and unobserved locations and the spatial correlation structure defined by the variogram. For maximum temperatures, a Gaussian variogram structure was used, with a partial sill of 0.004, a range of 0.5 and a nugget of 0.0005. For minimum temperatures an Exponential variogram structure was a better fit, with a smaller range of 0.25, as shown in Figure 4.7. These parameters ensure that λ_i effectively captures spatial dependence, assigning higher weights to closer observed points and lower weights to farther ones.

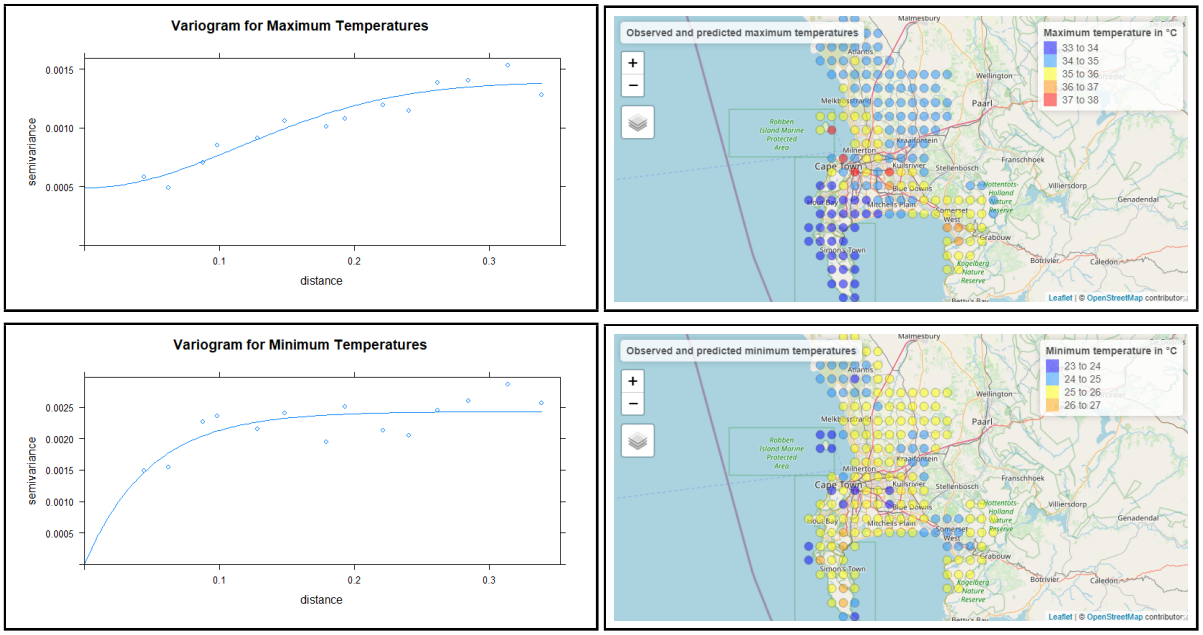

Figure 4.7: The top left panel shows the variogram for maximum temperatures. The top right panel illustrates the observed and predicted maximum temperature values across the City of Cape Town. The bottom left panel displays the variogram for minimum temperatures. The bottom right panel shows the observed and predicted minimum temperature values. Map data © OpenStreetMap contributors, under the Open Database License (ODbL).

A combination of both maximum and minimum temperatures are used to create

© University of Pretoria

UNIVERSITEIT VAN PRETORIA
UNIVERSITY OF PRETORIA
YUNIBESITHI YA PRETORIA

the final temperature attribute. Nodes are classified as "hot days" if they experience maximum summer temperatures above 35°C and minimum summer temperatures above 25°C, aligning with criteria identified by Heat Watch Cape Town[5] for high-temperature zones. All other nodes are classified into the "normal days" category.

4.4.2 Clusters and macro-regions

To illustrate the varying outcomes of clusters and macro-regions based on different attributes, multiple scenarios are investigated. The first scenario focuses on forming clusters and macro-regions by considering one attribute at a time, utilising $\hat{\mathbf{U}}$ to assess the impact of individual attributes. The second scenario examines the combined influence of all attributes, comparing the clusters generated under $\mathbf{P}_a$ with those derived from $\hat{\mathbf{U}}$.

Let $\mathbf{P}_a$ be constructed for three different scenarios: the first includes only temperature as an attribute, the second considers only ease of access as an attribute, and the third includes only demand as an attribute in G_a. When examining each attribute separately, the optimal number of clusters, determined by partitioning $\mathbf{S}(t) = (\mathbf{s}_1, \ldots, \mathbf{s}_{N+T})^T$ until the optimal clusters are obtained, corresponds to the number of levels in that attribute. For temperature, $K = z_1 = 2$ clusters are identified; for ease of access, $K = z_2 = 3$ clusters are identified; and for demand, $K = z_3 = 4$ clusters are identified. This is because there is no overlap or interference between attributes and transition probabilities between nodes. As a result, the alignment between the optimal number of clusters and the levels in the attribute is very distinct.

The number of macro-regions (Q) formed when considering only ease of access as an attribute is $Q = 19$, for demand $Q = 24$, and for temperature $Q = 5$. In all cases, the number of clusters (K) is less than the number of macro-regions ($K < Q$) because macro-regions are formed using spatial connections and clusters. When a cluster contains nodes that belong to the same cluster but are not spatially adjacent, these nodes are assigned to separate macro-regions.

With a single attribute, equation (4.9) converges rapidly, and the final solution for

[5] StoryMap by CAPA Strategies, *Heat Watch Cape Town: Community Heat Mapping in Cape Town, South Africa*, https://storymaps.arcgis.com/stories/35fd2bf7e70c448ab0a58245d2f2cd0b (accessed August 20, 2024)

© University of Pretoria

$\hat{\mathbf{U}}$ closely resembles the initial solution $\mathbf{U}(0)$, obtained when clustering $\mathbf{P}_a$. The macro-regions, formulated using structural edges and cluster membership as indicated in equation (4.5), are illustrated in Figure 4.8. When comparing Figure 4.6 to Figure 4.8, the macro-regions align naturally with the attributes on node level, as only one attribute is included in each case.

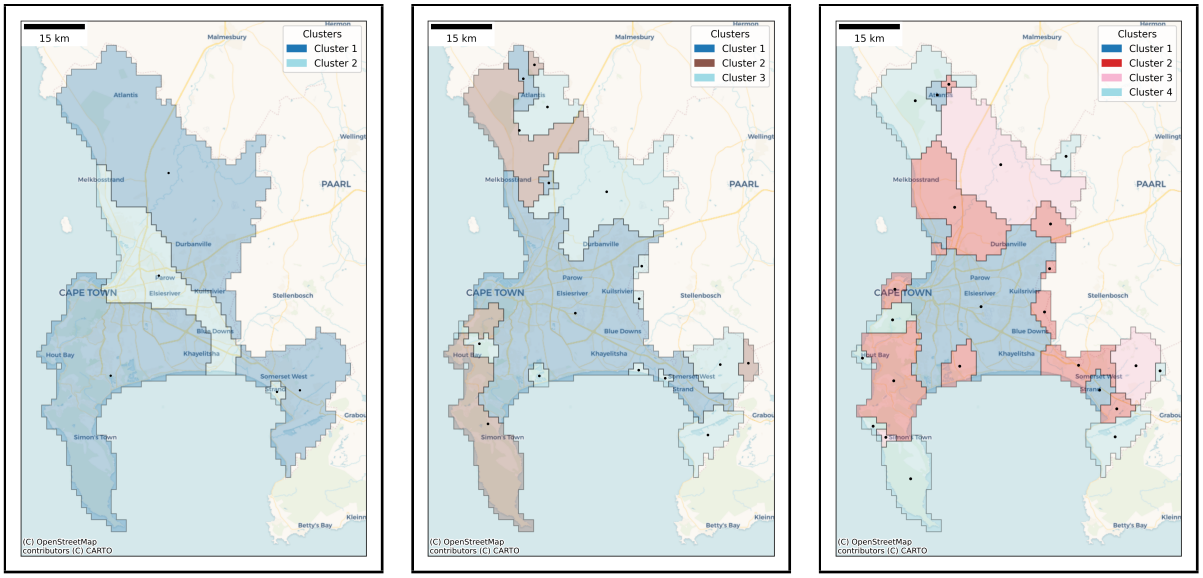

Figure 4.8: Representation of the temperature, ease of access, and demand attribute at cluster and macro-region level. The map illustrates how attributes are aggregated into clusters and macro-regions based on structural edges and spatial connections. Map data © OpenStreetMap contributors, under the Open Database License(ODbL).

However, when considering all attributes together, with $T = z_1 + z_2 + z_3 = 9$ different attribute levels across the three, defining macro-regions becomes more challenging. The optimal number of clusters, as identified from the elbow method is $K = 15$, from which $\mathbf{U}(0)$ is initially derived. Using the cluster memberships from $\mathbf{U}(0)$ together with structural edges $(v_i, v_j) \in E$, $Q = 358$ macro-regions are obtained, as shown in the first image in Figure 4.9. Although the k-means method minimises the distance between the initial cluster centroids and the transition probabilities of the nodes, the resulting solution is not spatially optimal. It leads to very small macro-regions that reflect minor differences in the data, rather than smoothing the spatial solution to create more realistic and applicable regions.

© University of Pretoria

When applying the iterative process outlined in equation (4.9), the process converges at $t = 33$, and the macro-regions obtained using structural edges $(v_i, v_j) \in E$ and $\hat{\mathbf{U}}$ are shown in the second image of Figure 4.9. The resulting macro-regions are more spatially smoothed out, which leads to a reduction of $Q = 358$ to $Q = 55$ macro-regions. The macro-regions in the second image of Figure 4.9 form spatially cohesive areas that reflect underlying structural links and combinations of temperature, ease of access, and demand patterns.

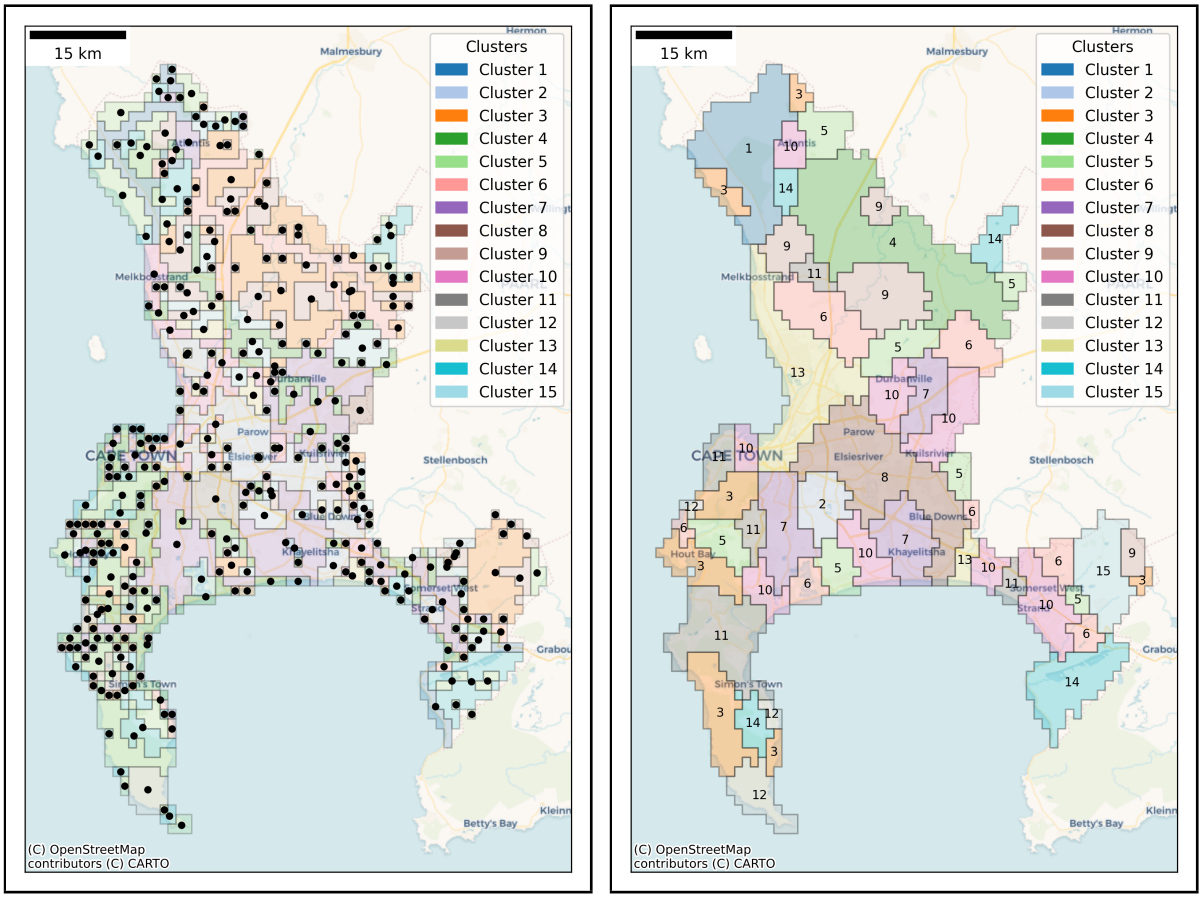

Figure 4.9: Macro-regions constructed using the initial cluster membership ($\mathbf{U}(0)$, left) and the final cluster membership ($\hat{\mathbf{U}}$, right). Map data © OpenStreetMap contributors, under the Open Database License (ODbL).

© University of Pretoria

UNIVERSITEIT VAN PRETORIA
UNIVERSITY OF PRETORIA
YUNIBESITHI YA PRETORIA

4.4.3 Attribute segmentation

An attribute segment is a description of a cluster based on the modal attributes observed within that cluster (and consequently the macro-regions associated with that cluster) when considering all levels of the attributes. For this application, attribute segmentation provides a unique description of the combination of all levels observed for temperature, ease of access and demand.

Even though $K = 15$ clusters are identified in the final cluster membership $\hat{\mathbf{U}}$, as shown in Figure 4.9, multiple clusters share the same prominent attributes when considering all levels across temperature, ease of access and demand. In total, there are $R = 9$ distinct attribute segments, which span over the $K = 15$ clusters and are classified as shown in Table 4.1.

Cluster	**Road Type**	**Temp**	**Demand**	**Attribute Segmentation**
C_1	Other	Normal	None	ONN
C_2	Principal	Normal	High	PNH
C_3	Other	Normal	None	ONN
C_4	Suburb	Normal	Low	SNL
C_5	Suburb	Normal	Low	SNL
C_6	Suburb	Normal	Mid	SNM
C_7	Principal	Normal	High	PNH
C_8	Principal	Hot days	High	PHH
C_9	Principal	Normal	Low	PNL
C_{10}	Principal	Normal	High	PNH
C_{11}	Principal	Normal	Mid	PNM
C_{12}	Other	Normal	None	ONN
C_{13}	Principal	Hot days	Mid	PHM
C_{14}	Suburb	Normal	None	SNN
C_{15}	Suburb	Normal	Low	SNL

Table 4.1: Distinct clusters with mode value of ease of access, temperature and demand

The assignment of the attribute segments can be described as follows:

- **ONN**: Other roads, normal temperature, and no demand.
- **PNH**: Principal roads, normal temperature, and high demand.

© University of Pretoria

UNIVERSITEIT VAN PRETORIA
UNIVERSITY OF PRETORIA
YUNIBESITHI YA PRETORIA

- **SNL**: Suburb roads, normal temperature, and low demand.
- **SNM**: Suburb roads, normal temperature, and mid-level demand.
- **SNN**: Suburb roads, normal temperature, and no demand.
- **PHH**: Principal roads, high temperature (hot days), and high demand.
- **PNM**: Principal roads, normal temperature, and mid-level demand.
- **PHM**: Principal roads, high temperature (hot days), and mid-level demand.
- **PNL**: Principal roads, normal temperature, and low demand.

As part of an exploratory descriptive analysis focused on the clusters, macro-regions and attribute segments, the potential correlations between these and the average sales for POIs are explored. When examining the macro-regions with which the POIs overlap, it is observed that only the macro-regions linked to the set of clusters $\{C_2, C_7, C_8, C_{10}, C_{11}, C_{13}\}$ overlap with POIs. These clusters are associated with only four attribute segments: PNH, PHH, PNM, and PHM. This suggests that the macro-regions from a location perspective and attribute perspective exhibit unique qualities that align closely with POI placement. The attribute segmentation, average sales, and total number of stores for each cluster that overlaps with at least one POI are summarised in Table 4.2.

Cluster	Attribute Segmentation	Average Sales	Total Stores
C_2	PNH	8.98	2
C_7	PNH	6.65	11
C_8	PHH	8.18	3
C_{10}	PNH	5.98	19
C_{11}	PNM	5.29	4
C_{13}	PHM	7.5	9

Table 4.2: POI average sales per cluster and attribute segmentation

It is noted that all clusters listed in Table 4.2 have principal roads as their primary road type, indicating high accessibility. Notably, both clusters C_8 and C_{13}, with average sales above 7.5, are associated with hot days in the temperature attribute, suggesting a potential link between elevated temperatures and increased demand. The demand

© University of Pretoria

levels across these clusters are generally mid or high. The placement of POIs overlaid with clusters and attribute segments shown at the macro-regions level is illustrated in Figure 4.10.

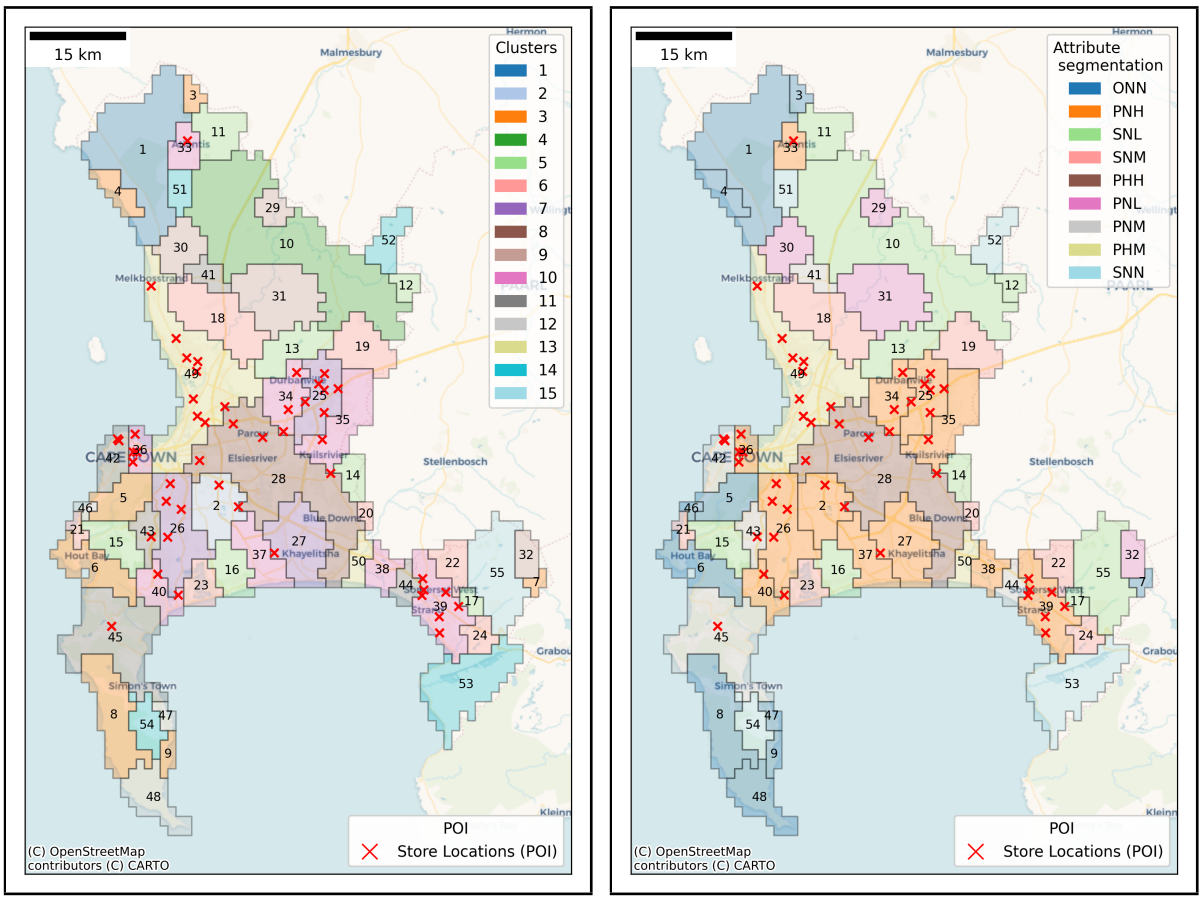

Figure 4.10: POI locations and macro-regions over clusters (left) and attribute segmentation (right). Map data © OpenStreetMap contributors, under the Open Database License (ODbL).

Cluster C_2 exhibits a high average sales value despite not being associated with an attribute segment typically linked to elevated sales. The increased sales observed in C_2 could be attributed to other influencing factors, such as the size of the store, its operating hours, the availability of stock or the store's location.

The effect of incorporating attribute segmentation to predict supply at a POI level will be tested using a SAR model. This will involve incorporating the location of a macro-region, or more specifically, the location of a store within a macro-region, along with attribute segments. Attribute segments will be included as aspatial covariate inputs,

© University of Pretoria

UNIVERSITEIT VAN PRETORIA
UNIVERSITY OF PRETORIA
YUNIBESITHI YA PRETORIA

with their influence further integrated into the covariates spatial weights matrix. This approach will be applied in the next section to predict the average number of sales per POI.

4.4.4 SAR model with attribute segmentation

A SAR model [10] is utilised to account for spatial dependence in the data by incorporating a spatial weights matrix ($\mathbf{W}$) that captures the relationships or proximities between different regions. In this study, we apply a SAR model to assess whether attribute based spatial segments impact the prediction of the summer average sales of a diarrhoea medication across 48 pharmaceutical POIs, $P = \{P_1, \ldots, P_M\}, M = 48$, located in the City of Cape Town.

Attribute based spatial segmentation is expected to contribute to the predictive power of the model by grouping regions based on shared characteristics. However, since attribute segmentation alone does not capture store-level differences, the quantitative variable operating hours (OpHours), representing the total number of hours a store is open during the week, is included as an additional covariate. Incorporating OpHours accounts for variations in operational time across stores, which likely influences sales performance. This combination of regional-level and store-level covariates provides a comprehensive basis for the spatial regression model.

Before fitting the SAR model, a general linear model was first applied to predict log-transformed sales, per POI, using the covariates OpHours and the attribute segmentations (PHH, PNM, PHM, with PNH as the reference category). Moran's I statistic [10] was calculated for the residuals of this model, yielding $I = 0.143$, with a variance of 0.006 and a p-value of 0.019. These results indicate statistically significant spatial autocorrelation in the residuals, justifying the use of a spatial regression approach. The SAR model builds upon the spatial regression framework [48] defined as

$$\mathbf{y} = \mathbf{X}\boldsymbol{\beta} + \mathbf{u} + \boldsymbol{\epsilon} \tag{4.11}$$

where $\mathbf{y}$ is the $M \times 1$ vector of log-transformed average sales for each POI, $\mathbf{X}$ is the $M \times p$ matrix of explanatory variables including OpHours and attribute segmentations (PHH,

© University of Pretoria

UNIVERSITEIT VAN PRETORIA
UNIVERSITY OF PRETORIA
YUNIBESITHI YA PRETORIA

PNM, PHM, with PNH as the reference category), $\boldsymbol{\beta}$ is the $p \times 1$ vector of regression coefficients and p the number of parameters, $\mathbf{u} \sim \mathcal{N}(0, \boldsymbol{\Sigma})$ is the latent spatial random error and $\boldsymbol{\epsilon} \sim \mathcal{N}(0, \sigma_\epsilon^2 \mathbf{I})$ is the independent error term.

For SAR models, the covariance structure is defined as

$$\boldsymbol{\Sigma} = \sigma_u^2 \left((\mathbf{I} - \mathbf{C})(\mathbf{I} - \mathbf{C})^\top \right)^{-1}$$

where $\mathbf{C} = \rho \mathbf{W}$, with $\mathbf{W}$ the spatial weights matrix and ρ the SAR smoothing parameter [48]. The weights matrix $\mathbf{W}$ incorporates both spatial and attribute-based proximities between regions, as defined by [19]

$$w_{ij} = \exp\left(-\left(\alpha u_e + (1 - \alpha) d_{ij}\right)\right) \tag{4.12}$$

where d_{ij} represents the standardised Euclidean distance between locations i and j and u_e reflects the absolute difference in the environmental covariates between two locations. Traditionally, in equation (4.12), u_e is based on the absolute difference of a quantitative environmental covariate. However, in this study, the environmental covariates are non-ordinal qualitative values. Consequently, we construct u_e based on attribute segmentation similarity, such that $u_{e_{ij}} = 0$ if POI i and j belong to the same attribute segmentation (associated with the overlapping macro-region) and $u_{e_{ij}} = 1$ if they belong to different attribute segmentations.

The parameter α controls the balance between spatial distance and attribute similarity ($\alpha \in [0, 1]$). For $\alpha = 0$, the weights depend entirely on spatial distance, while for $\alpha = 1$, they depend solely on attribute similarity. The SAR model for this application is formulated as

$$y = \beta_0 + \beta_1 \text{OpHours} + \beta_2 \text{PHH} + \beta_3 \text{PNM} + \beta_4 \text{PHM} + u + \epsilon. \tag{4.13}$$

This model is tested across all levels of α, starting at 0 (indicating that only spatial distance is considered) and increasing in increments of 0.05 up to 1 (indicating that only the attribute segmentation environmental effect is considered). In addition to evaluating the model's performance, the significance of the variables is assessed at all levels of α. The operating hours (OpHours) were found to be significant at all levels of α. However,

© University of Pretoria

UNIVERSITEIT VAN PRETORIA
UNIVERSITY OF PRETORIA
YUNIBESITHI YA PRETORIA

to test the effect of including attribute segmentation, we cannot rely solely on the p-values from the model output, as these values are dependent on the chosen reference category. Therefore, to quantify the significance of including attribute segmentation, we use a likelihood ratio test [17] to compare Model A, which has p_A parameters, with Model B, which has p_B parameters, as shown in the following equation

$$\begin{aligned} &\text{Model A: } y = \beta_0 + \beta_1 \text{OpHours} + u + \epsilon \\ &\text{Model B: } y = \beta_0 + \beta_1 \text{OpHours} + \beta_2 \text{PHH} + \beta_3 \text{PNM} + \beta_4 \text{PHM} + u + \epsilon. \end{aligned} \tag{4.14}$$

Under H_0, we are testing whether the categorical covariate, attribute segmentation, doesn't have a significant effect on the model, i.e., $H_0 : \beta_2 = \beta_3 = \beta_4 = 0$. Under H_0, assuming that Model A is sufficient, denote the fitted values as $\hat{y}_A$, which produces the log-likelihood l_A. Similarly, for Model B with fitted values $\hat{y}_B$, the log-likelihood is l_B. The log-likelihood ratio test (LRT) statistic [17] for comparing Models A and B is

$$L = 2(l_B - l_A) \sim \chi^2_{p_B - p_A}. \tag{4.15}$$

Testing both the model performance and significance of the covariates as indicated in equations (4.14) and (4.15), the final results of the SAR model outlined in equation (4.13) are presented in Figure 4.11 for all values of α ranging from 0 to 1 in increments of 0.05.

From the results in Figure 4.11 it can be noted that at $\alpha = 0$, we observe the lowest $R^2 = 40.27$, and the attribute segmentation covariates are not significant in the model (p-value(LRT)=0.52). As the value of α increases, the R^2 value also increases, reaching a maximum of 45.476, after which it begins to decrease again. The attribute segmentation covariates are significant for values of $0.5 \leq \alpha \leq 0.95$. From the results in Figure 4.11, $\alpha = 0.65$ produces the best model, with the highest R^2 and all variables being significant.

When considering the effect of all covariates in Figure 4.11 with the reference level for the attribute segmentation covariate being PNH (top right image), it can be observed that all other covariates have a positive effect on the log-transformed value of average sales. The PHH level has the strongest effect, followed by PHM, both of which are associated with the "hot days" attribute. When the reference level is changed to PHM,

© University of Pretoria

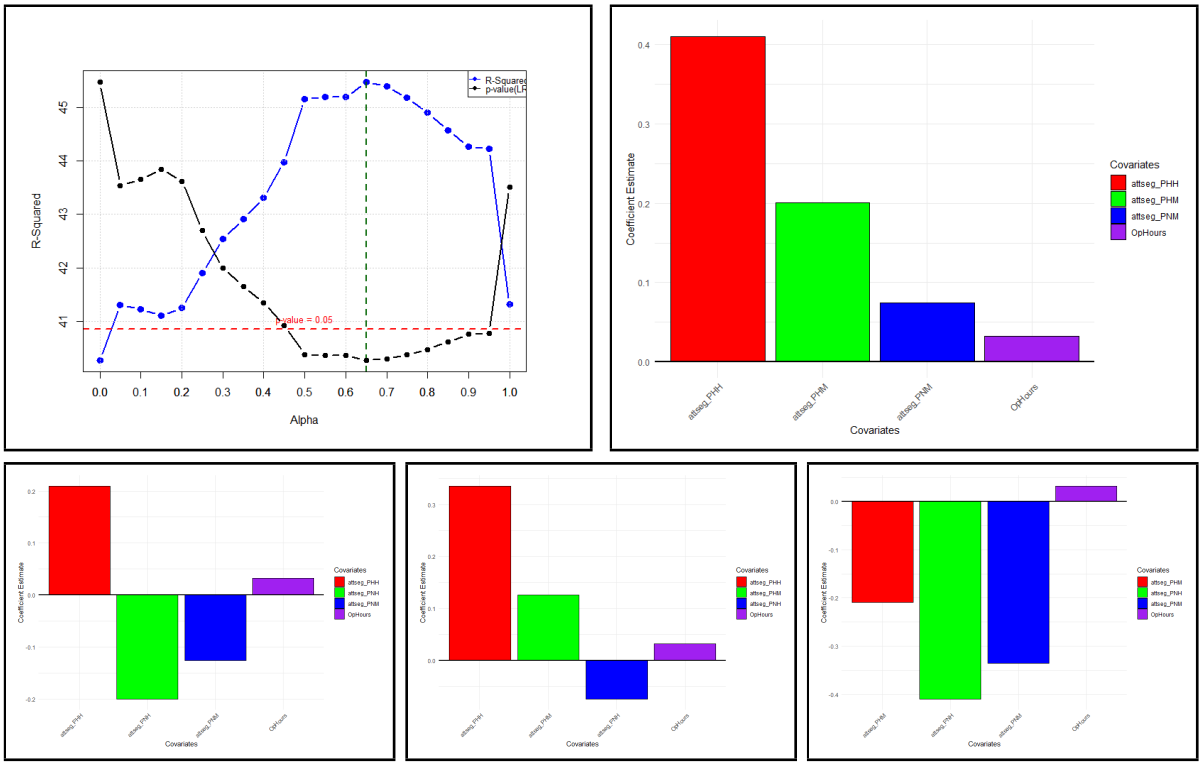

Figure 4.11: Top-left: R-squared and p-value (LRT) trends for varying α in the SAR model. Top-right: Coefficient estimates with reference level PNH. Bottom-left: Coefficient estimates with reference level PHM. Bottom-middle: Coefficient estimates with reference level PNM. Bottom-right: Coefficient estimates with reference level PHH.

PNM, and PHH, as shown in Figure 4.11, the operating hours consistently have a positive effect, while the impact of PHH and PHM remains substantial. In the last image, where PHH is the reference level, all other levels exhibit a negative effect relative to PHH, which is expected since PHH is associated with the highest average sales.

Upon investigation of the $Q = 55$ macro-regions, five have been identified as having the potential to exhibit positive average sales despite currently lacking allocated POIs. Among these, three macro-regions are classified as spatially inaccessible regarding access to the specific POI in question, suggesting high sales potential if accessibility issues are addressed as shown in the second row of images in Figure 4.12.

Conversely, other spatially inaccessible regions, such as those segmented under the ONN attribute segment, will not benefit from adding a POI due to their characteristics, including limited road access, typical temperature ranges, and a lack of demand as

© University of Pretoria

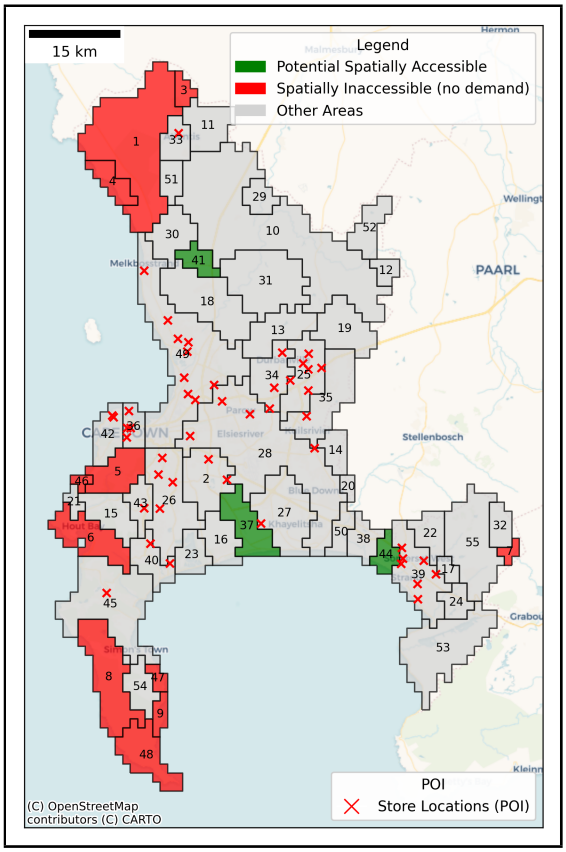

Figure 4.12: Highlighting spatially inaccessible areas and potential spatially accessible (w.r.t this specific POI). Map data © OpenStreetMap contributors, under the Open Database License (ODbL).

indicated on Figure 4.12. This segmentation provides a clear rationale for why certain areas remain spatially disjoint and do not warrant further resource allocation.

4.5 Discussion

The advantages of attribute based spatial segmentation lie in its ability to generate clusters that are tailored to the specific characteristics and needs of different regions. By incorporating spatial proximity along with environmental and other relevant attributes, this approach ensures that resource allocation aligns closely with local demands. The methodology supports realistic macro-regions, creating attribute segments that reflect area similarities and enable targeted planning and optimisation efforts.

© University of Pretoria

UNIVERSITEIT VAN PRETORIA
UNIVERSITY OF PRETORIA
YUNIBESITHI YA PRETORIA

The application of this methodology to predict the average sales of an over-the-counter diarrhoea medication in South Africa provides valuable insights into its practical utility. The use of attribute segmentation captures the interactions between environmental, spatial and demand-related factors, revealing patterns that would not be evident through traditional clustering approaches.

SAR models [10] are utilised to account for spatial dependence in the data by incorporating a spatial weights matrix that captures the relationships or proximities between different regions. In this study, we apply a SAR model to assess whether attribute based spatial segments impact the prediction of summer average sales of a diarrhoea medication. While SAR models are widely used for spatial dependency modelling, their application in this research is specifically aimed at macro-region optimisation by incorporating attribute based segmentation as covariates to enhance predictive accuracy and spatial coherence.

Beyond the SAR models applied in this research, other spatial regression methods could also be explored as potential alternatives. For instance, geographically weighted regression (GWR) [20] allows for localised relationships between predictors and outcomes, enabling the analysis of spatial heterogeneity across regions. Similarly, spatial error models (SEM) and spatial lag models (SLM) [11] address spatial dependence in error terms or outcomes. These models are particularly relevant when interactions between regions play a critical role in shaping outcomes, as is often the case in spatial planning applications. The application of this work however lies in the integration of attribute based spatial segmentation as covariates in the spatial prediction, enhancing the adaptability of resource planning models to diverse and geographically nuanced contexts. Future work could explore alternative spatial regression techniques to compare their effectiveness in different resource planning and decision-making scenarios.

This methodology can be applied to any geographical region, G_a, provided the areas exhibit similar environmental or attribute based characteristics to ensure consistent and meaningful clusters. For instance, in South Africa, Gauteng and the Western Cape demonstrate vastly different patterns in terms of population size and climate, necessitating separating the regions to capture their unique regional dynamics effectively.

The grid size and area size can be adjusted to a finer scale for more precise POI

© University of Pretoria

UNIVERSITEIT VAN PRETORIA
UNIVERSITY OF PRETORIA
YUNIBESITHI YA PRETORIA

optimisation within towns or cities. However, our application was limited by insufficient records at a smaller sized geographical region to thoroughly test the methodology. When working with smaller areas, it is essential to ensure adequate variability in the chosen area attributes, as environmental factors such as temperature may show minimal variation within a small region.

It is important to highlight that only one pharmaceutical chain was analysed in South Africa, although multiple smaller pharmacies also sell the same over-the-counter medication that was used in this application. The investigated chain is primarily situated in easily accessible areas with at least mid sized population, but incorporating smaller suburban pharmacies into the analysis could improve demand predictions by capturing broader sales patterns, including areas with lower demand.

The optimal number of clusters was determined using the elbow method, providing a robust starting point for segmentation. However, since the iterative clustering approach continuously updates until an optimal solution is reached, an adaptive process could also be employed to dynamically determine the most appropriate number of clusters. In addition, k-means clustering is known to be sensitive to initial conditions, which can sometimes lead to different final cluster assignments depending on the starting centroids. To address this, different initialisations of k-means were tested, including k-means++, which is designed to improve clustering stability by spreading out initial centroids [43]. This method selects the first centroid randomly and assigns subsequent centroids based on maximum squared distance, ensuring that initial centroids are pushed as far apart as possible. Despite these variations in starting centroids, the same clustering solution was consistently obtained and the number of iterations remained largely unchanged. Future research could further explore adaptive validation techniques that refine K dynamically, ensuring that clustering solutions remain optimal across different macro regions and attribute segments.

Attribute based spatial segmentation demonstrates the potential to significantly improve spatial planning and resource optimisation by tailoring macro-regions based on geographic and attribute based factors. By leveraging probabilistic clustering and iterative refinement, it offers adaptable, data-driven solutions to assist in city planning and resource allocation. The adaptability of this framework ensures it can be customised

© University of Pretoria

UNIVERSITEIT VAN PRETORIA
UNIVERSITY OF PRETORIA
YUNIBESITHI YA PRETORIA

to address diverse regional needs and different industries, making it a powerful tool for optimising service and infrastructure planning.

4.6 Conclusion

Our research presents a novel framework for spatial planning and resource optimisation, leveraging attribute-based spatial segmentation. This study integrates probabilistic clustering structures with iterative refinement processes to produce tailored macro-regions that align with both regional attributes and geographic needs. The methodology stands out by ensuring the precise delineation of service catchment areas, optimising POI placements, and addressing spatially accessible as well as disjoint areas through adaptive segmentation.

Unlike traditional connectivity-based clustering approaches, our model incorporates spatial and attribute-based proximities, dynamically adapting to local conditions and providing actionable insights into the unique characteristics of diverse geographic regions. By integrating spatial regression analysis, including a SAR model, the framework not only accounts for spatial dependence but also quantifies the role of attribute segmentation and store-level characteristics, such as operating hours, in predicting POI-level outcomes.

The results demonstrate the potential of this methodology to significantly improve resource allocation and service optimisation, particularly in heterogeneous environments. The adaptability of the proposed framework ensures its applicability across various industries and regions, making it a robust tool for informed decision-making in urban planning, retail, and healthcare resource management.

© University of Pretoria

Chapter 5

Conclusion

Effective spatial planning and resource optimisation are essential for ensuring equitable access to services and resources across diverse regions. This chapter summarises the key contributions from each of the three research papers (Section 5.1) and explores how they collectively enhance accessibility and resource allocation through fuzzy lattice data structures and attribute based spatial segmentation.

In addition, we discuss the selection methods used to determine attributes and weights, as well as key considerations when working with label disconnected graphs (Section 5.2). A thorough examination of the data limitations encountered in this research is presented in Section 5.3, highlighting potential challenges and areas for improvement.

This is followed by an outline of future research directions in Section 5.4, which identifies ways to refine and expand these methodologies. Finally, Section 5.5 presents a high-level synthesis of findings, offering a structured overview of how the methodologies interconnect to form a comprehensive spatial decision making framework.

5.1 Chapter discussions

5.1.1 Fuzzy lattice data structure

Chapter 2 introduced the concept of fuzzy lattice catchment areas, which create overlapping catchment areas using probabilistic label propagation. This approach ensures a more even distribution of demand and supply by enabling communities to choose from

© University of Pretoria

UNIVERSITEIT VAN PRETORIA
UNIVERSITY OF PRETORIA
YUNIBESITHI YA PRETORIA

multiple POIs within their accessibility range. By incorporating drive-time thresholds, the methodology accounts for both service proximity and accessibility constraints, offering a more realistic depiction of service areas. While the approach offers flexibility and precision, challenges remain in handling natural barriers and refining label propagation assumptions. Future work may focus on adjusting edge weights to better capture geographic barriers and further relaxing label assumptions for broader applicability. Overall, fuzzy lattice catchment areas present a versatile tool for various industry applications, providing a data-driven approach to resource allocation and accessibility planning.

5.1.2 Attribute based fuzzy lattice data structure

Building on the first methodology, Chapter 3 expanded the fuzzy lattice framework by integrating attribute based connections. By combining structural network links with shared attributes such as environmental conditions, this method allowed for more effective label propagation and demand distribution. This dual consideration of structure and attributes enabled a nuanced understanding of network interactions beyond purely topological relationships. Although the study highlighted the potential of this approach, it acknowledged the need for flexible weighting of attributes and the limitations of analysing a single pharmaceutical chain. Incorporating additional socio-economic and contextual factors could further enhance the accuracy of demand predictions and accessibility models. Ultimately, the attribute based fuzzy lattice data structure offers a powerful means of capturing complex, context dependent relationships within networks, providing a more holistic approach to spatial accessibility analysis.

5.1.3 Attribute based spatial segmentation

Finally, Chapter 4 reversed the perspective of the methodologies discussed in Chapters 2 and 3 by focusing on attribute based spatial segmentation to identify potential spatially accessible regions. By incorporating spatial proximity, environmental attributes and other relevant factors, this approach ensured resource allocation was closely aligned with local demands. The methodology's adaptability allowed for the creation of meaningful clusters, enhancing planning efforts and enabling targeted interventions. Limit-

© University of Pretoria

UNIVERSITEIT VAN PRETORIA
UNIVERSITY OF PRETORIA
YUNIBESITHI YA PRETORIA

ations included data availability at finer spatial scales and the need for variability in chosen attributes when working in smaller regions. Despite these challenges, attribute-based spatial segmentation offers a flexible framework for optimising service placement and tailoring resource allocation to diverse regional needs. Its iterative clustering and probabilistic structures provide a dynamic and responsive approach to spatial planning, enhancing service accessibility and infrastructure development.

5.2 Attributes, weights and label connectivity

The selection of attributes and their assigned weights plays a critical role in shaping the outcomes of the model. Each attribute contributes to the modelling framework by capturing key factors affecting demand distribution and accessibility to POIs. For each application and region, the choice of attributes needs to be tailored to reflect local conditions, infrastructure and demand characteristics.

The choice of attributes will vary depending on the type of service or goods a POI provides. For example, school placements may require an assessment of the number of residents under the age of 18, while planning for old-age homes would consider demand only from populations above a certain age threshold. Similarly, local conditions, such as infrastructure quality and geographical barriers, need to be assessed in order to accurately reflect real-world accessibility and service provision. These factors ensure that the model remains adaptable and relevant to different spatial planning applications.

The attributes selected in this research were determined based on data availability and their correlation with observed POI supply in a given area. Each individual use case and research question prioritises different attributes, depending on data availability and full geographical coverage that aligns with the research objectives. In Chapter 3, which examines summer sales of diarrhoea medication, factors such as accessibility to a POI and temperature were considered. Temperature was found to be highly significant in relation to sales, however, the low R-squared value of 0.1628 indicates that only 16.3% of the variability in sales can be explained by the model. This highlights the need for additional variables to improve predictive accuracy. However, due to a lack of full coverage for other potentially relevant factors such as economic constraints and

© University of Pretoria

UNIVERSITEIT VAN PRETORIA
UNIVERSITY OF PRETORIA
YUNIBESITHI YA PRETORIA

healthcare supply chain efficiency, these variables were not included in the study. Future research could explore ways to incorporate broader datasets to refine demand estimation and improve model performance.

Structual- and attribute- edge weights represent the relative importance of connections between nodes in the graph, where heavily weighted edges encourage strong connections. The structure edge weights reflects the importance of shared boundaries between structural nodes, whereas the attribute weights quantify the importance or influence of an shared attribute between structural nodes. If attribute connections are more important (similar economic profiles, income levels etc.), attribute edges will receive larger weights than structural edges, whereas if shared boundaries are more significant (natural boundaries, access to a service is explicitly limited to a designated neighbourhood etc.), structural connections will have larger weights than attribute connections. If both structural and attribute connections carry equal importance, they will be assigned equal weights to ensure a balanced influence. An edge weight can either be relative to a quantity for example in a social network the number of interactions (messages, common friends etc.) among users or it can simply be set to 1 to indicate that a link is present as discussed in [5]. In all applications considered in this research, the structural and attribute edge weights were set to 1, simply indicating the presence of a structural or attribute link. This approach was taken because quantifying a shared attribute between two regions is not as evident as in social networks, where a node typically represents a single individual. In contrast, regional nodes encompass multiple characteristics, with various underlying factors influencing their relationships. Future research will explore the impact of quantifying structural and attribute edge weights between regions, using an iteratively adjusted self-learning mechanism. This adjustment process dynamically modifies weights based on how well an attribute contributes to clustering—attributes that strongly differentiate clusters are assigned higher weights, whereas those with weaker clustering tendencies receive lower weights as discussed in [53].

All applications illustrated in Chapters 2, 3 and 4 were conducted in geographical regions where all nodes were label connected and could be assigned a probability. However, this assumption may not hold in non-urban areas with geographical barriers that restrict direct access to essential services. Geographical constraints such as mountains, rivers, or

© University of Pretoria

UNIVERSITEIT VAN PRETORIA
UNIVERSITY OF PRETORIA
YUNIBESITHI YA PRETORIA

a lack of road infrastructure may result in disconnected demand nodes that do not have feasible access to POIs. These regions will need to be treated differently by sectioning them off as separate geographical regions that maintain internal label connectivity. To apply fuzzy lattice data structures or attribute based fuzzy data structures, the graph must be label connected, otherwise $(\mathbf{I} - \mathbf{P}_{uu})^{-1}$ will not be invertible, preventing a solution from being obtained in Equations (2.4) and (3.7). Alternative methods for labelling disconnected graphs, as discussed in [21], can also be explored in future research.

Each research problem will require different attributes, weighting strategies and connectivity between nodes to reflect the unique characteristics of each domain. As future research expands the applicability of this approach, incorporating domain-specific weighting methods and adaptive clustering techniques will be essential to improving model performance and ensuring robust, context-sensitive results.

5.3 Data limitations

While this study presents a structured approach to catchment area estimation using structural and attribute properties, some data limitations such as incomplete GIS datasets, potential outdated socio-economic and demographic data and data biases must be acknowledged.

When considering the supply provided by a POI as done in Chapters 2, 3 and 4 some limitations needs to be addressed. The accuracy of healthcare resource data, particularly hospital bed capacity, is a significant challenge in a developing country such as South Africa. Variations exist between public and private hospital databases, and independent reports have raised concerns that some hospitals may have overstated their capacity due to budget constraints and shortages of healthcare professionals. Given these discrepancies, the estimated number of hospital beds per capita used in this study may be a conservative approximation. As the analysis relied on officially reported data, any unverified reductions in actual bed availability were not incorporated. Future studies should consider integrating real-time hospital capacity monitoring or independent verification methods to refine these estimates and improve transparency in healthcare resource allocation.

© University of Pretoria

UNIVERSITEIT VAN PRETORIA
UNIVERSITY OF PRETORIA
YUNIBESITHI YA PRETORIA

In addition to hospital bed capacity, pharmaceutical supply availability presents another limitation in this study. The analysis done in Chapters 3 and 4 focused on a single pharmaceutical chain operating in South Africa, however, many smaller pharmacies and independent suppliers that were not included in this analysis also sell the same medication. These smaller entities may not be formally registered, making comprehensive pharmaceutical sales data difficult to obtain. The investigated chain is also primarily located in easily accessible areas with at least mid sized population density, meaning that sale patterns derived from this dataset are unlikely to fully capture non-urban demand. Incorporating sales from smaller and independent pharmacies into future analyses could significantly improve supply allocation by broadening the dataset and capturing a more representative view of pharmaceutical consumption.

When considering the demand allocation there are also limitations in the data when considering how frequently the data is updated. The demand for each spatial grid is obtained from Lightstone (Pty) Ltd, which employs a modelling approach to estimate demand using census data and updates it annually with property registration and ownership data from the Deeds Office. However, census data is only updated once every decade, and population estimates based on deeds data do not capture informal settlements or rapidly developing non-urban areas where formal property registration is lacking. This means that some high-growth regions may have been underrepresented in demand estimation, potentially impacting spatial planning accuracy. The exclusion of unregistered households is a significant constraint in third world countries, as many regions do not maintain comprehensive records of informal housing. Future research can include alternative population estimation methods such as mobile network usage patterns or high-resolution satellite imagery as discussed in [8], to better capture evolving demographic trends.

Infrastructure accessibility, particularly road conditions and travel-time assumptions, poses a significant challenge in accurately predicting accessibility in developing countries. Road network accessibility was incorporated into the analysis to evaluate ease of access to POIs. However, the classification of road accessibility was based on official maps, as published by OpenStreetMaps, rather than real-time road quality assessments. This presents a major challenge in South Africa, where road conditions in many regions deteriorate

© University of Pretoria

UNIVERSITEIT VAN PRETORIA
UNIVERSITY OF PRETORIA
YUNIBESITHI YA PRETORIA

over time due to inadequate maintenance. As a result, the drive-time estimates used in this study may be overestimated, particularly in rural or non-urban areas where infrastructure quality is highly variable. The assumption that roads remain in their reported state does not account for deterioration, potholes, or seasonal flooding, all of which could significantly impact travel times. Furthermore, the fixed travel-time thresholds of 5-, 10-, and 15- minutes used in the study may not accurately reflect regional travel conditions. These thresholds assume consistent average speeds, which may not be realistic given the variability in road quality, congestion levels, and the presence of informal settlements. In some cases, what is classified as a 15-minute drive-time radius on an official road network may, in reality, take significantly longer due to poor road maintenance or unpaved routes that slow down travel. These thresholds can be further explored in future studies, potentially through real-time traffic data integration or dynamic drive-time calculations that adjust based on actual travel speeds rather than fixed assumptions as explored in [26].

Environmental data coverage introduces some challenges, particularly in capturing temperature variability across different regions. Temperature data for the study was sourced from both the South African Weather Services (SAWS) and OpenWeather to ensure adequate spatial representation. However, the limited number of official weather stations meant that interpolation techniques, specifically Ordinary Kriging, were required to estimate missing values across the study area. While Kriging is a well established method for spatial interpolation, uncertainties remain in regions where observed data points were sparse, leading to potential inaccuracies in temperature variability estimates. Expanding environmental monitoring networks or incorporating additional sources such as satellite-derived climate data could help improve spatial resolution and reduce uncertainty in future applications.

Considering the data limitation points raised, it is apparent that there is a need to consider strategies for improving data quality and accessibility in future research. Different use cases will require distinct approaches, but possible strategies include enhancing data-sharing agreements between public and private entities, increasing the frequency of spatial data updates. Volunteered geographic information [22] highlight how participatory data collection methods can supplement formal GIS databases, particularly in

© University of Pretoria

UNIVERSITEIT VAN PRETORIA
UNIVERSITY OF PRETORIA
YUNIBESITHI YA PRETORIA

regions with limited institutional capacity for frequent updates. In the healthcare domain, integrating electronic health records and mobile health data could help address data gaps in service accessibility. While each use case will have unique challenges, future studies should explore a combination of technological and participatory data collection strategies to enhance the accuracy and completeness of spatial datasets. Addressing these limitations will further strengthen the applicability of this approach in diverse settings, ensuring that spatial planning methodologies remain adaptive and reflective of real-world complexities.

5.4 Future work

In this research, the development of spatial catchment areas is advanced using fuzzy lattice structures and attribute-based modelling, paving the way for more adaptable and realistic service zones. This work also opens up several promising avenues for future exploration that extend its scope.

When comparing the fuzzy lattice model structure to traditional methods such as gravity models and network flow models, key differences emerge in how spatial relationships are represented. Gravity models assume a uniform distance-decay effect [50] which may oversimplify real-world accessibility patterns, whereas the fuzzy lattice approach allows for adaptive clustering based on both structural and attribute similarities, capturing more nuanced spatial interactions. Similarly, while network flow models are well-suited for optimising predefined transport networks, they rely on explicit flow constraints making them less effective for applications where demand patterns and accessibility evolve dynamically without fixed pathways. Future work can also include quantitatively comparing these approaches and assessing the performance trade-offs in different urban and non-urban contexts.

One key direction is the enhancement of data collection systems for recording and geocoding residential addresses of service users. In many low-resource settings, accurate geocoded data remains limited or inconsistent, posing challenges to precisely defining service catchment areas. Future efforts should focus on improving these data collection mechanisms, enabling more representative and adaptable models that can better serve

© University of Pretoria

UNIVERSITEIT VAN PRETORIA
UNIVERSITY OF PRETORIA
YUNIBESITHI YA PRETORIA

evolving community needs.

Additionally, although spatial proximity and key attributes were considered, incorporating the impact of seasonality on service demand and accessibility is another important area for future exploration. Developing dynamic models that account for temporal changes, such as population movements, would allow for more responsive and adaptive planning [7]. This aspect was not incorporated due to the availability of data. Furthermore, the attributes considered in the attribute based fuzzy lattice data structures and spatial segmentation approaches are not time-dependent. For instance, an attribute such as ease of access can have vastly different implications during peak and off-peak traffic times. Investigating a time-dependent approach that accounts for such variations is another promising direction for future research.

Future research could also explore the integration of mixed data clustering techniques with spatial regularisation, such as the Fuzzy C-Medoids Clustering for Mixed Data model with spatial constraints (FCMd-MD-SP) proposed by [18]. This model addresses the challenge of clustering datasets containing both quantitative and qualitative attributes by combining dissimilarity measures for each attribute type through a weighting system. The weights are optimised during the clustering process, reflecting the relevance of each attribute type, while a spatial penalty term ensures that membership degrees are spatially smoothed.

Applying this approach to the current methodology could refine the creation of spatially coherent macro-regions by dynamically weighting attributes and embedding spatial regularisation into the clustering process. This refinement would provide a more nuanced understanding of regional dynamics, further enhancing the adaptability of attribute-based spatial segmentation to real-world applications, and enabling more precise predictions of service demand and the identification of optimal POI placements.

Future research will also include a comprehensive quantitative comparative analysis between the fuzzy lattice model and existing approaches such as floating catchment area methods and gravity models. While this study demonstrates the effectiveness of the fuzzy lattice framework, and a comparison using a toy example is provided, a systematic evaluation of its performance relative to traditional models is still needed. This could involve benchmarking accessibility predictions, computational efficiency and model ro-

© University of Pretoria

UNIVERSITEIT VAN PRETORIA
UNIVERSITY OF PRETORIA
YUNIBESITHI YA PRETORIA

bustness across diverse urban and rural environments. To facilitate this comparison, simulated data can be used to test different scenarios and assess model performance under controlled conditions.

Finally, incorporating social factors, perceived service quality, and affordability into future models would deepen the understanding of service utilisation [32]. While this thesis primarily focused on spatial and attribute-driven approaches, considering these additional dimensions could provide a more comprehensive view of accessibility and inform targeted interventions.

5.5 Summary

Collectively, the three methodologies presented in this research offer a comprehensive framework for addressing spatial accessibility and resource optimisation across diverse regions. By leveraging probabilistic structures, attribute based linkages, and iterative clustering techniques, these approaches provide precise and adaptable solutions for creating tailored catchment areas, optimising POI placement and addressing spatially disjoint regions.

The fuzzy lattice model plays a foundational role by structuring spatial connectivity through probabilistic linkages, allowing for adaptive clustering based on both structural and attribute similarities. This ensures that spatial units are grouped in a way that captures both spatial coherence and attribute driven relationships, making it more flexible than traditional distance-based clustering methods.

Building on this, attribute based spatial segmentation enables a more contextually informed approach to defining demand regions, incorporating key factors such as accessibility, environmental influences, and socio-economic conditions. This segmentation method refines spatial decision making, ensuring that resource allocation and service distribution align with real-world demand patterns.

The integration of these segmented spatial structures into POI optimisation ensures that facility placement maximises accessibility while accounting for both structural connectivity and demand variation. This allows for the development of adaptive and equitable service regions, particularly in areas where geographical and aspatial barriers impact

© University of Pretoria

UNIVERSITEIT VAN PRETORIA
UNIVERSITY OF PRETORIA
YUNIBESITHI YA PRETORIA

accessibility. The ability to address spatially disjoint regions through attribute driven segmentation enhances service accessibility and infrastructure planning, making this approach valuable for urban planners, policymakers, and industry leaders.

This research highlights the importance of integrating structural and attribute based insights into spatial planning, acknowledging the complexities of geographic, environmental, and socio-economic factors. As regions continue to evolve and face changing accessibility challenges, the proposed spatial decision making framework provides a flexible and scalable methodology for adapting to new demands. This ensures equitable and efficient service provision across diverse landscapes.

Future work will further refine these models, expanding their applicability to more complex spatial environments and deepening their impact in both local and global contexts.

© University of Pretoria

Bibliography

[1] Jonas Lohmann Elkjær Andersen and Alex Landex. Catchment areas for public transport. *WIT Transactions on the Built Environment*, 101:175–184, 2008.

[2] Assaf Anyamba, Jennifer L Small, Seth C Britch, Compton J Tucker, Edwin W Pak, Curt A Reynolds, James Crutchfield, and Kenneth J Linthicum. Recent weather extremes and impacts on agricultural production and vector-borne disease outbreak patterns. *PloS One*, 9(3):e92538, 2014.

[3] Arik Azran. The rendezvous algorithm: Multiclass semi-supervised learning with Markov random walks. In *Proceedings of the 24th International Conference on Machine Learning*, pages 49–56, 2007.

[4] Punam Bedi and Chhavi Sharma. Community detection in social networks. *Wiley Interdisciplinary Reviews: Data Mining and Knowledge Discovery*, 6(3):115–135, 2016.

[5] Smriti Bhagat, Graham Cormode, and S Muthukrishnan. Node classification in social networks. *Social Network Data Analytics*, pages 115–148, 2011.

[6] Avrim Blum and Shuchi Chawla. Learning from labeled and unlabeled data using graph mincuts. In *Proceedings of the 18th International Conference on Machine Learning*, pages 19–26, 2001.

[7] Robert J Challen, Gareth J Griffith, Lucas Lacasa, and Krasimira Tsaneva-Atanasova. Algorithmic hospital catchment area estimation using label propagation. *BMC Health Services Research*, 22(1):1–12, 2022.

© University of Pretoria

UNIVERSITEIT VAN PRETORIA
UNIVERSITY OF PRETORIA
YUNIBESITHI YA PRETORIA

[8] CE Coetzee and EPJ Kleynhans. Estimating economic activity of South African provinces using satellite technology: An econometric panel data application. *Remote Sensing Applications: Society and Environment*, 23:100564, 2021.

[9] Goran Corluka. Tourism seasonality - An overview. *Journal of Business Paradigms*, 4(1):21–43, 2019.

[10] Noel Cressie. The origins of Kriging. *Mathematical Geology*, 22:239–252, 1990.

[11] David Darmofal. *Spatial Analysis for the Social Sciences*. Cambridge University Press, UK, 2015.

[12] Michelle de Klerk and Inger Fabris-Rotelli. Attribute based spatial segmentation for optimising POI placement. 2024. Unpublished results: under review.

[13] Michelle de Klerk and Inger Fabris-Rotelli. Hospital accessibility catchment areas as a fuzzy lattice data structure. In *ISPRS Annals of the Photogrammetry, Remote Sensing and Spatial Information Sciences*, volume X-4-2024, pages 99–106, 2024.

[14] Michelle de Klerk and Inger Fabris-Rotelli. Seasonal catchment areas using an attribute based fuzzy lattice data structure. 2024. Unpublished results: under review.

[15] Pasquale De Meo, Emilio Ferrara, Giacomo Fiumara, and Alessandro Provetti. Generalized louvain method for community detection in large networks. In *2011 11th International Conference on Intelligent Systems Design and Applications*, pages 88–93. IEEE, 2011.

[16] M. Duckham, M.F. Goodchild, and M. Worboys. *Foundations of Geographic Information Science*. CRC Press, London, 2003.

[17] Peter K Dunn and Gordon K Smyth. *Generalized Linear Models with Examples in R*. Springer, New York, 2018.

[18] Pierpaolo D'Urso, Livia De Giovanni, Lorenzo Federico, and Vincenzina Vitale. Fuzzy clustering of mixed data with spatial regularization. *Spatial Statistics*, 65:100874, 2025.

© University of Pretoria

UNIVERSITEIT VAN PRETORIA
UNIVERSITY OF PRETORIA
YUNIBESITHI YA PRETORIA

[19] Bedilu Alamirie Ejigu and Eshetu Wencheko. Introducing covariate dependent weighting matrices in fitting autoregressive models and measuring spatio-environmental autocorrelation. *Spatial Statistics*, 38:100454, 2020.

[20] A. Stewart Fotheringham, Chris Brunsdon, and Martin Charlton. *Geographically Weighted Regression: The Analysis of Spatially Varying Relationships*. Wiley, UK, 2003.

[21] Joseph A Gallian and Danielle Stewart. Properly even harmonious labelings of disconnected graphs. *AKCE International Journal of Graphs and Combinatorics*, 12(2-3):193–203, 2015.

[22] Michael F Goodchild. Citizens as sensors: the world of volunteered geography. *GeoJournal*, 69:211–221, 2007.

[23] Chéri A Green, Gerbrand G Mans, Mawande Ngidi, Zukisa Sogoni, and Johan Martiz. Using catchment area analysis and GIS based spatial analysis for prioritising spatial investment in non-metro South Africa. In *Proceedings of the 52nd ISOCARP Conference*, Durban, South Africa, September 2016. International Society of City and Regional Planners.

[24] Anil K Jain. Data clustering: 50 years beyond k-means. *Pattern Recognition Letters*, 31(8):651–666, 2010.

[25] Glen Jeh and Jennifer Widom. Simrank: A measure of structural-context similarity. In *Proceedings of the Eighth ACM SIGKDD International Conference on Knowledge Discovery and Data Mining*, pages 538–543, 2002.

[26] Shafiza Ariffin Kashinath, Salama A Mostafa, Aida Mustapha, Hairulnizam Mahdin, David Lim, Moamin A Mahmoud, Mazin Abed Mohammed, Bander Ali Saleh Al-Rimy, Mohd Farhan Md Fudzee, and Tan Jhon Yang. Review of data fusion methods for real-time and multi-sensor traffic flow analysis. *IEEE Access*, 9:51258–51276, 2021.

[27] Abdullah A Khan. An integrated approach to measuring potential spatial access to health care services. *Socio-Economic Planning Sciences*, 26(4):275–287, 1992.

© University of Pretoria

UNIVERSITEIT VAN PRETORIA
UNIVERSITY OF PRETORIA
YUNIBESITHI YA PRETORIA

[28] Diao Lin, Ruoxin Zhu, Jian Yang, and Liqiu Meng. An open-source framework of generating network-based transit catchment areas by walking. *ISPRS International Journal of Geo-Information*, 9(8):467, 2020.

[29] Hanyang Lin, Yongzhao Zhan, Zizheng Zhao, Yuzhong Chen, and Chen Dong. Overlapping community detection based on attribute augmented graph. *Entropy*, 23(6):680, 2021.

[30] Xin Luan, Lin Cheng, Yan Song, and Jinbao Zhao. Better understanding the choice of travel mode by urban residents: New insights from the catchment areas of rail transit stations. *Sustainable Cities and Society*, 53:101968, 2020.

[31] Wei Luo and Fahui Wang. Measures of spatial accessibility to health care in a GIS environment: Synthesis and a case study in the Chicago region. *Environment and Planning B: Planning and Design*, 30(6):865–884, 2003.

[32] Peter M Macharia, Nicolas Ray, Emanuele Giorgi, Emelda A Okiro, and Robert W Snow. Defining service catchment areas in low-resource settings. *BMJ Global Health*, 6(7), 2021.

[33] R. Minshull. *Regional Geography: Theory and Practice*. Taylor & Francis, New York, 2017.

[34] Gentille Musengimana, Fidele K Mukinda, Roderick Machekano, and Hassan Mahomed. Temperature variability and occurrence of diarrhoea in children under five-years-old in Cape Town metropolitan sub-districts. *International Journal of Environmental Research and Public Health*, 13(9):859, 2016.

[35] Andrew Ng, Michael Jordan, and Yair Weiss. On spectral clustering: Analysis and an algorithm. *Advances in Neural Information Processing Systems*, 14, 2001.

[36] David H Peters, Anu Garg, Gerry Bloom, Damian G Walker, William R Brieger, and M Hafizur Rahman. Poverty and access to health care in developing countries. *Annals of the New York Academy of Sciences*, 1136(1):161–171, 2008.

© University of Pretoria

[37] Alex Pothen. Graph partitioning algorithms with applications to scientific computing. In *Parallel Numerical Algorithms*, pages 323–368. Springer, 1997.

[38] Georgia Pozoukidou and Margarita Angelidou. Urban planning in the 15-minute city: Revisited under sustainable and smart city developments until 2030. *Smart Cities*, 5(4):1356–1375, 2022.

[39] Benjamin Rader, Christina M Astley, Kara Sewalk, Paul L Delamater, Kathryn Cordiano, Laura Wronski, Jessica Malaty Rivera, Kai Hallberg, Megan F Pera, and Jonathan Cantor. Spatial modeling of vaccine deserts as barriers to controlling SARS-CoV-2. *Communications Medicine*, 2(1):141, 2022.

[40] John Radke and Lan Mu. Spatial decompositions, modeling and mapping service regions to predict access to social programs. *Geographic Information Sciences*, 6(2):105–112, 2000.

[41] Usha Nandini Raghavan, Réka Albert, and Soundar Kumara. Near linear time algorithm to detect community structures in large-scale networks. *Physical Review E*, 76(3):036106, 2007.

[42] Yaxiong Shao and Wei Luo. Supply-demand adjusted two-steps floating catchment area (SDA-2SFCA) model for measuring spatial access to health care. *Social Science & Medicine*, 296:114727, 2022.

[43] Douglas Steinley. K-means clustering:A half-century synthesis. *British Journal of Mathematical and Statistical Psychology*, 59(1):1–34, 2006.

[44] Martin Szummer and Tommi Jaakkola. Partially labeled classification with Markov random walks. *Advances in Neural Information Processing Systems*, 14, 2001.

[45] Zhuolin Tao, Yang Cheng, Qingjing Zheng, and Guicai Li. Measuring spatial accessibility to healthcare services with constraint of administrative boundary: A case study of Yanqing District, Beijing, China. *International Journal for Equity in Health*, 17(1):1–12, 2018.

© University of Pretoria

UNIVERSITEIT VAN PRETORIA
UNIVERSITY OF PRETORIA
YUNIBESITHI YA PRETORIA

[46] Naftali Tishby and Noam Slonim. Data clustering by Markovian relaxation and the information bottleneck method. *Advances in Neural Information Processing Systems*, 13, 2000.

[47] Chieh-Yuan Tsai and Chuang-Cheng Chiu. Developing a feature weight self-adjustment mechanism for a k-means clustering algorithm. *Computational Statistics & Data Analysis*, 52(10):4658–4672, 2008.

[48] Jay M Ver Hoef, Erin E Peterson, Mevin B Hooten, Ephraim M Hanks, and Marie-Josèe Fortin. Spatial autoregressive models for statistical inference from ecological data. *Ecological Monographs*, 88(1):36–59, 2018.

[49] Ulrike Von Luxburg. A tutorial on spectral clustering. *Statistics and Computing*, 17:395–416, 2007.

[50] F. Wang. *Quantitative Methods and Socio-Economic Applications in GIS*. CRC Press, United States, 2014.

[51] S. Wierzchoń and M. Kłopotek. *Modern Algorithms of Cluster Analysis*. Springer International Publishing, Germany, 2017.

[52] Jierui Xie and Boleslaw K Szymanski. Labelrank: A stabilized label propagation algorithm for community detection in networks. In *2013 IEEE 2nd Network Science Workshop (NSW)*, pages 138–143. IEEE, 2013.

[53] Yang Zhou, Hong Cheng, and Jeffrey Xu Yu. Graph clustering based on structural/attribute similarities. *Proceedings of the VLDB Endowment*, 2(1):718–729, 2009.

© University of Pretoria